IDENTIFICATION OF THE ROLES PLAYED BY IKKε IN HEPATOCELLULAR AND COLORECTAL CARCINOGENESIS

A THESIS SUBMITTED TO

THE GRADUATE SCHOOL OF ENGINEERING AND SCIENCE

OF BILKENT UNIVERSITY

IN PARTIAL FULFILLMENT OF THE REQUIREMENTS FOR

THE DEGREE OF

MASTER OF SCIENCE

IN

MOLECULAR BIOLOGY AND GENETICS

By

Uğur Kahya

July 2018

IDENTIFICATION OF THE ROLES PLAYED BY IKKε IN HEPATOCELLULAR AND COLORECTAL CARCINOGENESIS

By Uğur Kahya

July 2018

We certify that we have read this thesis and that in our opinion it is fully adequate, in scope and in quality, as a thesis for the degree of Master of Science.

Serkan İsmail Göktuna (Advisor)

Murat Alper Cevher

Aytekin Akyol

Approved for the Graduate School of Engineering and Science:

Ezhan Karaşan

Director of the Graduate School of Engineering and Science

Abstract

IDENTIFICATION OF THE ROLES PLAYED BY IKKε IN HEPATOCELLULAR AND COLORECTAL CARCINOGENESIS

Uğur Kahya

M.S. in Molecular Biology and Genetics

Advisor: Serkan İsmail Göktuna

July, 2018

Hepatocellular carcinomas (HCC) and colorectal carcinomas (CRC) are among the most common cancers worldwide with high mortality rates. While HCC affecting mostly underdeveloped countries, CRC is a disease that mainly occur in more developed countries. As is known, CRC is the third most common cancer and the surgical removal of tumors upon early diagnosis is still the best tool in our hands, developing better strategies to cure patients with an advanced CRC has utmost importance. Furthermore, survival rates of HCC patients are very low as a result of poor prognosis and the most efficient therapy for HCC is organ transplantation. Sorafenib, a multikinase inhibitor, is the most effective chemotherapeutic agent in use for HCC leading drug resistance in HCC cells. Thus, alternative strategies should be developed to extend disease-free survival and to treat this cancer. One of the major risk factor for cancer is chronic inflammation and HCC is a good example of inflammation related cancer due to the fact that 90% of HCC cases are stem from inflammation and hepatic injury. As a result of unresolved chronic inflammation, sequential development of HCC occurs from fibrosis and cirrhosis. Moreover, tumor-associated inflammation can encourage tumor development in the gut, indicating central role for inflammation in the development of both sporadic CRC and CAC.

In this thesis, our aim was to understand the roles played by IKKε in hepatocellular and colorectal carcinogenesis. Our preliminary bioinformatics analysis with publicly available data has shown high amplification of IKKε in HCC patients *in silico*. Also, we showed that IKKε plays important roles in HCC cell proliferation and viability. Specifically, upon IKKε depletion, we observed reductions in HCC cell proliferation both *in vivo* and *in vitro*. Furthermore, increase epithelial markers upon IKKε loss was suggesting reversed EMT process in HEP3B cells. Consequently, IKKε could be a valuable prognostic biomarker and targeting IKKε may be a potential therapeutic strategy against HCC tumors. On the other hand, in CRC, we demonstrated that IKKε depletion conferred a growth advantage to IKKε depleted DLD1 and SW480 cells and resulted in an increased proliferation *in vivo* and *in vitro*, and induced formation of partial-EMT like features in DLD1 cells. Therefore, IKKε complementation may be a valuable potential therapeutic strategy against CRC tumors.

Keywords: HCC, CRC, EMT, IKKε, Inhibitor κB kinase subunit epsilon, metastasis

Özet

HEPATOSELLÜLER VE KOLOREKTAL KARSİNOGENEZDE IKKε'UN OYNADIĞI ROLLERİN BELİRLENMESİ

Uğur Kahya

Moleküler Biyoloji ve Genetik, Yüksek Lisans

Tez danışmanı: Serkan İsmail Göktuna

Temmuz, 2018

Hepatoselüler karsinomlar (HSK) ve kolorektal karsinomlar (KRK), yüksek mortalite oranlarıyla dünya çapında en sık görülen kanserler arasındadır. HSK çoğunlukla azgelişmiş ülkeleri etkilerken, KRK esas olarak daha gelişmiş ülkelerde görülen bir hastalıktır. Bilindiği gibi, KRK en sık görülen üçüncü kanserdir ve tümörlerin erken teşhisi üzerine cerrahi olarak çıkarılması hala elimizdeki en iyi araç olmakla birlikte, ileri KRK'lı hastaları iyileştirmek için daha iyi stratejiler geliştirmek son derece önemlidir. Dahası, HSK hastalarının hayatta kalma oranları, kötü prognoz nedeniyle çok düşüktür ve HSK için en etkili tedavi organ naklidir. Bir multikinaz inhibitörü olan Sorafenib, HSK için kullanılan en etkili kemoterapötik ajandır ancak ilaç direncine neden olmaktadır. Bu nedenle, hastalıksız sağkalımı uzatmak ve bu kanseri tedavi etmek için alternatif stratejiler geliştirilmelidir. Kanser için en önemli risk faktörlerinden biri kronik iltihaptır ve vakaların yaklaşık olarak % 90'ı inflamasyon ve karaciğer hasarından kaynaklanması nedeniyle, HSK enflamasyonla ilişkili kansere iyi bir örnektir. Çözülmemiş kronik inflamasyonun bir sonucu olarak, HSK sıralı bir şekilde fibrozis ve siroz'u takip ederek meydana gelir. Ayrıca, tümörle ilişkili inflamasyon bağırsaktaki tümör gelişimini teşvik edebilir, bu da hem sporadik KRK hem de kolit ilgili KRK gelişiminde inflamasyonun merkezi rolünü gösterir.

Bu tez çalışmasında, IKKε'nin hepatoselüler ve kolorektal karsinogenezde oynadığı rolleri anlamak amaçlanmıştır. Halka açık verilerle yapılan ilk biyoinformatik analizimiz, *in siliko* olarak HSK hastalarında yüksek IKKε amplifikasyonu göstermiştir. Ayrıca çalışmamızda, IKKε'nın HSK hücre proliferasyonu ve canlılığında önemli rol oynadığını gösterdik. Özellikle, IKKε tükenmesi üzerine, hem *in vivo* hem

de *in vitro* olarak HSK hücre çoğalmasında azalma gözlemledik. Ayrıca, IKKε kaybı üzerine epitel markörların artması, HEP3B hücrelerinde tersine çevrilmiş EMT sürecini düşündürdü. Sonuç olarak, IKKε değerli bir prognostik biyobelirteç olabilir ve IKKε'u hedeflemek HSK tümörlerine karşı potansiyel bir tedavi stratejisi olabilir. Diğer taraftan, KRK'da, IKKε tükenmesinin, IKKε susturulmuş DLD1 ve SW480 hücrelerine bir büyüme avantajı sağladığını, bu tükenmenin *in vivo* ve *in vitro* proliferasyon artışı ile sonuçlandığını ve DLD1 hücrelerinde kısmi-EMT benzeri özelliklerin indüklenmesini sağladığını gösterdik. Bu nedenle IKKε tamamlanması, KRK tümörlerine karşı değerli bir potansiyel tedavi stratejisi olabilir.

Anahtar Sözcükler: HSK, Kolon kanseri, EMT, IKKε, inhibitör κB kinaz alt birimi epsilon, metastaz

To my beloved family…

Sevgili Aileme…

Acknowledgements

I would like to express my sincere thanks to my advisor Assist. Prof. Dr. Serkan İsmail Göktuna and Dr. Tieu-Lan Chau for their endless patience, support and guidance that they have shown throughout my Master's studies. Also, I would like to express my gratitude to them for their valuable mentoring, trust and sharing their precious experiences on the field. I have accumulated very beautiful and valuable memories during this time that I will never forget in my life.

I would like to thank Lara Mai Göktuna, the youngest member of Göktuna Laboratory, for her cheerfulness and making us happy whenever she visits

I would like to express my sincere thanks to my colleagues Erta Xhafa and Zeynep Boyacıoğlu, for their friendship and their support during experiments.

Also, I would like to thank my friends Ertuğrul Gazi Yanar, Nevin Belder, Eda Süer and Muhammad Waqas Akbar for their valuable friendship, closeness and support.

I would like to thank Gamze Aykut, who helped in animal experiments, and Ulaş Saçıntı for taking care of animals.

I would like to thank Yavuz Ceylan, who always helped, and laboratory managers Pelin Makas, Seda Şengül Birkan and our technician Abdullah Ünnü.

Also, I would like to express my gratitude to Dr. Davide Monteferrario for his mentoring, trust and brotherhood in the past. In a very short time, I have accumulated very valuable and unforgettable memories.

I would like to extend my gratitude to TÜBİTAK and its valuable employees for supporting me financially during my graduate studies.

I also would like to express my endless gratitude to my valuable companion Ayşe Sedef Köseer, whom I met during my master’s, who has a very important place and special meaning for me, for her unconditional support, motivation and time.

And finally, I would like to express my utmost respect and gratitude to my mother Gülay Güler and my father Şenol Kahya, who are the best mother and father in the world, for their endless support, sacrifice, patience and all the goodness they have shown me.

The studies in this thesis was supported by TÜBİTAK project number: 116Z349

Teşekkürler

Tez danışmanım Yrd. Doç. Dr. Serkan İsmail Göktuna'ya, Yüksek Lisans çalışmalarım boyunca bana göstermiş olduğu sabır, destek ve benim için oldukça değerli olan rehberliği nedeniyle en içten teşekkürlerimi sunarım. Ayrıca, Yrd. Doç. Dr. Göktuna ve Dr. Tieu-Lan Chau'ya, bana tüm hayatım boyunca yön verip, yol gösterecek oldukça değerli deneyimlerini paylaştıkları ve kendileriyle çalışma imkanı verdikleri için minnettarlığımı sunarım. Kendileriyle geçirdiğim üç sene boyunca hayatım boyunca unutamayacağım çok güzel ve değerli anılar biriktirdim.

Bana karşı göstermiş olduğu sabır, anlayış, ve hoşgörü için, bıkmadan usanmadan defalarca bilimsel doğruları gösterdiği, tüm bilgi birikimini koşulsuz şartsız aktardığı, ve her zaman motive edici önderliği için Tieu-Lan Chau'ya,

Sık sık laboratuvarımızı ziyaret edip bizi neşelendirdiği ve mutlu ettiği için grubumuzun en küçük üyesi Lara Mai Göktuna'ya,

Gösterdikleri arkadaşlık ve deneyler sırasındaki destek ve yardımlarından dolayı çalışma arkadaşlarım Erta Xhafa ve Zeynep Boyacıoğlu'na,

Göstermiş oldukları cana yakınlık ve destekleri için arkadaşlarım Ertuğrul Gazi Yanar, Nevin Belder, Eda Süer ve Muhammad Waqas Akbar'a,

Hayvan deneylerinde yardımcı olan veteriner hekim Gamze Aykut ve hayvanların bakımını yapan Ulaş Saçıntı'ya,

Laboratuvarımızda ihtiyaç duyduğumuz her an yanımızda olan Yavuz Ceylan'a, laboratuvar sorumlularımız Pelin Makas, Seda Şengül Birkan'a ve teknisyenimiz Abdullah Ünnü'ye,

Bana bu alandaki ilk yurtdışı tecrübemde koşulsuz destek olup, hem bilimsel hem hayat ile ilgili tecrübelerini aktaran, adeta abilik yapan Dr. Davide Monteferrario'ya,

Yüksek lisans eğitimim süresince beni finansal olarak destekleyen TÜBİTAK ve kıymetli çalışanlarına,

Teşekkürlerimi sunarım.

Ayrıca, yüksek lisans eğitimim sırasında tanıştığım ancak benim için çok önemli bir yere ve anlama sahip olan, koşulsuz şartsız destekçim, motivasyon kaynağım ve en umutsuz olduğum anlarda umut aşılayan çok değerli yoldaşım Ayşe Sedef Köseer'e

Ve son olarak, hayatımın her alanında destek olan, dünyanın en iyi, en fedakar, en şefkatli anne ve babası olan annem Gülay Güler ve babam Şenol Kahya'ya bana göstermiş oldukları sonsuz destek, fedakarlık, sabır, ve tüm iyilikler için,

Sonsuz saygı, minnet ve şükranlarımı sunarım.

Bu tez dahilindeki çalışmalar TÜBİTAK 116Z349 numaralı proje ile desteklenmiştir.

Table of Contents

Abstract iii

Özet v

Acknowledgements viii

Teşekkürler ix

Table of Contents xi

List of Figures xv

List of Tables xvii

Abbreviations xviii

Chapter 1 1

Introduction 1

1.1 Liver cancer 1

1.1.1 Hepatocellular carcinoma 3

1.1.1.1 Epidemiology of HCC 4

1.1.1.2 Major causes of HCC 5

1.1.1.3 Early molecular changes and driver pathways in Hepatocellular carcinogenesis 6

1.1.1.4 Microenvironment in HCC 8

1.2 Colorectal cancer 8

1.2.1 Risk factors 9

1.2.2 Epidemiology of CRC 10

1.2.3 Genetics of CRC 11

1.3 Inflammation and Cancer 13

1.4 The roles of IKKε in cancer and immunity 14

Chapter 2 17

Aim of the study 17

Chapter 3 19

Materials and Methods 19
3.1 Materials 19
3.1.1 General Laboratory Reagents and Chemicals 19
3.1.2 Cell culture reagents and chemicals 22
3.1.3 Antibodies 24
3.1.4 Nucleic Acids 26
3.1.5 Primers 30
3.1.6 Equipment 32
3.2 Media and Solutions 33
3.2.1 General Laboratory Solutions 33
3.2.2 Cell Culture Media and Solutions 35
3.3 Methods 36
3.3.1 Maintenance of human cell lines 36
3.3.2 siRNA transfection of human cell lines 37
3.3.3 shRNA transfection of human cell lines 38
3.3.4 *In vitro* wound healing assay 39
3.3.5 Determination of cell proliferation by using Cell Titer Glo reagent 39
3.3.6 Determination of cell proliferation by using Real Time Cell Analyzer ... 39
3.3.7 Determination of cell migration by using Real Time Cell Analyzer 40
3.3.8 Determination of cell invasion by using Real Time Cell Analyzer 40
3.3.9 Colony formation assays 41
3.3.10 RNA Isolation from human cell lines and quality determination 42
3.3.11 cDNA synthesis from isolated RNAs 42
3.3.12 qPCR and analyses of gene expression 42
3.3.13 Total protein isolation and quantification 43
3.3.14 SDS-PAGE 45
3.3.15 Western blot 46

3.3.16 Preparation of competent *Escherichia coli* DH5α 46

3.3.17 Bacterial transformation..47

3.3.18 Plasmid isolation and sequencing 47

3.3.19 Design and annealing of synthetic guide RNAs 47

3.3.20 Restriction of LentiCRISPRv2 plasmid and insertion of sgRNAs 48

3.3.21 Flow Cytometry analyses of EdU staining 49

3.3.22 Creation of *in vivo* tumor xenograft models 49

3.3.23 Creation of *in vivo* tumor metastasis models 50

3.3.24 Statistical Analyses 50

Chapter 4 51

Results 51

4.1 Analysis of IKKε expression in cell lines and patient materials *in silico*....51

4.2 Endogenous IKKε expression levels in HCC and CRC cell lines 54

4.3 The role of IKKε in HCC cell viability...55

4.4 The role of IKKε in HCC cell proliferation 58

4.5 The role of IKKε in HCC cell migration 59

4.6 The role of IKKε in epithelial-to-mesenchymal transition of HEP3B cells 62

4.7 The effect of IKKε loss in HEP3B xenograft growth *in vivo*. 64

4.8 The effects of IKKε loss in CRC cell proliferation and anchorage independent growth of CRC cells...65

4.9 The role of IKKε in CRC cell migration...68

4.10 The role of IKKε in epithelial-to-mesenchymal transition of CRC cells 70

4.11 The effect of IKKε loss in SW480 xenograft growth *in vivo*. 73

Chapter 5 74

Discussion 74

Chapter 6 79

Conclusion and Future perspectives 79

Bibliography **81**

Appendix **88**

Copyright Permissions 89

List of Figures

Figure 1.1. Age standardized incidence rates of liver cancer by sex and location. 1

Figure 1.2. Classification of malignant neoplasms of the liver. 2

Figure 1.3. BCLC classification system and treatment choices for hepatocellular carcinoma. 4

Figure 1.4. Major causes of hepatocellular carcinoma. 5

Figure 1.5. Mechanisms of HCC progression and related genes. 7

Figure 1.6. Age standardized incidence rates of colorectal cancer by sex and location. 9

Figure 1.7. Progression of normal colon to CRC.. 12

Figure 4.1. Gene Expression data for IKKε extracted from Cancer Cell Line Encyclopedia by using Gene-centric RMA-normalized mRNA expression data. 51

Figure 4.2. IKKε amplification in cBioPortal TCGA patient cancer tissues. 52

Figure 4.3. Kaplan Meier survival curves representing a gender or stage specific effects of IKKε expression in HCC patient prognosis.. 53

Figure 4.4. Measuring endogenous IKKε expression levels in HCC cell lines via western blot. 54

Figure 4.5. Measuring endogenous IKKε expression levels in CRC cell lines via western blot. 55

Figure 4.6. *In vitro* end-point viability assay in IKKε depleted HEP3B, PLC/PRF/5, SNU182, SNU387 and SNU423 cell lines.. 57

Figure 4.7. Copy number data for IKKε and TLR3 extracted from Cancer Cell Line Encyclopedia by using normalized copy number data. 57

Figure 4.8. *In vitro* real time cell proliferation assay in IKKε depleted HEP3B cells.. 58

Figure 4.9. The effect of siRNA mediated transient IKKε depletion in HCC cell migration via *in vitro* wound healing assay. 60

Figure 4.10. The effect of shRNA mediated stable IKKε depletion in HCC cell migration via *in vitro* wound healing assay. 61

Figure 4.11. The effect of IKKε depletion in epithelial-to-mesenchymal transition in HEP3B cells. 63

Figure 4.12. The effect of IKKε loss in tumorigenicity of HEP3B cells *in vivo*. 65

Figure 4.13. *In vitro* real end-point and real time cell proliferation assay in IKKε depleted DLD1 and SW480 cells.. 66

Figure 4.14. The effects of IKKε depletion in viability and anchorage independent growth of DLD1 cells.. 67

Figure 4.15. The effects of IKKε loss in SW480 colony formation. 68

Figure 4.16. The effect of shRNA mediated IKKε depletion in DLD1 cell migration via *in vitro* wound healing and RTCA migration assays. 69

Figure 4.17. The effect of CRISPR/Cas9 mediated IKKε depletion in SW480 cell migration via *in vitro* wound healing assay. 70

Figure 4.18. Expression of EMT markers upon IKKε depletion in DLD1 cell line. ...71

Figure 4.19. Expression of EMT markers upon IKKε depletion in SW480 cell line. .72

Figure 4.20. The effect of IKKε loss in SW480 xenograft growth *in vivo*. 73

List of Tables

Table 3.1. Routinely used reagents, chemicals, enzymes, and kits for general laboratory purposes 19

Table 3.2. Routinely used Media, reagents, chemicals for cell culture experiments...23

Table 3.3. Used Antibodies...25

Table 3.4. List and sequences of nucleic acids that are used for gene editing............27

Table 3.5. Used Primers..30

Table 3.6. Used equipment for the experiments 33

Table 3.7. Routinely used buffers and solutions...34

Table 3.8. Cell lines and their growth media 35

Table 3.9. qPCR protocol..43

Table 3.10. Preparation of BSA dilutions..44

Table 3.11. Components and composition of separating and stacking gels 45

Abbreviations

AKT	Akt Serine/Threonine Kinase
APC	Adenomatous Polyposis Coli
BCLC	Barcelona Clinic Liver Cancer
BSA	Bovine Serum Albumin
CAC	Colitis Associated Cancer
Cas9	CRISPR Associated Protein 9
CC	Cholangiocarcinoma
CCLE	Cancer Cell Line Encyclopedia
CIP	Calf İntestinal Phosphatase
CIS	Chromosomal İnstability Syndrome
CK2α	Casein Kinase 2a
CRC	Colorectal Carcinoma
CRISPR	Clustered Regularly Interspaced Short Palindromic Repeats
CTNNB1	Catenin (Cadherin-Associated Protein), Beta 1
PBS	Phospho Buffer Saline
EDTA	Ethylenediaminetetraacetic Acid
EGFR	Epidermal Growth Factor Receptor
EMT	Epithelial-To-Mesenchymal Transition
FAP	Familial Adenomatous Polyposis
FBS	Fetal Bovine Serum
GFP	Green Fluorescence Protein

HBV	Hepatitis B Virus
HCC	Hepatocellular Carcinoma
HCV	Hepatitis C Virus
HGDN	High Grade Dysplastic Nodules
HSK	Hepatosellüler Karsinom
IBD	Inflammatory Bowel Disease
IκB	Inhibitor Of Nuclear Factor Kappa B
IKKα	Inhibitor Of Nuclear Factor Kappa B Kinase Subunit Alpha
IKKβ	Inhibitor Of Nuclear Factor Kappa B Kinase Subunit Beta
IKKε	Inhibitor Of Nuclear Factor Kappa B Kinase Subunit Epsilon
IRF3	Interferon Regulatory Factor 3
IRF7	Interferon Regulatory Factor 7
LGDN	Low Grade Dysplastic Nodules
LOH	Loss Of Heterozygosity
LPS	Lipopolysaccharide
MAPK	Mitogen-Activated Protein Kinase
MSI	Micsosatellite İnstability
mTOR	Mechanistic Target Of Rapamycin Kinase
NAFLD	Non-Alcoholic Fatty Liver Diseae
NASH	Non-Alcoholic Steatohepatitis
NF-κB	Nuclear Factor Kappa B
NOC	N-Nitroso Compounds

qRT-PCR	Quantitative Real Time Polymerase Chain Reaction
RB	Retinoblastoma
ROS	Reactive Oxygen Species
RTCA	Real Time Cell Analysis
SBA	Secondary Bile Acids
SDS	Sodium Dodecyl Sulfate
Ser	Serine
sgRNA	Synthetic Guide RNA
shRNA	Short Hairpin RNA
siRNA	Small İnterfering RNA
STAT	Signal Transducer And Activator Of Transcription Protein
TAE	Tris Acetate-Edta
TANK	Traf Family Member Associated Nfkb Activator
TBK1	Tank Binding Kinase 1
TCGA	The Cancer Genome Atlas
TCR	T Cell Receptor Signaling
Th17	T Helper 17 Cell
Thr	Threonine
TLR	Toll Like Receptor

Chapter 1

Introduction

1.1 Liver cancer

Liver cancer is the sixth most common cancer worldwide with 800.000 new cases diagnosed per year [1]. However, it is the second leading cause of the cancer related deaths worldwide due to very high mortality rates associated with this disease (e.g., 5-year life-expectance after diagnosis is only 5-10%) [2]. Liver cancer related deaths show a great geographical disparity and liver cancer incidence and mortality rates are much higher in under-developed locations most probably due to infectious causes,

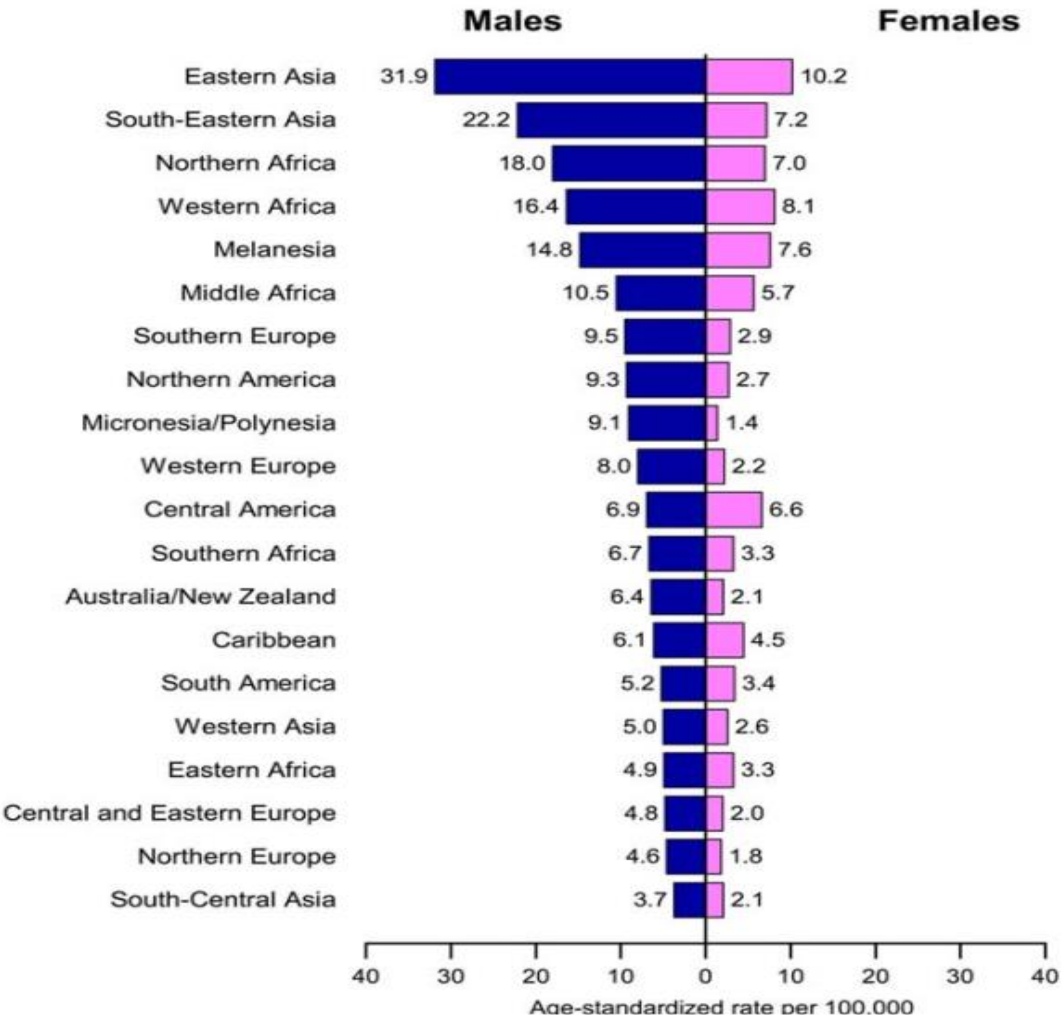

Figure 1.1. Age standardized incidence rates of liver cancer by sex and location. (Reprinted with the permission from Ref. [1], John Wiley and Sons)

improper of sanitary conditions and inadequate access to medical services (Figure 1.1) [1, 3]. Moreover, liver cancer incidence is more common in men compared to women in spite of the geographical location (Figure 1.1) cause of which is not fully understood yet [1, 2].

Malignant liver neoplasms can be classified as primary or secondary according to the site of origin of the tumor cells (Figure 1.2). 95% of the hepatic malignancies are of secondary neoplasms originated from elsewhere in the body and these kind of malignancies are the indicator of the systemic spread [3]. Hepatocellular carcinomas (HCCs) and cholangiocarcinoma (CC) and are the most common primary malignant neoplasms of the liver. While HCCs usually develop from hepatocytes in cirrhotic livers and constitute 70 to 90% of primary liver cancers [4-7] CCs are originated from inflamed intrahepatic or extrahepatic bile ducts [3, 4, 6, 7]. Although CC is less frequently observed worldwide, its occurrence is quite high in some parts of Asia due to the high prevalence of *Clonorchis sinensis* and *Opisthorcis viverrini* infections, so-called liver flukes [4, 6, 7]. Since HCC can better model inflammation driven liver carcinogenesis, in the following parts we will only get further insights about this cancer.

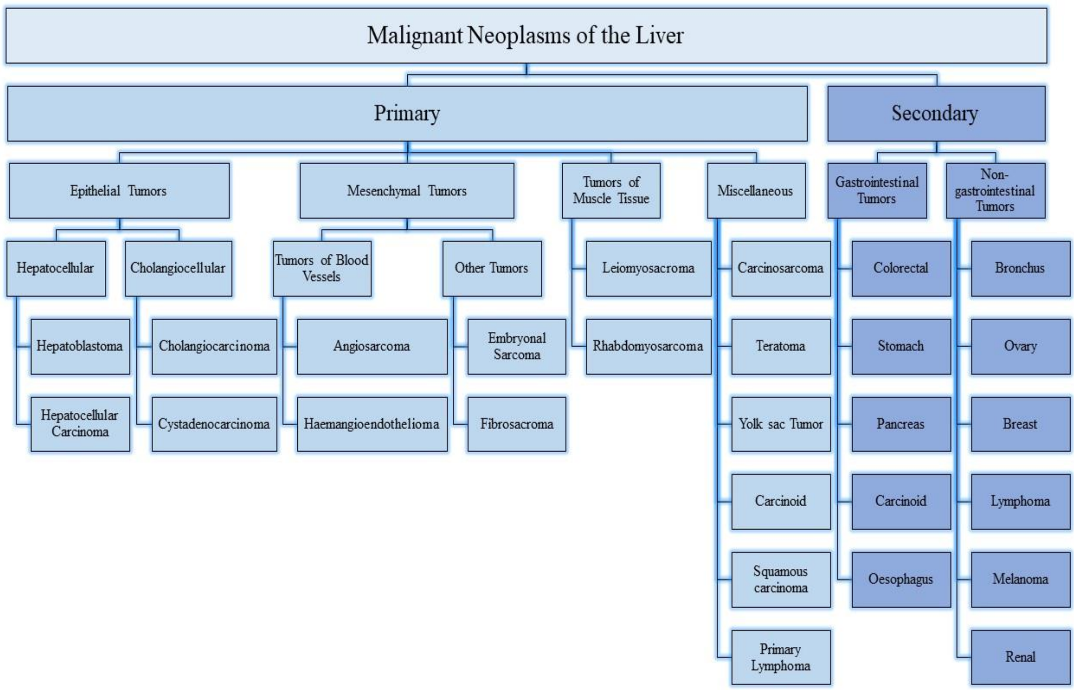

Figure 1.2. Classification of malignant neoplasms of the liver. (Adopted from the Ref. [4] with the permission of Elsevier)

1.1.1 Hepatocellular carcinoma

As we mentioned earlier, hepatocellular carcinoma (HCC) is the 6th most common cancer and the second most frequent reason for cancer-related deaths worldwide with over 600.000 casualties every year [1, 3]. This is partially due to very bad prognosis of HCC patients, survival rates of whom range between 6 to 20 months after diagnosis [8, 9]. The most effective therapeutic option for HCC is organ transplantation since standard chemo- and radiotherapies, effective for other cancers, rather lead to drug resistance or compensatory proliferation in HCC due to high regenerative potential of hepatocytes [5]. Currently, HCC tumor cells gain resistance against sorafenib, the most effective chemotherapeutic agent in use for HCC at the moment. Still sorafenib treatment marginally improves the advanced/metastatic HCC patient prognosis by only 3 months. Thus, strategies to treat this cancer or to extend disease-free survival of the patients are urgently needed [8, 10].

Among the primary causes of HCC, infections caused by hepatitis B virus (HBV) and hepatitis C viruses (HCV) together with the aflatoxin and alcohol exposure can be counted [11-14]. Moreover, it is also reported that adeno-associated virus 2 infection can cause HCC without preceding cirrhosis [15]. Although HCC is a deadly disease, primary prevention is possible via HBV vaccination, lifestyle changes, and chemoprevention [1, 9, 11, 13]. For HCC patients, there are several treatment options such as transplantation, systemic therapies and liver resection. Barcelona Clinic Liver Cancer (BCLC) system is used to classify HCC (Figure 1.3) instead of TNM system (tumor, lymph nodes and metastasis) which is used for the staging most of the malignant tumors except HCC [12].

There are two molecular subclasses of HCC, proliferative and non-proliferative classes, identified based on genomic studies [6-8]. Proliferative class identified in detail via the advancement of cell proliferation and cell cycle progression related signals resulting more aggressive HCC incidence [6-9] whereas non-proliferative class protects normal like molecular peculiarities of hepatic physiology [9]. Main characteristics of proliferative class are the activation of pathways related to cell survival and proliferation which leads to more aggressive phenotype, less differentiation (e.g., increase in α-fetoprotein) and poor prognosis. Some proliferative or pro-survival pathways like AKT/mTOR, TGFβ, IGF, RAS/MAPK are activated at varying levels in HBV-driven hepatocellular carcinogenesis [7, 10-14]. Non-proliferative class of HCC is generally influenced by the WNT/β-catenin activation as well as by the immune response. Additionally, significant enrichment of classical WNT signaling as well as *GLUL* and *LGR5*, well-known targets of WNT, has been detected in non-proliferative class [12, 14]. As well as alterations in the WNT/β-catenin pathway, extensive increase in chromosome 7 causing overexpression of EGFR in men due to transposon activity is also observed in some of the tumors in this subclass [15].

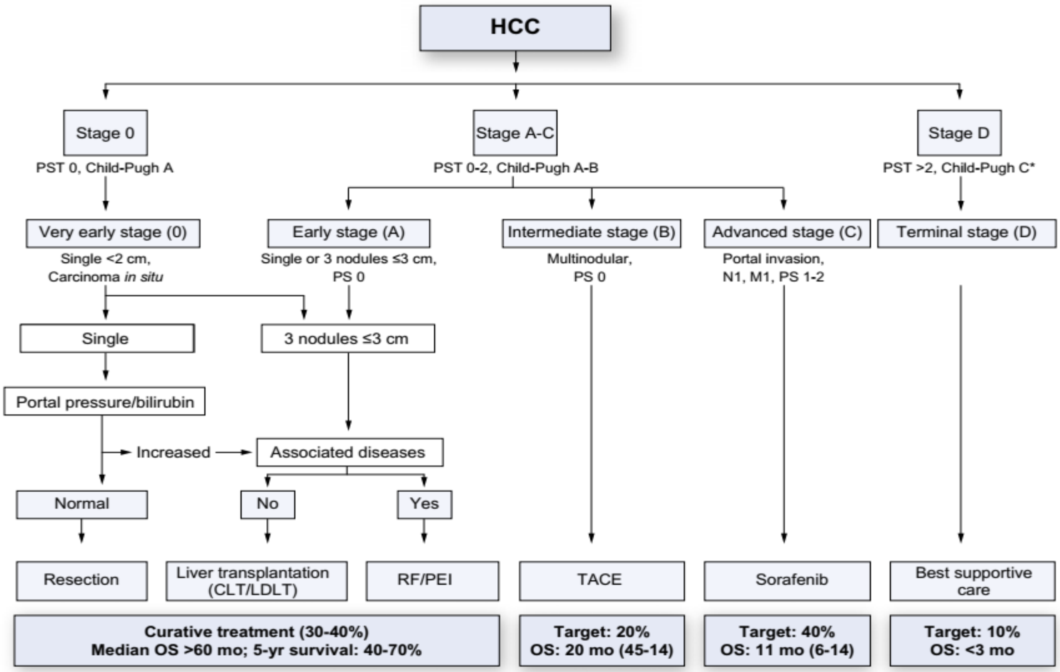

Figure 1.3. BCLC classification system and treatment choices for hepatocellular carcinoma. (Reprinted with the permission from Ref [16], Elsevier),

1.1.1.1 Epidemiology of HCC

As we mentioned earlier, HCC incidences around the world are not uniformly distributed according to geological locations or populations [1, 17]. There is a strong correlation between chronic viral infections driven hepatitis and HCC incidence [18]. While HBV is a DNA virus provoking insertional mutagenesis leading to cirrhosis and chronic HBV infections-related HCC are more common in sub-Saharan Africa and in Asia, HCV is a RNA virus and responsible for the HCC incidences occurred in Europe, Japan, and North America [1, 17-19]. Moreover, aflatoxin B1 exposure is another main cause of HCC together with HBV infections in Africa [20]. Additionally, HCC prevalence in men compared to women is more common worldwide independent of populations or geographical distribution (Figure 1.1) [1, 3]. This phenomenon may be due to the tendency of men to consume more alcohol and cigarettes than women. Besides, high HBV and HCV infection can be influenced by androgenic hormones as well, which put the men at higher risk of developing hepatitis and HCC [17].

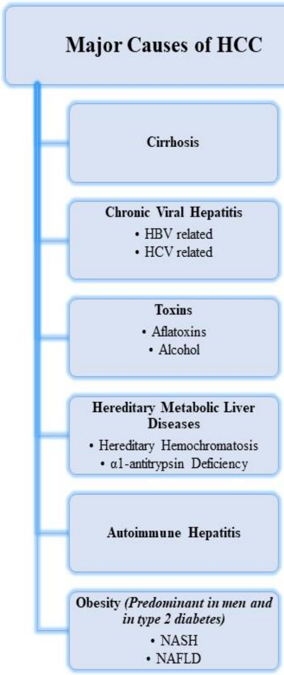

Figure 1.4. Major causes of hepatocellular carcinoma. (Adopted from the Ref. [4] with the permission of Elsevier)

1.1.1.2 Major causes of HCC

There are several causes, namely cirrhosis, viral infections, liver toxins, hereditary or autoimmune diseases and obesity, associated with the risk of HCC development (Figure 1.4). About 80% of HCC patients are suffering from the cirrhosis, which makes cirrhosis the primary cause of HCC development [17, 21]. Cirrhosis is developed after long term chronic liver disease (hepatitis) and associated with reduced hepatocyte proliferation which is a sign of diminished hepatic regenerative capacity [22, 23]. It is well-known that chronic HBV infections are the main risk factor for HCC in which some patients might establish HCC even in the absence of preceding history of cirrhosis [24-26]. Except from viral infection-driven or aflatoxin-driven cirrhosis, there are also other causes which may support the development of HCC. These factors are mainly affecting the people in the Western countries. The other factors that may cause HCC development include obesity, type 2 diabetes, heavy alcohol consumption, and smoking. Especially, obesity or type 2 diabetes significantly increase the likelihood of developing nonalcoholic steatohepatitis (NASH) or nonalcoholic fatty liver disease (NAFLD), which may turn into cirrhosis or HCC later on [17, 27, 28].

1.1.1.3 Early molecular changes and driver pathways in Hepatocellular carcinogenesis

Malignant transformation of cirrhosis into HCC is a multi-stage process (Figure 1.5) where low-grade dysplastic nodules (LGDNs) are developed due to surrounding of damaged cells such as stem cells, progenitor cells, and mature hepatocytes by fibrosis [9]. Inactivating mutations in the gene coding the telomerase reverse transcriptase (*TERT)* malfunction of which cause cell senescence and apoptosis due to the shortened telomeres are responsible for the elevated risk of cirrhosis [29, 30]. As a result, maintenance of telomeres is crucial for the initiation and advancement of HCC [31, 32]. Although telomerase expression is not usually seen in normal hepatocytes, reactivation of it is needed for both rampant proliferation of hepatic tumor cells and the promotion of hepatocellular carcinogenesis[22]. Reactivation of telomerase occurs in LGDNs due to point mutations affecting *TERT* promoter [9, 17, 33]. As a result, cirrhotic liver cells skip senescence and proceed further to early HCC by following high-grade dysplastic nodules (HGDNs). Consequently, this sequence of changes results in the formation of advanced HCC were telomerase still active and stable [9, 17, 33].

Through induction of chronic inflammation, HCV and HBV viral infections shape the initial molecular changes contributing malignant transformation (Figure 1.5). HBV caused insertion of viral DNA to the *TERT* promoter in hepatocytes leading activation of telomerase [29, 30]. Furthermore HBV may also trigger the activation of oncogenes such as *MLL4*, *CCNE1*, *SENP5* in hepatocytes [30, 34, 35]. Finally, together with HBV infection, aflatoxin exposure triggers formation of DNA adducts especially in tumor suppressor genes like *TP53* [20].

Different somatic mutations in malignant neoplasms result in the formation of unique HCC genomes [17]. Among the pathways involved in progression of HCC (Figure 1.5), maintenance of telomeres is the primary factor in which telomerase is overexpressed in 90% of HCC cases [36]. Moreover, WNT activating *CTNNB1* mutations are among the most frequent cause of highly transformed tumors in patients without HBV infection [36]. In addition to *CTNNB1* mutations, mutations in *AXIN1*, *APC*, and *ZNRF3* genes may also lead to activation of WNT/β-catenin pathway in HCC [9, 33]. Also in HCC patients with aflatoxin exposure, *TP53* as well as the *RB1* and *CDKN2A* genes are found to be inactivated via mutations causing alteration of the cell cycle and resulting in a poor prognosis [37, 38]. RAS-RAF-MAPK and PI3K-AKT-mTOR pathways are also activated in nearly 10% of HCC due to the amplification of the locus containing *FGF3*, *FGF4*, and *FGF19* genes. Furthermore, PI3K-AKT-mTOR signaling may be activated via the mutations resulting in inactivation of *TSC1* and *PTEN* tumor suppressor genes. On the other hand, RAS-RAF-MAPK may also be activated by the inactivation of RSK2 protein [38, 39]. Another altered driver mechanism in HCC progression is the chromatin remodeling complex. Besides inactivating mutations of *ARID1A* and *ARID2* genes which have tumor suppressor function in BAF and PBAF chromatin complexes together with *SETDB1* overexpression accompanies poor prognosis as well as cancer cell growth through *TP53* methylation [37, 40-42].

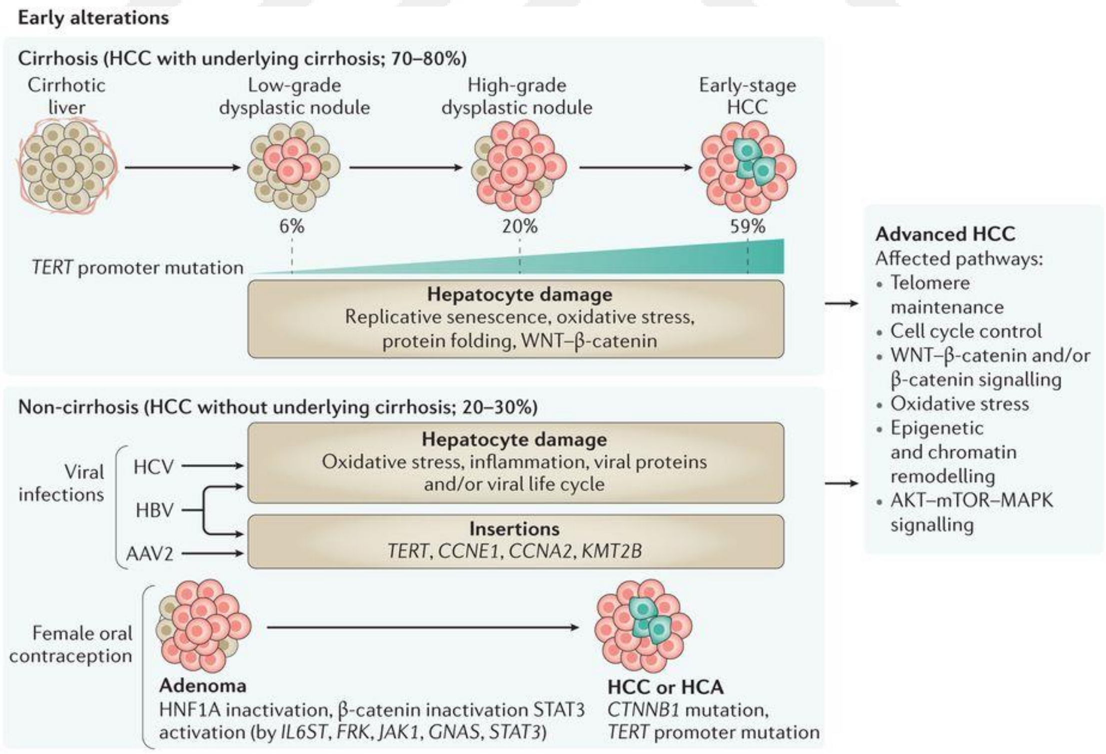

Figure 1.5. Mechanisms of HCC progression and related genes. (Reprinted with the permission from Ref [33], MacMillan Publishers Limited)

1.1.1.4 Microenvironment in HCC

A changed microenvironment is now thought to be a key activating feature of cancer, and it is known that it participates in all stages of malignant progression from the first transitional stages to the invasion and metastasis.[43, 44]. HCC is a prototypical example of inflammation related cancer. About 90% of the HCC burden associated with long-standing hepatitis, indicating important role of microenvironment in the pathogenesis of this disease [45]. Activation of EGF, IL-6, NF-κB signaling is found in liver parenchyma whose destruction is associated with fibrosis and cirrhosis but not in tumors [45]. Furthermore, Tumor growth in certain mouse models (e.g., IKKβ(EE)^{Hep} mice [46]) is promoted by the interactions of multiple cell types (e.g., lymphocytes, stellate cells, and macrophages) with hepatocytes in chronically inflamed liver [45, 46]. Macrophages in chronic inflammatory hepatic infiltrate release TNF and make hepatocytes more impervious to apoptosis and hence promotes carcinogenesis [47]. Moreover, JAK-STAT and NF-κB signaling pathways are induced by inflammatory cytokines in chronically inflamed liver and cause further promotion of HCC [45, 47-49]. Hence, inflammation of the liver is a key mechanism in HCC development [45]. Hepatic stellate cells are originated from liver sinusoids are responsible for maintenance of hepatic homeostasis [45, 50]. Due to their intermediary role in cirrhosis and fibrosis after the liver injury, it is thought that detection of stellate gene expression signature in HCC is an indication of poor prognosis [45, 50]. Thus, fibrosis and cirrhosis can be thought as a causes of HCC.

1.2 Colorectal cancer

Colorectal cancer is the third most common cancer and the fourth leading cause of cancer related deaths [1]. Unlike liver cancer, CRC is almost equally prevalent in men and women [51]. As of 2012, more than 1 million CRC cases had been diagnosed annually, about half of which will succumb to death later on during the disease development [1]. In contrast to liver cancer, which was affecting mostly underdeveloped countries, CRC is a disease that mainly occur in developed countries such as USA, Australia, and Western Europe (Figure 1.6) [1, 51]. As the number of CRC cases increase, mortality rates decrease due to improvements in diagnostic tools, colorectal cancer screening and treatment options [1]. Early diagnosis of CRC is crucial, like other cancers, to improve the survival chances of the patients [1, 51].

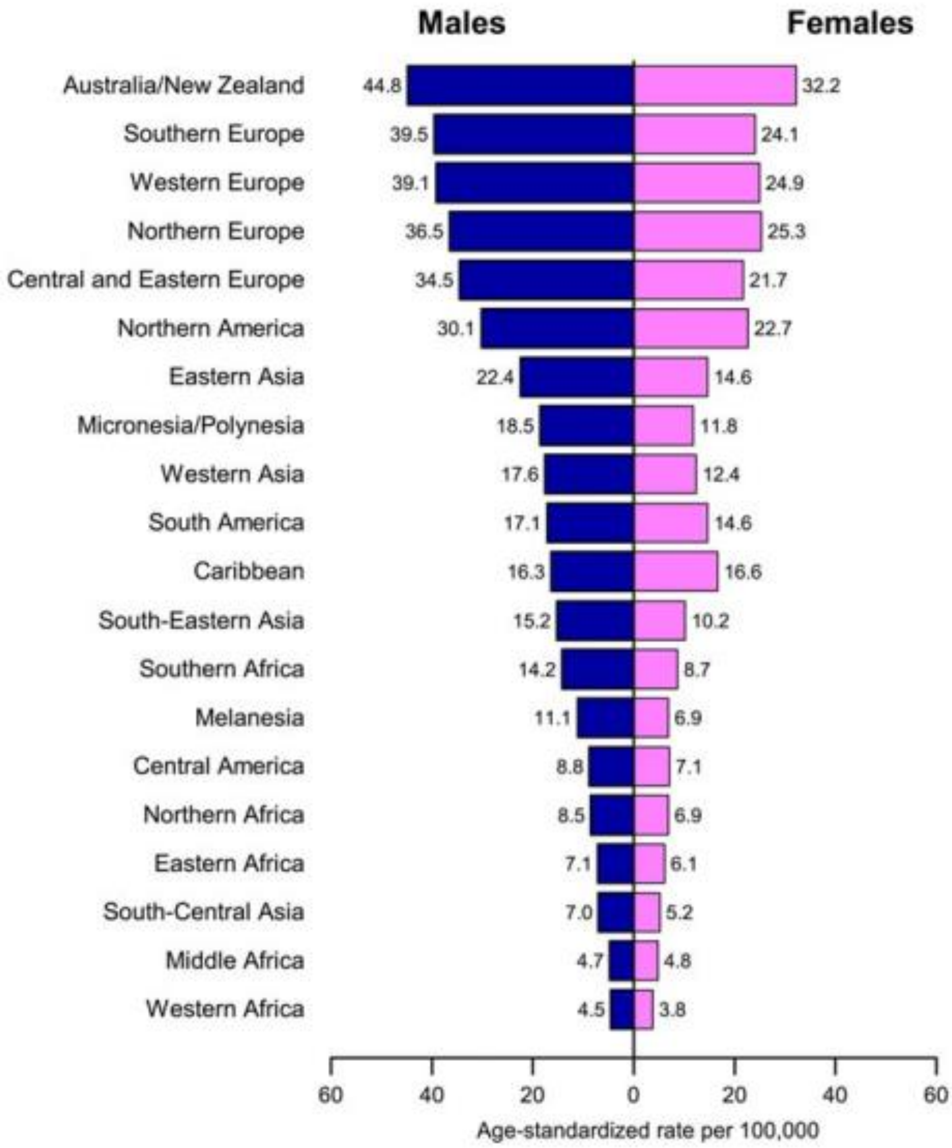

Figure 1.6. Age standardized incidence rates of colorectal cancer by sex and location. (Reprinted with the permission from Ref. [1], John Wiley and Sons)

1.2.1 Risk factors

Risk factors can be classified as environmental risk factors and hereditary (genetic) factors [51]. Environmental risk factors can be grouped as nutritional factors, obesity and physical activity, tobacco and alcohol consumption [51-54]. Tobacco, alcohol and processed-meat consumption increases the CRC development risk not only through their carcinogen constituents but also through supporting inflammation within intestinal epithelia [55, 56].

Eating habits also affect the CRC risk. Western diet, rich in fats, is one of the most important risk factor for CRC development. Fat rich diet favors the growth of a microflora that produces phenols, ammonia, and hydrogen sulfide, all of which may have varying effects in cytotoxicity, mutability and induction of chronic inflammation in the intestines [21, 51, 56]. For example, upon absorption, ammonia has to be metabolized in colonocytes to prevent its cytotoxic effects. However, its metabolites such as nitric oxides (N-nitroso compounds (NOC)) [56]. NOC formed from nitrosamines and nitrosamides can cause formation of DNA adducts resulting in mutations in tumor suppressor and oncogenes [56]. Moreover, lithocholic acid and deoxycholic acids are well-known secondary bile acids (SBA) and their fecal concentrations found to be high in people with increased risk of CRC development [21, 51, 57]. SBA found to alter the proliferation of intestinal epithelial cells through increased mutability of tumor cells, hence, it was suggested that SBA might have role in the initiation and progression of CRC [21, 56]. [21, 56]. Mechanistically, SBA-induced tumorigenicity is due to ROS formation and resulting genomic instability in intestinal epithelia. [57]. On the other hand, calcium, multivitamins, dietary fiber, tea and coffee consumption is correlated with reduced CRC risk [51, 57].

High body mass index and low physical activity are associated with higher risk of CRC [21, 51, 57]. However, increased physical activity may lower CRC development risk through enhancing metabolic rate, gut motility and oxygen uptake and reducing insulin resistance and blood pressure [21, 51, 57].

1.2.2 Epidemiology of CRC

Although CRC incidence rates are high in North America, Australia, and Europe, incidence rates in South-Central Asia and Africa are relatively low showing a trends as countries with high-income has the highest risk of developing CRC due to their westernized eating habits [1, 3]. However, with the developments in CRC screening methods and improved therapies, CRC mortality rates were decreased in most of the countries [58, 59]. Despite reduction of CRC mortality rates, some East European and South American countries demonstrated increased CRC incidence and mortality [27, 60].

1.2.3 Genetics of CRC

Most of the CRC cases are sporadic in origin and the rest are either hereditary or related to IBD [61]. Hereditary colorectal cancers are very important for the understanding of cancer development [21]. Hereditary colorectal cancer constitute Peutz-Jeghers syndrome, serrated polyposis and juvenile polyposis, familial adenomatous polyposis (FAP) and hereditary nonpolyposis colorectal cancer (HNPCC) also known as lynch syndrome [21, 51]. Mutation in tumor suppressor *APC* gene, controlling the WNT/β-catenin signaling, results in familial adenomatous polyposis (FAP) development [62]. Individuals with FAP disease (who have inherited a deleterious APC allele) may lose the second allele through loss of heterozygosity (LOH) very early in their life and develop numerous adenomatous polyps which usually turn to adenocarcinomas later on [62]. Mutation in DNA mismatch repair genes such as; *MSH2, MSH6, EPCAM, PMS2,* and *MLH1* associated to lynch syndrome [62, 63]. Due to problems in mismatch repair, accumulation of DNA mutations results in microsatellite instability (MSI) [62, 63]. Individuals with HNPCC develops fewer adenomas [63].

Genetics of colorectal carcinogenesis follow a multistep model in which multiple mutations in oncogenes and tumor suppressor genes occur in stepwise manner [64, 65]. At the bottom of crypts, stem cells generates large number of colonocytes in which have had the risk of accumulation of mutations [23, 66]. After production of colonocytes, these cells move towards the colonic lumen from crypt bottom [23, 66]. Despite production of large number of colonocytes at crypt bottom, proliferation rate in colonic mucosa kept constant due to balance between activity of proto-oncogenes and tumor suppressor genes which fine tunes proliferation and cell death [57]. Mismatch repair, nucleotide excision, base excision and double strand break repair systems efficiently scan genome to detect faulty nucleotides and repair them [57]. If replication errors identified by DNA repair systems, cell cycle delayed or arrested in G1 phase by tumor suppressor genes for the maintenance of faulty regions [67, 68]. When mutations are hard to repair or too broad, cells may undergo apoptosis [69].

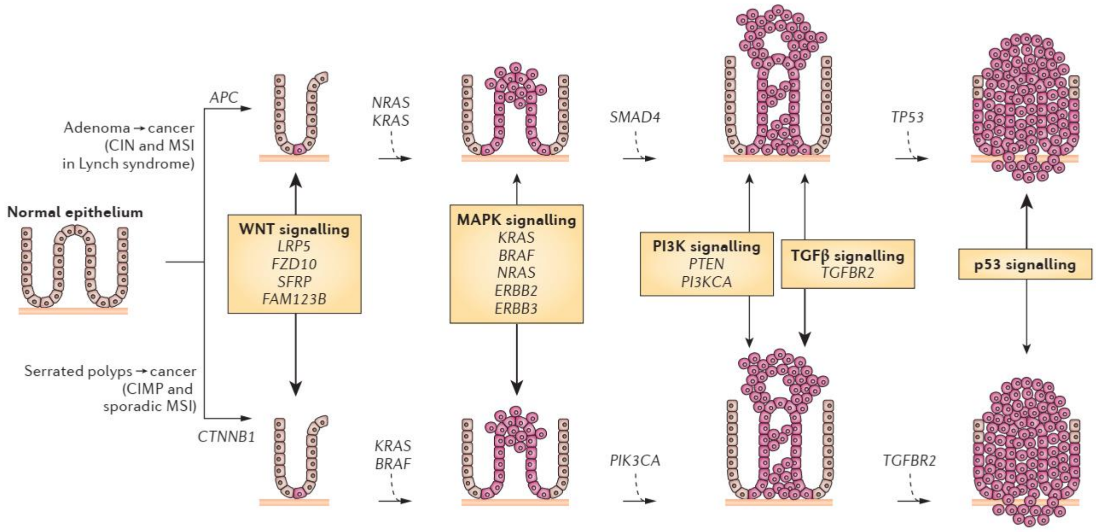

Figure 1.7. Progression of normal colon to CRC. Top pathway results in formation of adenocarcinomas from tubular adenomas whereas bottom pathway results in formation of serrated CRC from serrated adenomas. (Reprinted with the permission from Ref [21], MacMillan Publishers Limited)

In the canonical model of CRC formation, cancers emerge from polyps and progress to early adenoma which later turn to progressed adenoma and finally they advance into adenocarcinoma. There are two well characterized pathways, namely chromosome instability pathway (CIS) and microsatellite instability pathway (MSI), for CRC development (Figure 1.7) [21, 57].

CIS-driven CRC development pathway is marked with the aggregation of mutations in the genes playing roles in cell cycle, apoptosis and intercellular signaling such as *APC*, *KRAS* and *TP53 [57]*. *KRAS* is a proto-oncogene which is prone to point mutations and amino acid substitutions resulting in its activation as an oncogene [70]. Although activating mutations of *KRAS* following the loss of tumor-suppressor *APC* leads to the transformation of dysplastic regions to cancer, *KRAS* mutations alone can only cause development of serrated adenomas or carcinomas [70-72]. Due to the important roles played by *KRAS* under EGFR signaling, presence of activating mutations in this gene decrease treatment efficacy of EGFR inhibitors in CRC therapy [73]. Additionally, mutations in *BRAF*, downstream effector of *KRAS*, are considered as a sign of worse prognosis in microsatellite stable (or CIS) CRC whereas they are considered as a sign of better prognosis in microsatellite instable CRC [74, 75]. *APC* is a tumor suppressor gene functioning in cell orientation, cell proliferation, transcription and intercellular communication [21, 57]. Together with other partner proteins, it regulates WNT pathway by tight control of cytoplasmic β-catenin. As a result, loss of *APC* is a common theme both in hereditary FAP and sporadic CRC and is observed in about 90% of all CRC cases [21, 57]. *TP53* is another important tumor suppressor which detects mutations and DNA replication errors. Later, it stops cell cycle progression to fix the problems by DNA repair enzymes or it induces apoptosis via caspase pathway [21, 57]. Thus, *TP53* mutations are crucial for progression to carcinoma [21, 57]. On the other hand, serrated or MSI adenocarcinomas arise due to abnormally functioning mismatch repair system which lost its function to correct errors and to maintain genomic stability [21, 63].

1.3 Inflammation and Cancer

Inflammation is known as one of the natural defense mechanism of the body against external and internal dangers occurred through joint action of infiltrating leukocytes, tissue regeneration and cytokine secretion [76]. Inflammation should be resolved, after elimination of pathogens or when the tissue integrity is restored. Nevertheless, chronic inflammation is taken place upon failure of resolution of the inflammatory pathways [76]. One of the major risk factor for cancer is chronic inflammation. It was previously shown that individuals with inflammatory disorders such as Crohn’s disease, Ulcerative colitis, and hepatitis were demonstrated to have increased risk for cancer [21, 45, 51, 77]. HCC is a good example of inflammation related cancer due to the fact that 90% of HCC cases are stem from inflammation and hepatic injury [44, 78, 79]. As a result of unresolved chronic inflammation, sequential development of HCC occurs from fibrosis and cirrhosis [44, 78, 79]. Regardless of the differences between the various etiological factors, there is a common theme in HCC development, the maintenance of a wound healing response activated by parenchymal cell death and the resulting inflammatory cascade [44, 78, 79]. Hence, it is crucial to identify the basic inflammatory signal pathways leading to chronic liver damage, dysplasia, and their progression into HCC [44, 78, 79]. Moreover, tumor-associated inflammation can encourage tumor development in the gut, indicating central role for inflammation in the development of both sporadic CRC and CAC [44]. Therefore, chronic inflammation follows tumor development and vice versa [44]. Upon tumor formation, additional mutations and epigenetic alterations may be accumulated due to the localized inflammatory microenvironment [80-82]. Moreover, clinically detectable inflammation predates initiation of tumor in the case of CAC [83]. However, CRC tumors do not come out within the context of previous inflammation [83]. Thus, it is not likely that inflammation have determinative role in CRC initiation [83]. Moreover, most of the tumor promoting cytokines activates NF-κB in inflammatory and pre-malignant cells. Abnormal NF-κB activation was observed in half of the CRC and CAC tumors [80-82]. NF-κB may promote tumorigenesis via increased cell proliferation and angiogenesis, advanced metastasis and cell invasion and inhibition of cell death [80-82, 84]. Additionally, chronic inflammation can speed up progression of cancer by reshaping the tumor microenvironment by continuous secretion of cytokines and proteases as well as production of ROS and nitric oxides [76]. For this reason, it is important to identify the molecules that regulate inflammatory pathways in cancer [84]. Due to its wide ranging roles in tissue regeneration and inflammation, NF-κB signaling pathway has placed to the center of the inflammatory pathways regulating tumor microenvironment and cellular plasticity [76]. While susceptibility to cancer development increased by chronic inflammation, tumor promotion in cancers, which are not linked to preceding inflammation, could be promoted with an inflammatory tumor microenvironment generated by NF-κB signaling [76].

1.4 The roles of IKKε in cancer and immunity

Inhibitor of Kappa Light Polypeptide Gene Enhancer in B-Cells, Kinase Epsilon (IKKε) is a non-canonical IκB kinase with 66% sequence homology to TBK1 which is a related non-canonical IκB kinase [85]. In Addition to its homology to TBK1, IKKε has 33% homology to the IKKα and 31% homology to the IKKβ which are canonical IκB kinases [85, 86]. Many previous studies has shown the importance of IKKε in cell transformation and innate immunity [85]. Additionally, IKKε is overexpressed and act like oncogene in glioma [87], esophageal squamous cell carcinoma [88], gastric cancer [89], non-small lung cancer [90], pancreatic ductal adenocarcinoma [91], prostate cancer [92, 93], ovarian cancer [94, 95], breast cancer [96-98] which makes it an important target to combat to treat cancer. IKKε protein is identified as crucial for cell transformation in some cancers. Together with MEK, it can compensate the loss of PI3K activation and help transformation cells [97, 99, 100]. Oncogenic properties of

IKKε can also be related to its downstream targets, such as NF-κB signaling [98]. IKKε activates NF-κB pathway via phosphorylation of p65 at Ser536 [101]. Phosphorylation of an important breast cancer tumor suppressor CYLD at Ser418, also known as an NF-κB inhibitor, by IKKε results in its inactivation and reduction in its deubiquitinase activity [96]. Similarly, TRAF2 is also phosphorylated by IKKε which cause elevated activity and ubiquitination of TRAF2 [99, 102]. Activation of TRAF2 and suppression of CYLD synergizes for enhanced survival of breast cancer cells [72]. In the downstream of IKK□, tumor growth can also be regulated by the help of STAT3 and NF-κB, important regulators of inflammation and tumor microenvironment, via production of inflammatory cytokines to support tumor development [82, 103].

It was also demonstrated that AKT pathway could be activated via direct phosphorylation of Ser473 and Thr308 amino acids on AKT by IKKε [58, 59, 100]. Activated AKT induces pro-survival signaling and cause inhibition of FOXO3a via phosphorylation at Ser32, Ser253 and Ser315 which leads to enhanced cell survival and evading from apoptosis [58]. Similar to AKT, IKKε is also able to regulate FOXO3a stability via direct phosphorylation at Ser644 [104]. Moreover, in ovarian cancer, IKKε is found to regulate metastasis and invasion by modulating genes affiliated with tumor metastasis, as well as, IKK□ overexpression is correlated with chemoresistance and poor prognosis [94, 95]. On the other hand, ectopic expression of CK2α in breast cancer cell lines resulted in an increase of IKKε expression which further enhanced NF-κB activation, a critical factor for the pathogenesis of breast cancer [105]. Moreover, Göktuna et al. showed that IKKε behave like pro-survival kinase restricting TNF and caspase 8 dependent apoptosis upon constitutive WNT activation in intestinal epithelial cells [65]. IKKε, a pro-survival kinase, integrates LPS and IL17A signaling cascades to support WNT driven tumor development [65].

IKKε is mostly expressed in macrophages and T lymphocytes, and activated by LPS treatment, TNFα, IL-1β, IL-6 and upon induction of TCR signaling [86, 106]. Consequently, IKKε can suppress T lymphocyte activation via inhibition and phosphorylation of NFATc1 [107, 108]. Moreover, IKKε is a downstream of TLR pathway and vital for both IFNβ regulation and TLR induced activation of IRF3 and IRF7 which makes IKKε a fundamental player of innate immunity regulating IRF and NF-κB [109]. DNA binding and nuclear localization of IRF3 is induced upon phosphorylation of its Ser386 residue by IKKε that results in an increased IFNβ production upon Sendai virus infection [110]. As well as NF-κB and IRF3 activation, IKKε can also phosphorylate STAT1 at its Ser708 for an efficient antiviral response to stimulate ISGF3 formation [111]. Hence, IKKε has a pivotal role to equilibrate Type I and Type II interferon pathway levels [109]. IKKε takes part in Th17 lymphocyte maintenance by phosphorylation of Act1 altering IL-17 signaling as well as inhibition of GSK3α upon IKKε activating IL-1 stimulation [107, 108]. These studies showing how important IKKε is for inflammation and tumor development [65]. Also, increased NF-κB activation in mice fed with western diet results in an elevated IKKε activity in adipocytes, adipose tissue macrophages and liver [112]. Moreover, obesity and chronic inflammation was not observed in IKKε knockout mice indicating that IKKε may be an important target in combating inflammatory diseases such as obesity and cancer [112].

Chapter 2

Aim of the study

Hepatocellular carcinoma is the 6th most common cancer and the second leading cause of cancer related death and also colorectal cancer is the third most common cancer and the fourth leading cause of cancer related deaths. HCC patients have very bad prognosis, survival rates of whom range between 6 to 20 months after diagnosis. That's why, it is important to develop new therapies. Regardless of the developments in the therapy and diagnosis of these cancers, it is crucial to understand the tumorigenesis as well as metastasis of HCC and CRC to develop top-notch therapies or diagnostic markers.

NF-κB signaling pathway, an important regulator of inflammation and tumor microenvironment, has placed to the center of the inflammatory pathways regulating tumor microenvironment and cellular plasticity. Cell survival, invasion, proliferation and inflammatory immune responses are various important physiological functions which are regulated by NF-κB and it is proposed that NF-κB is a pivotal link between inflammation and cancer due to its activation in variety of tumors. While susceptibility to cancer development increased by chronic inflammation, tumor promotion in cancers, which are not linked to preceding inflammation, could be promoted with an inflammatory tumor microenvironment generated by NF-κB signaling. IKKε and TBK1, non-canonical inhibitor of κB kinases, act as an effector of NF-κB to promote tumorigenesis providing a bridge between NF-κB mediated inflammation and cancer. Besides NF-KB signaling, IKKε and TBK1 can also activates interferon signaling by phosphorylating IRF3 and IRF7. Hence, they regulate immune response in lymphocytes and myeloid cells, and related target cytokine expression by controlling the expression of Type I IFNs, IFNα and IFNβ. Thus, we hypothesized that IKKε may be involved in tumorigenesis and metastasis of hepatocellular and colorectal carcinomas. Our aims to validate this hypothesis are as follows;

- To understand oncogenic and metastatic roles played by IKKε.

- To understand exact mechanisms and biological functions through which IKKε exerts oncogenic and metastatic roles
- To understand potential targeting of IKKε for HCC and CRC therapy.

Chapter 3

Materials and Methods

3.1 Materials

3.1.1 General Laboratory Reagents and Chemicals

Routinely used general laboratory reagents and chemicals comprise substances utilized for common techniques such as western blotting, cloning, qPCR. Vendor companies and the Catalog numbers of mentioned materials used in this study are listed in Table 3.1.

Table 3.1. Routinely used reagents, chemicals, enzymes, and kits for general laboratory purposes

Catalog #	Name	Company (Country)
M3148	2-mercaptoethanol	Sigma-Aldrich (USA)
100995	2-Propanol	Merck (Germany)
1610148	40% Acrylamide/Bis Solution 37.5:1	Bio-Rad (USA)
5039	Agar (microbiology grade)	Sigma-Aldrich (USA)
BHE500	Agarose-Biomax	Prona (Spain)
A2941	Ammonium per sulfate	Applichem (Germany)
A0839	Ampicillin	Applichem (Germany)
sc-2323	Bovine Serum Albumin (BSA)	Santa Cruz Biotechnology (USA)
R0580S	BsmBI restriction enzyme	New England BioLabs (USA)

Table 3.1. Routinely used reagents, chemicals, enzymes, and kits for general laboratory purposes

Catalog #	Name	Company (Country)
M0290S	Calf Intestinal Phosphatase (CIP)	New England BioLabs (USA)
C10633	Click-iT Plus EdU Alexa Fluor 488 Flow Cytometry Assay Kit	Invitrogen (USA)
11697498001	cOmplete, Protease inhibitor cocktail tablets	Roche (USA)
A3672	Dimethyl sulfoxide (DMSO)	Applichem (Germany)
D2500-01	E.Z.N.A. Gel Extraction Kit	Omega bio-tek (USA)
D6922-02	E.Z.N.A. Plasmid DNA Maxi Kit	Omega bio-tek (USA)
D6943-01	E.Z.N.A. Plasmid DNA Mini Kit	Omega bio-tek (USA)
R6834-02	E.Z.N.A. Total RNA Kit I	Omega bio-tek (USA)
00-6993-50	eBioscience 7-AAD Viability Staining Solution	Invitrogen (USA)
BMS500FI/300	eBioscience Annexin V-FITC Apoptosis Detection Kit	Invitrogen (USA)
A3562	EDTA	Applichem (Germany)
32221	Ethanol	Sigma-Aldrich (USA)
FD0454	FastDigest Esp3I	Thermo Scientific (USA)
K1991	FastDigest Value Pack	Thermo Scientific (USA)
41003-T	GelRed Nucleic Acid Gel Stain, 10,000X, 0.1 mL in water	Biotium (USA)

Table 3.1. Routinely used reagents, chemicals, enzymes, and kits for general laboratory purposes

Catalog #	Name	Company (Country)
GLN001.1	Glycine	Bioshop (Canada)
K0691	GeneJET Gel Extraction Kit	Thermo Scientific (USA)
SM0311	GeneRuler 1 kb DNA Ladder	Thermo Scientific (USA)
27225	Glacial acetic acid	Sigma-Aldrich (USA)
15524	Glycerol	Sigma-Aldrich (USA)
100317	Hydrochloric acid	Merck (Germany)
1620177	Immobilion-P PVDF Membrane	Bio-rad (USA)
170-8891	iScript cDNA Synthesis Kit	Bio-Rad (USA)
D9307	JumpStart *Taq* DNA Polymerase	Sigma-Aldrich (USA)
MP0035	LookOut Mycoplasma PCR detection kit	Sigma-Aldrich (USA)
106.462	NaOH	Merck (Germany)
740424.10	NucleoBond Xtra Maxi EF	Macherey-Nagel (Germany)
26616	PageRuler Prestained Protein Ladder	Thermo Scientific (USA)
23227	Pierce BCA Protein Assay Kit	Thermo Scientific (USA)
32106	Pierce ECL Western Blotting Substrate	Thermo Scientific (USA)
71725	SDS	Sigma-Aldrich (USA)
S2002-5G	Sodium Azide	Sigma-Aldrich (USA)
47410 19318	Super RX-N	Fujifilm (Japan)

Table 3.1. Routinely used reagents, chemicals, enzymes, and kits for general laboratory purposes

Catalog #	Name	Company (Country)
34095	SuperSignal West Femto Maximum Sensitivity Substrate	Thermo Scientific (USA)
RR820L	SYBR *Premix Ex Taq* II (Tli RNaseH Plus), Bulk	TaKaRa (Japan)
M0202S	T4 DNA Ligase	New England BioLabs (USA)
M0201S	T4 Polynucleotide Kinase	New England BioLabs (USA)
1610801	TEMED	Bio-rad (USA)
T1503	Tris (Trizma Base)	Sigma-Aldrich (USA)
T8787	Triton X-100	Sigma-Aldrich (USA)
BE17-161E	Trypsin/EDTA (0.25%)	Lonza (Switzerland)
95039	Tryptone enzymatic digest from casein	Sigma-Aldrich (USA)
822184	Tween-20	Merck (Germany)
122799	XenoLight D-Luciferin Firefly, Potassium Salt	PerkinElmer (USA)
1.037.530.500	Yeast extract	Merck (Germany)

3.1.2 Cell culture reagents and chemicals

Routinely used cell culture media, reagents and chemicals to maintain the cells and to conduct experiments in cell culture have been listed in Table 3.2.

Table 3.2. Routinely used Media, reagents, chemicals for cell culture experiments

Catalog #	Name	Company (Country)
AF-100-15	Animal-Free Recombinant Human EGF	Peprotech (USA)
ant-bl-1	Blasticidin	Invivogen (USA)
G8090	Caspase-Glo 3/7 Assay	Promega (USA)
11644807001	Cell Proliferation Reagent (WST-1)	Roche (USA)
G7571	CellTiter-Glo Luminescent Cell Viability Assay	Promega (USA)
356231	Corning Matrigel Basement Membrane Matrix Growth Factor Reduced, Phenol Red Free	Corning (USA)
TLP5912	Dharmacon Trans-Lentiviral shRNA Packaging Kit with Calcium Phosphate Transfection Reagent	GE Healthcare (UK)
A3672	Dimethyl sulfoxide (DMSO)	Applichem (Germany)
BE12-614F	DMEM, High Glucose	Lonza (Switzerland)
31885-023	DMEM, Low Glucose	Gibco (USA)
BE12-707F	DMEM, Low Glucose	Lonza (Switzerland)
BE17-512F	Dulbecco’s Phosphate Buffered Saline	Lonza (Switzerland)
TLP4606	Expression Arrest Trans-Lentiviral Packaging Mix	Thermo-Fisher Scientific (USA)
S181H-500	Fetal Bovine Serum Heat Inactivated	Biowest (USA)
10131-027	Geneticin G418	Thermo-Fisher Scientific (USA)
301705	Hiperfect Transfection Reagent	Qiagen (Germany)

Table 3.2. Routinely used Media, reagents, chemicals for cell culture experiments

Catalog #	Name	Company (Country)
SH30258.02	HyClone Phosphate Buffered Saline (PBS)	GE Healthcare (UK)
BE17-605E	L-Glutamine	Lonza (Switzerland)
BE12-688F	McCoy's 5A medium	Lonza (Switzerland)
31985-070	Opti-MEM I	Gibco (USA)
DE17-602E	Pen-Strep	Lonza (Switzerland)
sc-134220	Polybrene	Santa Cruz Biotechnology (USA)
301105	PolyFect Transfection Reagent	Qiagen (Germany)
ant-pr-1	Puromycin	Invivogen (USA)
100-21	Recombinant Human TGF-β1 (HEK293 derived)	Peprotech (USA)
BE12-167F	RPMI 1640	Lonza (Switzerland)
5665817001	The xCELLigence Real-Time Cell Analyzer (RTCA) DP CIM-plate 16	Acea Biosciences (USA)
5469830001	The xCELLigence Real-Time Cell Analyzer (RTCA) DP E-plate 16	Acea Biosciences (USA)
BE17-161E	Trypsin/EDTA (0.25%)	Lonza (Switzerland)
E4981	ViaFect Transfection Reagent	Promega (USA)

3.1.3 Antibodies

Antibodies used in western blotting experiments have been listed in Table 3.3.

Table 3.3. Used Antibodies

Catalog #	Name	Company (Country)
7076S	Anti-mouse IgG, HRP-linked Antibody	Cell Signaling Technology (USA)
7074S	Anti-rabbit IgG, HRP-linked Antibody	Cell Signaling Technology (USA)
9664S	Cleaved Caspase-3 (Asp175) (5A1E) Rabbit mAb	Cell Signaling Technology (USA)
5605S	c-Myc (D84C12) Rabbit mAb	Cell Signaling Technology (USA)
sc-8426	E-cadherin Antibody (G-10)	Santa Cruz Biotechnology (USA)
sc-271269	ERK 1 Antibody (G-8)	Santa Cruz Biotechnology (USA)
sc-376114	IKK-i Antibody (A-11)	Santa Cruz Biotechnology (USA)
2905S	IKKε (D20G4) Rabbit mAb	Cell Signaling Technology (USA)
3416S	IKKε (D61F9) XP® Rabbit mAb	Cell Signaling Technology (USA)
T5168	Monoclonal Anti-α-Tubulin antibody produced in mouse	Sigma-Aldrich (USA)
14215S	N-Cadherin (13A9) Mouse mAb	Cell Signaling Technology (USA)
4060S	Phospho-Akt (Ser473) (D9E) XP® Rabbit mAb	Cell Signaling Technology (USA)

Table 3.3. Used Antibodies

Catalog #	Name	Company (Country)
8766S	Phospho-IKKε (Ser172) (D1B7) Rabbit mAb	Cell Signaling Technology (USA)
4370S	Phospho-p44/42 MAPK (Erk1/2) (Thr202/Tyr204) (D13.14.4E) XP® Rabbit mAb	Cell Signaling Technology (USA)
9255S	Phospho-SAPK/JNK (Thr183/Tyr185) (G9) Mouse mAb	Cell Signaling Technology (USA)
5483S	Phospho-TBK1/NAK (Ser172) (D52C2) XP® Rabbit mAb	Cell Signaling Technology (USA)
sc-166643	TANK Antibody (D-2)	Santa Cruz Biotechnology (USA)
3013S	TBK1/NAK Antibody	Cell Signaling Technology (USA)
sc-81417	Twist Antibody (Twist2C1a)	Santa Cruz Biotechnology (USA)
5741S	Vimentin (D21H3) XP® Rabbit mAb	Cell Signaling Technology (USA)
13663S	ZO-1 (D6L1E) Rabbit mAb	Cell Signaling Technology (USA)

3.1.4 Nucleic Acids

Nucleic acids such as siRNAs, sgRNAs, shRNAs and other vectors used in gene editing/targeting experiments have been listed in Table 3.4 with their target sequences and available descriptions.

Table 3.4. List and sequences of nucleic acids that are used for gene editing

Catalog #	Name	Company (Country)	Target Sequence/ Description
1027280	Negative Control siRNA	Qiagen (Germany)	Allstars Negative Control siRNA
VG-1000480436-mpn	IKBKE siRNA	Eurogentec (Belgium)	siRNA 1- GUGCGUGCAGAAGUAUCA AdTdT siRNA 2- GGUGAAUUUCAGUCAUUU AdTdT
RHS4346	GIPZ Non-silencing Lentiviral shRNA Control	GE Healthcare (UK)	sh_Scramble: ATCTCGCTTGGGCGAGAGT AAG
TLP5912	GIPZ Lentiviral Human IKBKE shRNA	GE Healthcare (UK)	shIKBKE_29: TGGACGACAACTCGCTGC A shIKBKE_43: TGTAGATGAAGTTCATCTT shIKBKE_67: TCATCTTGTCCAAACAGCA
SHC002 Sigma	pLKO.1-puro Non-Mammalian shRNA Control Plasmid DNA	Sigma-Aldrich (USA)	MISSION® pLKO.1-puro Non-Mammalian shRNA Control Plasmid DNA

Table 3.4. List and sequences of nucleic acids that are used for gene editing

Catalog #	Name	Company (Country)	Target Sequence/ Description
SHCLNG-NM_013254	MISSION Lentiviral Human TBK1 shRNA	Sigma-Aldrich (USA)	shTBK1_474: CCGGCCAGGAAATATCATGCGTGTTCTCGAGAACACGCATGATATTTCCTGGTTTTT shTBK1_1212: CCGGCGGGAACCTCTGAATACCATACTCGAGTATGGTATTCAGAGGTTCCCGTTTTTG shTBK1_1773: CCGGGCAGAACGTAGATTAGCTTATCTCGAGATAAGCTAATCTACGTTCTGCTTTTTG shTBK1_2355: CCGGATTTGATGTGGTCGTGTAAATCTCGAGATTTACACGACCACATCAAATTTTTG
Following synthetic sgRNAs used for CRISPR/Cas9 genome editing are designed by me via E-CRISPR Design (DKFZ)			
Scramble_UK	Non Targeting Control synthetic guide RNA (sgRNA)	NA	GCACTACCAGAGCTAACTCA

Table 3.4. List and sequences of nucleic acids that are used for gene editing

Catalog #	Name	Company (Country)	Target Sequence/ Description
IKBKE_12_6092	IKBKE Targeting synthetic guide RNA 1 (sgRNA)	NA	GTGCATCGCGACATCAAGCC
IKBKE_35_6092	IKBKE Targeting synthetic guide RNA 2 (sgRNA)	NA	GCATCCCGACATGTATGAGC
IKBKE_13_3046	IKBKE Targeting synthetic guide RNA 3 (sgRNA)	NA	GGCCACTGCCAGTGTGTACA
TBK1_58_11384	TBK1 Targeting synthetic guide RNA 1 (sgRNA)	NA	GGAAATATCATGCGTGTTAT
TBK1_2_22768	TBK1 Targeting synthetic guide RNA 2 (sgRNA)	NA	GACCCTTTGAAGGGCCTCGT
TANK_91_60186	TANK Targeting synthetic guide RNA 1 (sgRNA)	NA	GCAGAGAATACGTGAACAAC
TANK_98_80248	TANK Targeting synthetic guide RNA 2 (sgRNA)	NA	GCAGTCCTTTGCTCCATGAA

Table 3.4. List and sequences of nucleic acids that are used for gene editing

Catalog #	Name	Company (Country)	Target Sequence/ Description
52961	pLentiCRISPRv2	Addgene (USA)	backbone for CRISPR/Cas9 genome editing

3.1.5 Primers

Sequence of primers that are used for PCR applications and their amplicon size and melting temperatures are listed in Table 3.5. All primers were ordered from and synthesized by Oligomer Biotechnology Company (Ankara) and their concentrations were adjusted to 100 µM by reconstituting with ddH_2O. Upon reconstitution, primers were aliquoted and stored at -20°C freezer.

Table 3.5. Used Primers

Name of Primer	Sequence of Primer	Size of the amplicon (bp)
IKBKE 1 F	TGCGTGCAGAAGTATCAAGC	109
IKBKE 1 R	TACAGGCAGCCACAGAACAG	
IKBKE 2 F	CTGCATCCCGACATGTATGA	171
IKBKE 2 R	CCGGTACATGATCTCCTTGTT	
IKBKE 3 F	GAGCATCTACAAGCTGACAGAC	173
IKBKE 3 R	CAATGCTCCAGAGATCCACAG	
TBK1 1 F	GTGGTGGGTGGAATGAATCAT	51
TBK1 1 R	ATCACGGTGCACTATACCATTCTC	

Table 3.5. Used Primers

Name of Primer	Sequence of Primer	Size of the amplicon (bp)
TBK1 2 F	CAACCTGGAAGCGGCAGAGTTA	124
TBK1 2 R	ACCTGGAGATAATCTGCTGTCGA	
TBK1 3 F	GAAGGGCCTCGTAGGAATAAAG	142
TBK1 3 R	CCCGAGAAAGACTGCAAGAA	
TANK 1 F	CAAAGCCCTCAAATCTCGTAAAC	113
TANK 1 R	GTCCAGAAGTGGGAAGCTATTT	
TANK 2 F	CAGCTGTCACTTCAACAGACTA	97
TANK 2 R	GCAGAGGAACACAGCCATAA	
CDH1 F	CCCGGGACAACGTTTATTAC	72
CDH1 R	GCTGGCTCAAGTCAAAGTCC	
CDH2 F	ACAGTGGCCACCTACAAAGG	201
CDH2 R	CCGAGATGGGGTTGATAATG	
FN F	CTGGCCGAAAATACATTGTAAA	114
FN R	CCACAGTCGGGTCAGGAG	
KRT18 F	TGATGACACCAATATCACACGA	112
KRT18 R	GGCTTGTAGGCCTTTTACTTCC	
MMP9 F	GAACCAATCTCACCGACAGG	67
MMP9 R	GCCACCCGAGTGTAACCATA	
SNAI2 F	TGGTTGCTTCAAGGACACAT	66
SNAI2 R	GTTGCAGTGAGGGCAAGAA	

Table 3.5. Used Primers

Name of Primer	Sequence of Primer	Size of the amplicon (bp)
ZEB1 F	GGGAGGAGCAGTGAAAGAGA	70
ZEB1 R	TTTCTTGCCCTTCCTTTCTG	
ZEB2 F	AAGCCAGGGACAGATCAGC	74
ZEB2 R	CCACACTCTGTGCATTTGAACT	
ZO1 F	CAGAGCCTTCTGATCATTCCA	69
ZO1 R	CATCTCTACTCCGGAGACTGC	
GAPDH F	GCCCAATACGACCAAATCC	66
GAPDH R	AGCCACATCGCTCAGACAC	
EPCAM F	CGCAGCTCAGGAAGAATGTG	88
EPCAM R	TGAAGTACACTGGCATTGACG	
CLAUDIN7 F	CCACTCGAGCCCTAATGGTG	266
CLAUDIN7 R	GGTACCCAGCCTTGCTCTCA	
KRT19 F	CTTCCGAACCAAGTTTGAGAC	225
KRT19 R	GAATCCACCTCCACACTGAC	
VIMENTIN F	GGTGGACCAGCTAACCAACGA	183
VIMENTIN R	TCAAGGTCAAGACGTGCCAGA	

3.1.6 Equipment

Routinely used equipment are listed in Table 3.6.

Table 3.6. Used equipment for the experiments

Company	Name of the Equipment
Applied Biosystems (USA)	Polymerase Chain Reaction (PCR) Thermal cycler
Bio-Rad (USA)	PowerPac Basic
Thermo Scientific (USA)	NanoDrop ONE
Vilber Lourmat (Germany)	UV Transilluminator
Hettich (Germany)	-80ºC freezer
Amersham Life Science (UK)	Hyperprocessor
Nikon (Japan)	Eclipse TS100 Inverted light microscope
Nikon (Japan)	COOLPIX 4500 camera
Roche (Switzerland)	The LightCycler® 480 System
Leica Microsystems (Germany)	Leica MC120 HD, 2.5 Megapixel HD Microscope Camera
Leica Microsystems (Germany)	DMi8 S Platform, Inverted Microscope Solution
BioTek (USA)	Synergy HT Microplate Reader

3.2 Media and Solutions

3.2.1 General Laboratory Solutions

Routinely used buffers, solutions and their formulations have been listed in Table 3.7.

Table 3.7. Routinely used buffers and solutions

Buffer	For 1 L solution
Mild Stripping Buffer	15 g glycine; 1 g SDS; 10 ml Tween20; pH=2.2
Cell Lysis Buffer (1 ml)	25mM Hepes; 150mM NaCl; 0.5% Triton X-100; 10% Glycerol; 5mM Na_3VO_4; 25mM β-glycero phosphate; 25mM NaF; 0.1 Tablet cOmplete Protease inhibitor
TAE Buffer	4.84 gr Trizma Base; 1.14 ml Glacial acetic acid; 2 ml 0.5M EDTA
Wet Transfer Buffer	14.4 gr Glycine; 3.02 gr Trizma Base; 20% Methanol
Running Buffer (TGS Buffer)	14.4 gr Glycine; 3.02 gr Trizma Base; 1 gr SDS
2X Protein Loading Dye (50 ml)	6.25 ml 1M Tris-HCl (pH:6.8); 25 ml 10% SDS; 10 ml β-Mercaptoethanol; 20 ml glycerol; 0.008% Bromophenol blue
4X Protein Loading Dye (50 ml)	12.5 ml 1M Tris-HCl (pH:6.8); 5 gr SDS; 5 ml β-Mercaptoethanol; 10 ml glycerol; 0.004% Bromophenol blue
LB Broth	10 gr NaCl; 5 gr Yeast Extract; 10 gr Tryptone
LB Agar	10 gr NaCl; 5 gr Yeast Extract; 10 gr Tryptone; 15 gr Bacto agar
10% SDS	100 gr SDS (Heat to 68^{o}C for solubility)
1M Tris-HCL, pH:6.8	121 gr Trizma Base
1.5M Tris-HCL, pH:8.8	181.65 gr Trizma Base
APS 10%	100 gr $(NH_4)_2S_2O_8$

Table 3.7. Routinely used buffers and solutions

Buffer	For 1 L solution
Transformation Buffer	2 ml 0.5M PIPES Buffer (pH:6.7); 1.10 gr $MnCl_2.4H_2O$; 1.87 gr KCl; 0.22 gr $CaCl_2.2H_2O$
2xHBSS Buffer, pH:7.05 (25 ml)	10 ml 1M Hepes; 666 µl 3M KCl; 0.4 gr dextrose; 11.2 ml 5M NaCl; 0.0531gr Na_2HPO_4
0.5M EDTA, pH:8.0	186.12 gr $EDTA.Na_2.2H_2O$
Fixing/Staining Solution for Colony Formation	0.5 gr Crystal Violet (0.05% w/v); 27 ml 27% Formaldehyde (1%); 100 ml 10X PBS (1X); 10 ml Methanol (1%); 863 ml dH_2O
PolyHEMA solution (50 ml)	6 gr PolyHEMA; 47.5 ml absolute EtOH; 2.5 ml dH_2O

3.2.2 Cell Culture Media and Solutions

Cell lines and their growth media are listed in Table 3.8.

Table 3.8. Cell lines and their growth media

Cell Line	Growth Medium
DLD1	McCoy's 5A; 10% FBS; 1% Pen/Strep
HCT116	McCoy's 5A; 10% FBS; 1% Pen/Strep
HEK293FT	Normal DMEM; 10% FBS; 500 µg/ml geneticin
Hep3B	Normal DMEM; 5% FBS; 1% Pen/Strep
HT29	Normal DMEM; 10% FBS; 1% Pen/Strep: 1% L-glutamine;

Table 3.8. Cell lines and their growth media

Cell Line	Growth Medium
HUH7	Normal DMEM; 10% FBS; 1% Pen/Strep
HepG2	RPMI-1640; 10% FBS
PLC/PRF/5	High Glucose DMEM (4.5g/L); 10% FBS; 1% Pen/Strep; 1% L-glutamine
SNU182	RPMI-1640; 10% FBS; 1% Pen/Strep
SNU387	RPMI-1640; 10% FBS; 1% Pen/Strep
SNU423	RPMI-1640; 10% FBS; 1% Pen/Strep
SNU475	RPMI-1640; 10% FBS; 1% Pen/Strep
SW480-SG	Normal DMEM; 10% FBS; 1% Pen/Strep
SW480-FG	Normal DMEM; 10% FBS; 1% Pen/Strep: 1% L-glutamine; 1% NEAA; 1% Sodium Pyruvate

3.3 Methods

3.3.1 Maintenance of human cell lines

Cells are kept inside sterile cryovials in liquid nitrogen for further uses and they can be thawed and cultured for experiments when needed. To do this, cryovials are taken from liquid nitrogen tank and plunged to the water bath at 37ºC until diminutive ice ball left. Then, melted cell-freezing medium mixture is placed to the falcon tubes containing appropriate growth medium at 37ºC (Table 3.8). After that, falcon tubes are centrifuged at 1500 rpm for five minutes at RT (room temperature). Next, falcon tubes are taken from centrifuge and supernatant of the falcon tube are removed and the cell pellet are resuspended with suitable growth medium and transferred to T25 tissue culture coated flasks. Moreover, T25 Flasks are placed to the incubator that already adjusted to 37ºC and 5% CO_2 and are maintained there. Furthermore, depending on the cell type and the experimental needs, cell splitting can be done with the varying ratios such as; from 1:2 up to 1:10 ratios. In order to split the cells, growth medium is removed from the flasks and cells that are attached to the surface of the flask are washed with sterile 1X DPBS. Addition to this, cells are kept under Trypsin/EDTA (0.25%) for 2-3 minutes until they detached from the surface, this time usually changes depending on the cell line that are used. To use the cells in the experiments, they are needed to be counted. Thus, hemocytometer is used for cell counting under inverted light microscope via loading 10 µl of well mixed cell suspension to the hemocytometer. Afterwards, desired concentrations of the cells are prepared by dilutions and cells are used for experiments depending on the purpose. Finally, cells can be stored and frozen in cryovials for further use by the help of freezing medium that composed of 90% FBS and 10% DMSO. To freeze the cells, medium of the cells are removed from the flasks and cells washed with DPBS. After that, cells are kept under Trypsin/EDTA (0.25%) for 2-3 minutes until they detached from the surface and detached cells washed with medium and centrifuged at 1500 rpm for five minutes at RT. Moreover, cell pellets are resuspended in freezing medium and distribute to the cryovials. Furthermore, cryovials are placed to the -20ºC freezer for 2 hours. By following that, vials are placed to the -80ºC for overnight and then placed to liquid nitrogen. All used cell lines were tested for mycoplasma contamination by using LookOut Mycoplasma PCR Detection Kit (Sigma-Aldrich, USA) and were observed to be clean.

3.3.2 siRNA transfection of human cell lines

For 12 well plates, cells were seeded as triplicates. For each wells 500 µl of optimem added to 1.5 ml eppendorf tube and 0.25 µl of IKKε targeting siIKKε1 (100µM) and siIKKε2 (100µM) constructs were added to the medium. After vortex and spin down, 7.5 µl of Hiperfect was added to this mixture and 10 minutes of incubation were conducted. Furthermore, final mixture was added to the wells as 500 µl per well. After 6 hours, 500 µl of appropriate medium was added to the wells. Last but not least, medium is totally changed with the appropriate growth medium 24 hours after transfection.

For 96 well plates, cells were seeded as triplicates. For each wells 50 µl of optimem added to 1.5 ml eppendorf tube and 0.05 µl of IKKε targeting siIKKε1 (100µM) and siIKKε2 (100µM) constructs were added to the medium. After vortex and spin down, 0.75 µl of Hiperfect was added to this mixture and 10 minutes of incubation were conducted. Furthermore, final mixture was added to the wells as 50 µl per well. After 6 hours, 50 µl of appropriate medium was added to the wells. Last but not least, medium is totally changed with the appropriate growth medium 24 hours after transfection.

3.3.3 shRNA transfection of human cell lines

First of all, HEK293FT cells were seeded to 6 well plates as 1 million cells per well. The other day, 6µg of targeting plasmid was added to 1.5ml eppendorf. By following that,4.3 µl of packaging plasmid was added to the same tube. Moreover, 15 µl of $CaCl_2$ was also added to the same tube. After that, volume of the tube was completed to 150 µl with sterile ddH_2O. Then, tube was vortexed and spun. Later, 150 µl of 2x HBSS were added on top of the mixture as dropwise while mixing with vortex. By following 3 minutes of incubation at room temperature, total of 300 µl of mixture was added on top of the HEK293FT cells as dropwise. After 14 hours of incubation, cells were examined under fluorescent microscope and GFP expression was observed. Subsequently, medium of HEK293FT cells were changed and 5% FBS containing reduced serum media was added to the wells to induce virus production and to reduce growth of HEK293FT cells. Additionally, cells to be depleted were also seeded to 6 well plate for transduction. On the next day, Virus sups were filtered and applied to the 6 well plate of cells to be depleted for first transduction. After that, 5% FBS containing reduced serum media was added to the 6 well plate of FT cells for second round of virus production. The other day, second round of transduction was conducted. 24 hours after second transduction, medium of cells to be depleted were changed with the appropriate growth medium to remove medium with virus sups. Later, puromycin were introduced to the medium of depleted cells so that untransduced cells eliminated. Due to massive cell death, medium of the cells were changed and the confluency of the cells reaches to 100%, protein isolation was performed and protein samples were quantified and western blot experiment was conducted to check depletion status.

3.3.4 *In vitro* wound healing assay

For wound healing assay, different amount of cells for different cell lines were seeded to 12 well plate as triplicates per constructs in normal growth medium. When the cells reach the confluency on the next day, scratches were introduced with 200 µl pipette tips, and the wells were washed with PBS and media was added. Photos were taken at 12 hr intervals. The gap width of the scratches in the first and the last time point were determined using Image J. Subsequently, measured values were normalized according to initial time point of each group and related graphs were sketched by using GraphPad Prism 7.0 software.

3.3.5 Determination of cell proliferation by using Cell Titer Glo reagent

Cells were seeded into 96 well plate to be 5000 cells/well for Hep3B, SNU182, SNU387, SNU423 and PLC/PRF/5 (or 5000 cells/well for SNU475). 24 hours later, appropriate treatment like PolyI:C treatment or siRNA transfection was conducted. For PolyI:C treatment, cells were treated with 50 ng/ml and 100ng/ml final concentration of polyI:C. Then, 1 volume of Cell Titer Glo reagent was added to each well. After 5 minutes of incubation on shaker at 300 rpm, content of the wells transferred to opaque reading plate and luminescence of the samples were measured by using BioTek Synergy HT Microplate Reader. Subsequently, measured values were normalized according to control group and graph were sketched by using GraphPad Prism 7.0 software.

3.3.6 Determination of cell proliferation by using Real Time Cell Analyzer

First of all, E-plate was opened and 75 µl of appropriate growth medium was added to each well of the RTCA E-plate by reverse pipetting. Then, RTCA software was opened and slots that were used was selected, activated and labeled via software. Next, background measurement and experimental step were added from schedule page. Later, sweep interval was adjusted to 10 minutes and total step time for experimental step was adjusted to 120 hours. Subsequently, message part of the software was controlled whether any pin gives error before starting to the background measurement. Furthermore, plate was placed to the slot and background measurement were taken. After background measurement, 10,000 cells/well were loaded to E-plate by reverse pipetting. Moreover, plate was placed to the slot on the RTCA machine after 30 minutes of incubation of the cells to let them attach to the bottom of the plate and experiment started. At the end of the experiment, measurements were taken and data were normalized according to initial time point of each group and related graphs were sketched by using GraphPad Prism 7.0 software.

3.3.7 Determination of cell migration by using Real Time Cell Analyzer

Initially, CIM-plate was opened and 160 µl of appropriate growth medium was added to the bottom chamber by reverse pipetting. Then, 50 µl of reduced serum media was added to top chamber after it was placed on top of the bottom chamber. Then, assembled chambers were incubated at 37 ºC for 1 hour. After that, RTCA software was opened and slots that were used was selected, activated and labeled. Next, background measurement and experimental step were added from schedule page. Later, sweep interval was adjusted to 15 minutes and total step time for experimental step was adjusted to 96 hours. Subsequently, message part of the software was controlled whether any pin gives error before starting to the background measurement. Furthermore, plate was placed to the slot and background measurement were taken. After background measurement, 30,000 cells/well were loaded in 100 µl of reduced serum media to the top chamber of CIM-plate by reverse pipetting. Moreover, plate was placed to the slot on the RTCA machine after 30 minutes of incubation of the cells to let them attach to the bottom of the plate and experiment started. At the end of the experiment, measurements were taken and data were normalized according to initial time point of each group and related graphs were sketched by using GraphPad Prism 7.0 software.

3.3.8 Determination of cell invasion by using Real Time Cell Analyzer

Firstly, CIM-plate was opened and 160 µl of appropriate growth medium was added to the bottom chamber by reverse pipetting. Next, 50 µl of matrigel was placed to the top chamber and 30 µl of it pipetted back. Later, plate was left in incubator for matrigel to dry. Then, 50 µl of reduced serum media was added to top chamber after it was placed on top of the bottom chamber. Then, assembled chambers were incubated at 37 ºC for 1 hour. After that, RTCA software was opened and slots that were used was selected, activated and labeled. Next, background measurement and experimental step were added from schedule page. Later, sweep interval was adjusted to 15 minutes and total step time for experimental step was adjusted to 96 hours. Subsequently, message part of the software was controlled whether any pin gives error before starting to the background measurement. Furthermore, plate was placed to the slot and background measurement were taken. After background measurement, 30,000 cells/well were loaded in 100 µl of reduced serum media to the top chamber of CIM-plate by reverse pipetting. Moreover, plate was placed to the slot on the RTCA machine after 30 minutes of incubation of the cells to let them attach to the bottom of the plate and experiment started. At the end of the experiment, measurements were taken and data were normalized according to initial time point of each group and related graphs were sketched by using GraphPad Prism 7.0 software.

3.3.9 Colony formation assays

SW480 and HT29 cells were cultured as 1,000 cells per well of a 6-well plate, in at least triplicates and were grown for 10 days, until colonies visible to eye formed. During this period, medium of the cells were changed every 3 – 4 days. Subsequently, media were removed and fixing/staining solution (Table 3.7) added to the wells to cover the dish. Furthermore, 20 minutes of staining at room temperature was conducted. Then, fixing/staining solution were removed from the wells and plates were washed one at a time by dipping into bucket of water in the sink with the water continuing to run. After air dry, plates were scanned and photos were analyzed to count the colonies by using Clono-Counter.

Also, PolyHEMA assay were conducted to check colony formation with DLD1 cells. For this purpose, PolyHEMA solution was prepared according to (Table 3.7) and this mixture was incubated in water bath at 37 ºC for 48-72 hours by shaking time to time. Then, solution was distributed to the wells of 96 well plate as 50 µl per well. Following that, plate was incubated at 37 ºC, 5% CO_2 until it gets dried. Furthermore, 2,500, 5000, and 10,000 cells were seeded to polyHEMA coated 96 well plate in at least triplicates in 100 µl medium with 10% FBS and were grown for 4 days, Lastly, cell growth was monitored by adding 10 µl of Cell Proliferation Reagent (WST-1) and subsequent incubation of the plate at 37 ºC, 5% CO_2 for 4 hours. At the end of the incubation, absorbance of the samples was measured at 440 nm using a microplate reader. Also, photos of the colonies were recorded to determine the size manually.

3.3.10 RNA Isolation from human cell lines and quality determination

To isolate RNAs from the cell lines, E.Z.N.A. Total RNA Kit I was used and all RNA isolation procedures was conducted according to kits user's manual. Then, isolated RNAs were quantified by using 1.5 µl of samples via NanoDrop ONE spectrophotometer. After isolation and quantification, samples were stored at -80ºC freezer.

3.3.11 cDNA synthesis from isolated RNAs

cDNAs were synthesized by the use of 1 µg of isolated and quantified total RNA samples together with iScript cDNA Synthesis Kit (Bio-Rad, USA) according to supplied protocol. Secondly, synthesized cDNAs were stored at -20ºC freezer for further use.

3.3.12 qPCR and analyses of gene expression

The LightCycler® 480 System (Roche, Switzerland) was used to quantify the expression of the genes with the help of SybrGreen assay. Each gene was run as duplicate for each sample. cDNA samples were diluted as 1:4. Total volume of qPCR reaction was 10 µl and which composed of mixing 5 µl of SybrGreen (Takara, Japan), 0.5 µl of Forward and Reverse Primer mixture (Table 3.5), 1 µl of 1:4 diluted cDNA and 3.5 µl of nuclease free water per well of 96 well plate. Protocol for the qPCR reaction was adjusted according to Table 3.9.

Table 3.9. qPCR protocol

Denaturation	**1 cycle**
	30 seconds at 95 ºC with the ramp rate 4.4 ºC/sec
PCR	**40 cycles**
	5 seconds at 95 ºC with the ramp rate 4.4 ºC/sec 30 seconds at 60 ºC with the ramp rate 2.2 ºC/sec (Single acquisition)
Melting	**1 cycle**
	5 seconds at 95 ºC with the ramp rate 4.4 ºC/sec 60 seconds at 60 ºC with the ramp rate 2.2 ºC/sec 95 ºC with the ramp rate 1.1 ºC/sec (Continuous acquisition, 5 per ºC)
Cooling	**1 cycle**
	30 seconds at 50 ºC with the ramp rate 2.2 ºC/sec

When qPCR reaction is done, derived Ct values (cycle number where the fluorescence exceeds the fixed threshold) of each sample normalized according to the housekeeping gene, *GAPDH*, belongs to that sample. Then, values of each duplicate were averaged and graphs representing the relative expression of the desired gene were sketched.

3.3.13 Total protein isolation and quantification

Growth medium of the cells were removed from cell culture dish and cells were washed with 1X PBS. After that, PBS having growth medium remnants were replaced with cold 1X PBS. Then, cell culture dish was scraped to collect all the cells from the dish by using scraper. Next, cells were collected into falcon tubes and centrifuged at 13000 rpm at 4 ºC for 5 minutes. After centrifugation, supernatant was emptied and cell pellet was resuspended with cell lysis buffer (Table 3.7). After 15 minutes of incubation on ice, centrifugation was conducted at 13000 rpm at 4 ºC for 10 minutes. Finally, supernatant having proteins are transferred to another 1.5 ml of Eppendorf tube and stored at -80 ºC freezer. For quantification of isolated proteins, 1 µl of isolated proteins were mixed with 99 µl dH_2O and 75 µl of 2 mg/ml concentrated Bovine Serum Albumin (BSA) solution was mixed with 1425 µl of dH_2O to prepare 0.1 mg/ml concentrated BSA working solution. From this working solution, different dilutions were prepared as follows in Table 3.10.

Table 3.10. Preparation of BSA dilutions

Dilutions	Volume from Working Solution (0.1 mg/ml)	Volume of dH_2O	Final Concentration of the dilutions
1	0 µl	100 µl	0 ng/µl
2	10 µl	90 µl	10 ng/µl
3	20 µl	80 µl	20 ng/µl
4	30 µl	70 µl	30 ng/µl
5	40 µl	60 µl	40 ng/µl
6	50 µl	50 µl	50 ng/µl
7	70 µl	30 µl	70 ng/µl
8	100 µl	0 µl	100 ng/µl

At the end of the preparation of dilutions according to Table 3.10, dilutions are added to the 96 well plate vertically as triplicates and unknown proteins which were isolated from cells were also loaded to the same 96 well plate horizontally as triplicates. Furthermore, 10 ml of Solution A and 200 µl Solution B of Pierce BCA Protein Assay Kit (Thermo Scientific, USA) were mixed and distributed to each well of 96 well plate as 100 µl mixture per well. After incubation of 96 well plate at 60 ºC for 40 minutes, absorbance of the plate was measured and recorded at 562 nm wavelength by using

BioTek Synergy HT Microplate Reader. Recorded values were used to sketch standard curve to determine the concentration of unknown proteins.

3.3.14 SDS-PAGE

Gels for SDS-PAGE experiment are prepared as in Table 3.11.

Table 3.11. Components and composition of separating and stacking gels

Components	**Separating Gel (Resolving Gel)**			**Stacking Gel**
	12%	**10%**	**8%**	
Acrylamide	4.8 ml	4 ml	3.2 ml	0.6 ml
dH_2O	4.2 ml	5 ml	5.8 ml	3.5 ml
Glycerol	1.5 ml			**Not added**
Tris-HCl 1.5M pH 8.8	3.75 ml			
Tris-HCl 1M pH 6.8	**Not added**			625 µl
EDTA 0.25M	375 µl			125 µl
SDS 10%	300 µl			100 µl
APS 10%	125 µl			60 µl
TEMED	15 µl			10 µl

Gels were run at 120V until the SDS loading dye gets through to the end of the gel in 1X running buffer prepared according to Table 3.7.

3.3.15 Western blot

With the help of 1X Transfer buffer (Table 3.7) and wet transfer system (Biorad), proteins that were run in SDS gel were transferred to the PVDF membrane at 250mA for 2 hours. For big proteins, transfer step was conducted at 30mA for overnight. To do a transfer, PVDF membrane was activated in 100% methanol for 30 seconds and then immersed into 1X transfer buffer. Later, transfer sandwich was formed by using whatman papers, sponge, activated PVDF membrane and run SDS gel. After the transfer step, membrane was incubated in blocking solution that is composed of 10% milk powder dissolved in 1X TBS-T buffer for one hour at room temperature. When the blocking step over, blocked membrane was washed three times for 10 minutes by using TBS-T buffer on shaker at room temperature. Moreover, Membrane was incubated in primary antibody (Table 3.3) prepared in 5% BSA and supplemented with NaZ in TBS-T at 4ºC for overnight. Also, membrane was taken from primary antibody and washed three times for 10 minutes by using TBS-T buffer on shaker at room temperature. By following that, secondary antibody incubation for 1 hour at room temperature was conducted. Last, membrane was washed again three times for 10 minutes by using TBS-T buffer on shaker at room temperature and was developed with the help of ECL system.

3.3.16 Preparation of competent *Escherichia coli* DH5α

5 ml of *Escherichia coli* DH5α cells has grown in LB Broth while shaking in the incubator at 37 ºC. Subsequently, overnight grown starter culture was seeded to 250 ml flask of LB Broth as 1/100 of the volume. Moreover, OD value of the culture was followed at 595λ wavelength until reaches to the 0.6Å. Then, culture was chilled for 10 minutes on ice and subsequently centrifuged at 2000 rpm for 10 minutes at 4 ºC. Furthermore, supernatant was discarded from the tube and remaining pellet was resuspended in 10 ml of ice cold 0.1M $CaCl_2$. Centrifugation at 2000 rpm for 10 minutes at 4 ºC was repeated but this time pellet was resuspended in 5 ml of ice cold 0.1M $CaCl_2$ and left overnight at 4 ºC. Finally, 5 ml of 50% Glycerol solution mixed with 5 ml of bacterial suspension and dispensed into 100 µl aliquots which then frozen immediately in liquid nitrogen and stored at -80 ºC freezer.

3.3.17 Bacterial transformation

Competent *Escherichia coli* DH5α cells were taken from -80 ºC freezer and thawed on ice for 15 minutes. Meanwhile, LB agar plates containing appropriate antibiotic were also taken out to room temperature. Subsequently, 100ng of plasmid DNA was mixed with 20 µl of competent cells in a microcentrifuge tube by flicking the tube. Next, Plasmid DNA and competent cell mixture was incubated later on ice for 30 minutes. Heat shock of transformation tube was conducted by placing the tube into 42 ºC water bath for 45 seconds by following incubation on ice. When heat shock was completed, tube replaced back on ice for 2 minutes and grown in the shaking incubator for 45 minutes at 37 ºC with 250 µl of LB broth medium. After outgrowth step, transformants were plated on LB agar plates and incubated overnight at 37 ºC.

3.3.18 Plasmid isolation and sequencing

Transformed colonies were picked from LB agar plate as single colony and dipped couple of times in 5 ml of LB broth medium in 15 ml falcon tube. After that, falcon tube was incubated in the shaking incubator at 37 ºC for overnight. Moreover, tube was centrifuged at 4000 rpm for 10 minutes to get bacterial pellet and DNA isolation was conducted by using E.Z.N.A. Plasmid DNA Mini Kit (Omega bio-tek, USA) according to manufacturer's protocol. Later, isolated DNA was quantified by measuring samples via NanoDrop ONE (Thermo Scientific, USA). Isolated DNAs were stored at -80 ºC freezer. Then, isolated plasmid DNAs were diluted to 50 ng/µl concentration depending on the requirements of the PRZ Biotech company for sanger sequencing reaction. Subsequently, sequencing peaks were analyzed by using chromas software and sequence alignment was done by using MUSCLE which is available in EMBL-EBI website (https://www.ebi.ac.uk/Tools/msa/muscle/).

3.3.19 Design and annealing of synthetic guide RNAs

Synthetic guide RNAs (sgRNAs) targeting against human IKBKE, TBK1, and TANK genes (Table 3.4) were designed by using E-CRISP, an online tool to design gRNA sequences and evaluate Clustered Regularly Interspaced Short Palindromic Repeats (CRISPR). For this purpose, default settings were preferred. As a result, list of nucleotide sequences targeting above mentioned genes were presented together with their Specificity, Annotation and Efficiency scores. Among the number of successful designs, two or three sequences were preferred and their complementary sequences were also produced and sticky ends sequences for cloning were also added. All in all, oligoes were ordered from PRZ Biotech company for further steps. Moreover, 1 µl of each oligoes (100µM), 1 µl of 10X T4 ligation buffer, 0.5 µl of T4 kinase (New England Biolabs, USA) and 6.5 µl of nuclease free sterile water were mixed for annealing reaction and annealing mixture was incubated at 37 ºC for 30 minutes before incubation at 95 ºC for 5 minutes and then decreasing the temperature from 95 ºC to 25 ºC as 5 ºC/min. Later on, annealed oligoes were diluted into sterile water as 1:200 for ligation reaction.

3.3.20 Restriction of LentiCRISPRv2 plasmid and insertion of sgRNAs

LentiCRISPRv2 is a plasmid that developed by Zhang lab [113] and accommodating two expression cassettes, hSpCas9 and the chimeric guide RNA. It can be digested by *BsmB*I, and a pair of annealed oligoes can be cloned into the single guide RNA scaffold. To digest the 5 µg of lentiCRISPRv2 plasmid, 2 µl of *BsmB*I restriction enzyme (New England Biolabs, USA (10 unit/ µl)), and 2.5 µl of Buffer 3 was mixed and the volume was completed to 25 µl by using nuclease free sterile water. Moreover, reaction mixture was incubated in thermal cycler for 1 hour at 55 ºC before being inactivated for 10 minutes at 80 ºC. Following that, dephosphorylation of the digested plasmid with Calf Intestinal Phosphatase (CIP) (NEB, USA) for 1 hour at 37 ºC in thermal cycler by mixing 1 µl of CIP with the previous digestion mixture. Subsequently, mixture was run on 1% Agarose gel for separation of bands with 120 V to purify 12kb long cut LentiCRISPRv2. Later, gel was imaged and only 12 kb digested plasmid containing part was cut and eluted from the gel by using GeneJET Gel Extraction Kit (Thermo Scientific, USA) according to manufacturer’s protocol. Later, 50 ng of eluted 12kb long cut LentiCRISPRv2 plasmid, 1 µl of diluted oligo duplex, 1 µl of 10X T4 ligation buffer, 0.5 µl of T4 ligase (New England Biolabs, USA) were mixed and the volume was completed to 10 µl by using nuclease free sterile water. At the end, ligation reaction was started at 16 ºC for overnight.

3.3.21 Flow Cytometry analyses of EdU staining

400,000 cells were plated in wells of 12-well plates as triplicates and were grown in normal growth conditions for 24 hours. Subsequently, EdU reagent was added to the wells to be 10µM final concentration and incubated for 2 hours. Moreover, cells were immediately collected in PBS by the help of scraper, followed by centrifugation at 1500 g for 5 min, at +4°C. After that, cells washed with 3 ml of 1% BSA in PBS before dislodging and mixing the pellet in 100 µl of Click-iT fixative. After that, incubation at room temperature for 15 minutes in the dark was conducted following wash step with 3 ml of 1% BSA in PBS. Remaining pellet was resuspended in 100 µl of 1X Click-iT saponin-based permeabilization and wash buffer and was incubated for 15 minutes. Later, Click-iT Plus reaction cocktail was prepared according to manual of the product and 0.5 ml of this mixture was added to each sample and incubated for 30 minutes at room temperature in the dark. Cells were washed with 3 ml of 1X Click-iT saponin-based permeabilization and wash buffer one more time and were resuspended in 90 µl of 1X Click-iT saponin-based permeabilization. Before staining the cells for DNA content with 5 µl of 7AAD for 10 minutes, RNAse treatment was conducted by the addition of 5 µl of RNAse for 5 minutes. At the end, cells were centrifuged at 1500 rpm at +4 ºC for 5 minutes and resuspended in 700 µl of permeabilization buffer to read the samples via flow cytometry.

3.3.22 Creation of *in vivo* tumor xenograft models

6 to 8 weeks old athymic nude mice were provided by the animal facility of the Bilkent University, Department of Molecular Biology and Genetics with the ethical permission of local ethics committee of Bilkent University. To create *in vivo* tumor xenograft model, 5 million Scrambled and IKBKE depleted Hep3B cells per mice, as it would be 2.5 million per flank of mice in 100 µl, and 10 million of Scrambled and IKBKE depleted SW480 cells per mice, as it would be 5 million per flank of mice in 100 µl, were cultured and prepared in cell culture. After that, cells were mixed with equal volume of matrigel and subcutaneously injected to the flanks of mice. Subsequently, tumor formation was followed by palpation for the first week and then tumors and weight of the animals were started to measure twice a week by digital caliper. Finally, experiment was ended by looking out for humane endpoint. After the end of the experiment, animals were sacrificed and tumors were extracted. Extracted tumors were

washed with PBS before transferring and incubating them in falcons containing 10% formalin for 1 hour at 4 ºC. Next, 10% formalin was replaced with 15% sucrose solution and incubated for 3 hours at 4 ºC. After that, 15% sucrose was replaced with 30% sucrose solution and incubated overnight at 4 ºC. At the end of this procedure, tumors were removed from 30% sucrose solution and embedded into plastic block by using OCT and stored at -80 ºC.

3.3.23 Creation of *in vivo* tumor metastasis models

6 to 8 weeks old athymic nude mice were provided by the animal facility of the Bilkent University, Department of Molecular Biology and Genetics with the ethical permission of local ethics committee of Bilkent University. To create *in vivo* tumor metastasis model, 2 million Scrambled and IKBKE depleted luciferase tagged DLD1 cells per mice were cultured and prepared in cell culture. After that, cells were intravenously injected through the tail vein of mice. Subsequently, metastases were followed monthly by using *in vivo* cell imager (IVIS) with the injection of D-Luciferin to the mice according to weight of the animal. Finally, Experiment was ended by looking out for humane endpoint. After the end of the experiment, animals were sacrificed and organs were extracted. Extracted organs were washed with PBS before transferring and incubating them in falcons containing 10% formalin for 1 hour at 4 ºC. Next, 10% formalin was replaced with 15% sucrose solution and incubated for 3 hours at 4 ºC. After that, 15% sucrose was replaced with 30% sucrose solution and incubated overnight at 4 ºC. At the end of this procedure, organs were removed from 30% sucrose solution and embedded into plastic block by using OCT and stored at -80 ºC.

3.3.24 Statistical Analyses

All statistical analyses were performed in GraphPad Prism 7.0 software, if not otherwise stated.

Chapter 4

Results

4.1 Analysis of IKKε expression in cell lines and patient materials *in silico*

After bioinformatic analyses conducted by using Cancer Cell Cycle Encyclopedia (CCLE) and cBioPortal TCGA patient cancer tissue databases, it was found that HCC and CRC cell lines were among the most IKKε expressing cell lines (Figure 4.1). Similarly, findings from the cBioPortal platform revealed that IKKε underwent high gene amplification in liver cancers and mRNA levels were relatively elevated (Figure 4.2).

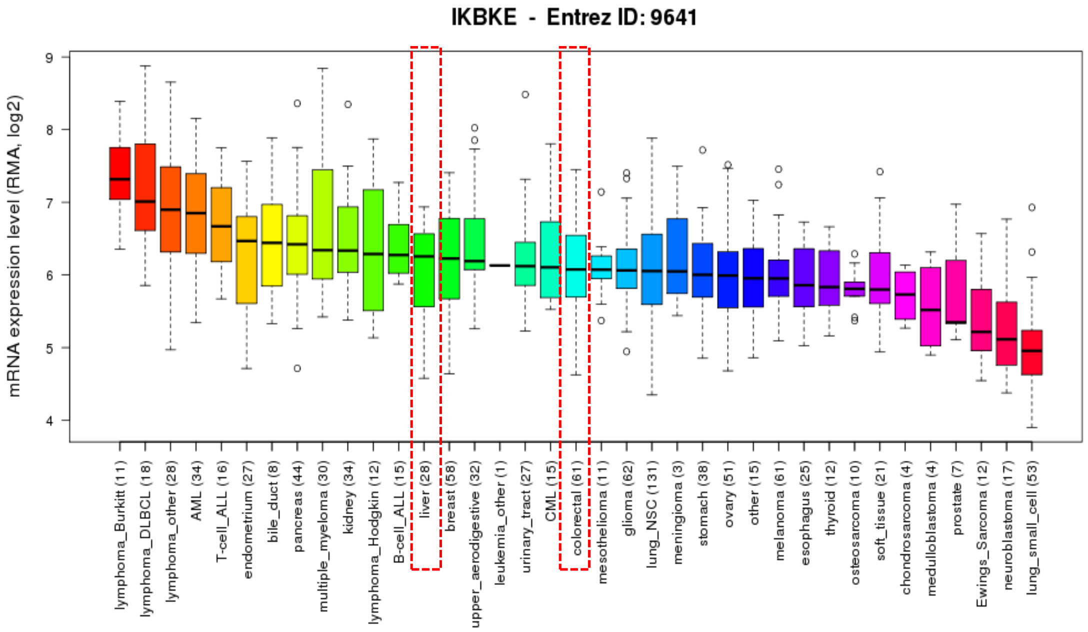

Figure 4.1. Gene Expression data for IKKε extracted from Cancer Cell Line Encyclopedia by using Gene-centric RMA-normalized mRNA expression data.

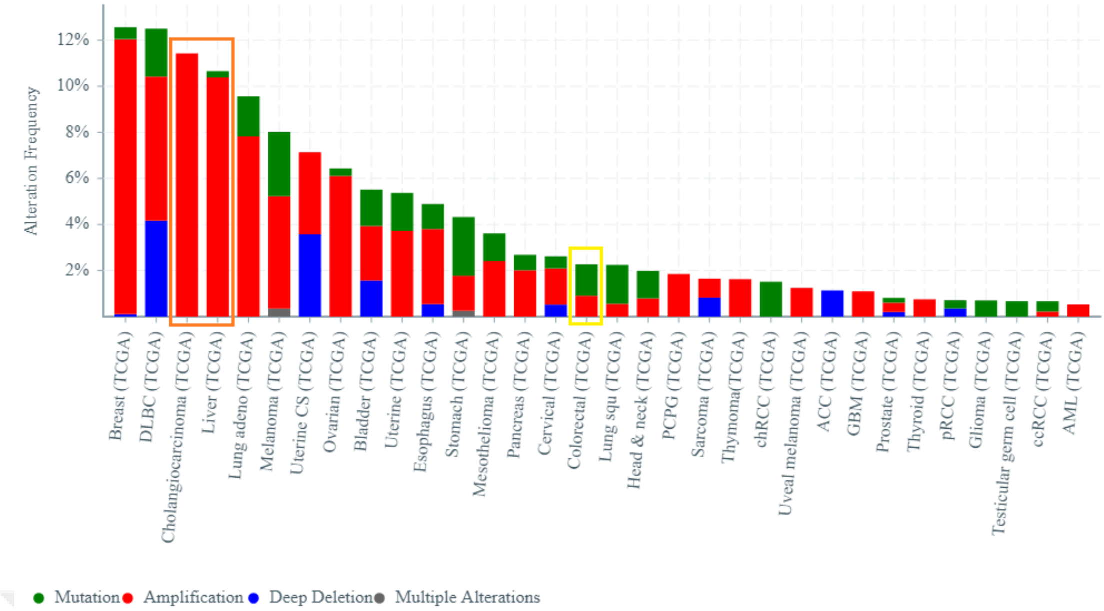

Figure 4.2. IKKε amplification in cBioPortal TCGA patient cancer tissues. According to the cBioPortal database, both cholangiocarcinoma and HCC are among the cancers in which IKKε is the most amplified. (red: amplification; blue: deletion; green: mutation; Orange rectangle is showing cholangiocarcinoma and liver, Yellow rectangle is showing Colorectal cancer)

Moreover, Kaplan-Meier survival curves were plotted by using RNAseq data from KM Plot database [114] based on IKKε levels in HCC patients (Figure 4.3). HCC patients with high IKKε expression have significantly reduced median survival compared to patients with low IKKε expression (Figure 4.3A). After further analysis, it was observed that median survival of male patients with high IKKε expression is significantly lower compared to males with low IKKε expression (Figure 4.3B), whereas female patients with either high or low IKKε expression in HCC cohort does not represent such significance (Figure 4.3C). Additionally, Male HCC patients with high IKKε expression demonstrate meaningful decrease in median survival in later stages, with poorer prognosis (Figure 4.3D, 4.3E and 4.3F).

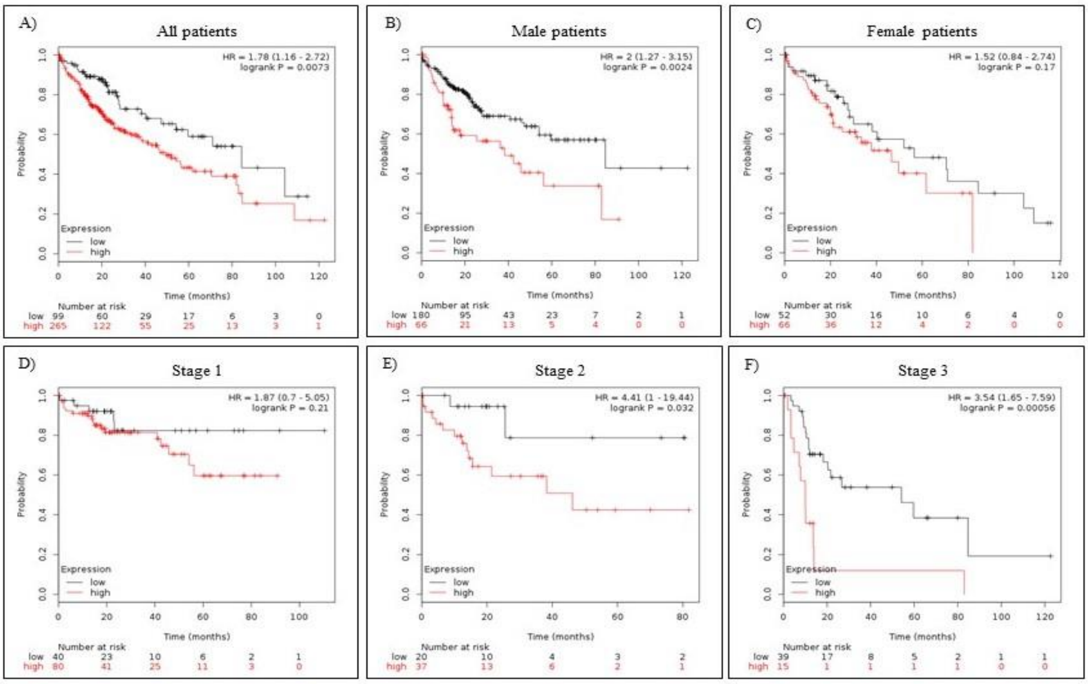

Figure 4.3. Kaplan Meier survival curves representing a gender or stage specific effects of IKKε expression in HCC patient prognosis. Graphs prepared by using mRNA RNAseq data of KM Plot database [114] according to IKKε level in HCC patients (n=364) A) All patient samples without any gender separation showed significant reduction in the median survival of the cohorts with high IKKε expression (Low expression cohort (LEC)= 84.4 months, High expression cohort (HEC)= 49.7 months (p=0.0073)) B) Male patient samples (n=246) demonstrated significant reduction in the median survival of the cohorts with high IKKε expression (LEC= 84.4 months, HEC= 38.3 months (p=0.0024)) C) Female patient samples (n=118) revealed non-significant reduction in the median survival of the cohorts with high IKKε expression (LEC= 56.5 months, HEC= 46.6 months (p=0.1659)) D) Stage I male cohort (n=120) showed non-significant reduction in the median survival of the cohorts with high IKKε expression (p=0.2073) E) Stage II male cohort (n=57) revealed significant reduction in the median survival of the cohorts with high IKKε expression (p=0.0318) F) Stage III male cohort (n=54) demonstrated non-significant reduction in the median survival of the cohorts with high IKKε expression (LEC= 54.1 months, HEC= 10 months (p=0.0006)) (red: high; black: low)

In addition to these preliminary observation in HCC, Göktuna et al. [65] shown that IKKε has important roles in the development of colon cancer in their previous studies. By using the *Apc*$^{+/min}$*-Ikbke*$^{-/-}$ mice (Wnt-driven tumor model), they have shown that tumor burden and tumor growth were greatly reduced. Furthermore, when in situ hybridization and IKKε mRNAs were examined in the same tumor model, it was found that IKKε was predominantly expressed in transformed epithelia and its expression increased through the tumor development.

4.2 Endogenous IKKε expression levels in HCC and CRC cell lines

In order to determine the cell lines to be used for the further experiments in this study, endogenous IKKε expression levels of HCC (Figure 4.4) and CRC (Figure 4.5) cell lines available in our laboratory were determined by western blot.

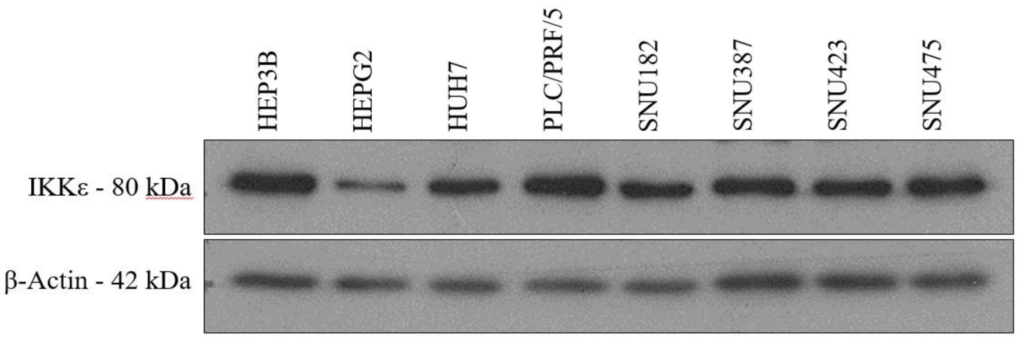

Figure 4.4. Measuring endogenous IKKε expression levels in HCC cell lines via western blot. After blotting proteins, antibodies against IKKε and β-Actin (loading control) was used to identify their relative protein levels. 20 µg of protein sample per cell line were used in this experiment.

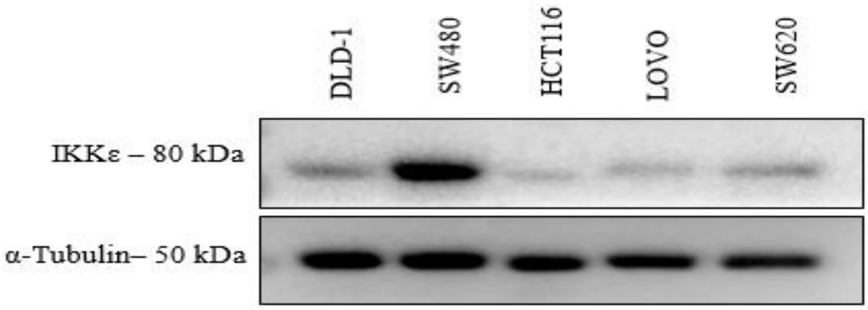

Figure 4.5. Measuring endogenous IKKε expression levels in CRC cell lines via western blot. After blotting proteins, antibodies against IKKε and β-Actin (loading control) was used to identify their relative protein levels. 20 μg of protein sample per cell line were used in this experiment.

Although all available HCC cell lines were used in some of the experiments throughout this study, HEP3B cell line, which has the highest IKKε expression among others, has been used the most. Subsequently, SW480, which has the highest IKKε expression, and DLD-1 cell lines were the CRC cell lines that were used in this study.

4.3 The role of IKKε in HCC cell viability

As it was shown previously by Göktuna et al. [65], IKKε has pro-survival role in colorectal cancer. For this reason, IKKε in HEP3B, PLC/PRF/5, SNU182, SNU387 and SNU423 cell lines were depleted by using IKKε targeting siRNA and treated with three different concentrations of PolyI:C (0 ng/ml, 50 ng/ml, and 100 ng/ml) which is a synthetic double-stranded RNA that imitates pathogen infection and cause immune system activation to induce apoptosis in cancer cells that express TLR3 [115]. By doing that, the role of IKKε in HCC cell viability was tried to be understood by end-point measurement via Cell Titer Glo assay. Although siRNA mediated IKKε depletion of the cells were successful (Figure 4.6), HEP3B (Figure 4.6A), SNU387 (Figure 4.6D), PLC/PRF/5 (Figure 4.6B) cells demonstrated a significant decrease in cell viability upon different concentration of PolyI:C underlining the pro-survival role of IKKε promoting HCC cell survival, especially HEP3B cells showed the most significant decrease (20% inhibition of cell viability after depletion, 55% inhibition of cell viability upon 50 ng/ml PolyI:C and 60% inhibition of cell viability after 100 ng/ml PolyI:C) whereas SNU182 (Figure 4.6C) cell line didn't show any decrease in cell viability and SNU 423 (Figure 4.6E) cell line only show a substantial reduction when it was treated with 100ng/ml of PolyI:C.

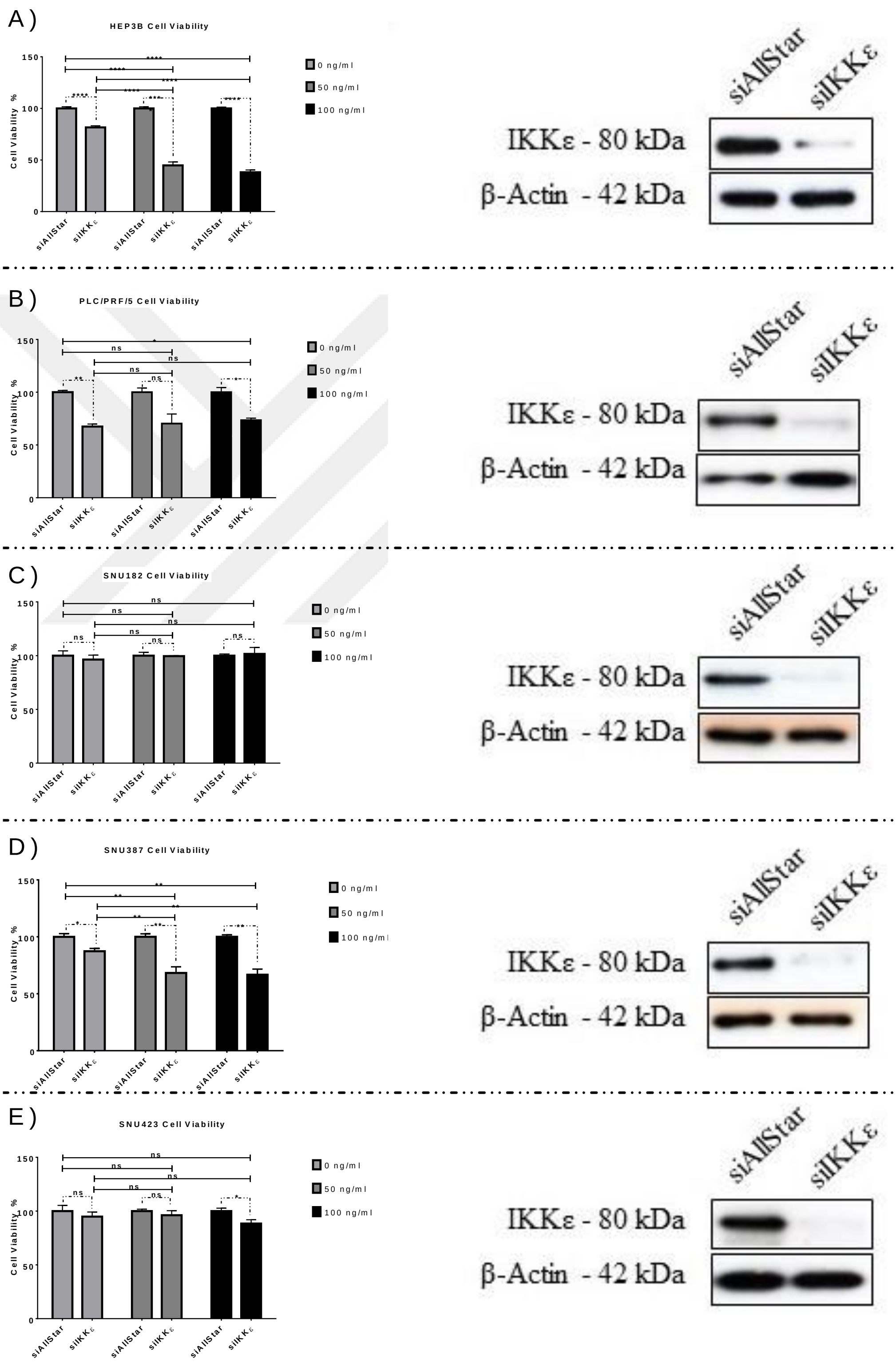

Figure 4.6. *In vitro* end-point viability assay in IKKε depleted HEP3B, PLC/PRF/5, SNU182, SNU387 and SNU423 cell lines. Cell lines were treated with 0 ng/ml, 50 ng/ml, and 100 ng/ml PolyI:C concentrations following siRNA mediated IKKε depletion and viability of the cells were measured by using Cell Titer Glo reagent. A-E) Viability of cell lines and western blot images representing siRNA-mediated IKKε knockdown. Data shown as mean ± SEM of triplicate wells, A) HEP3B cell line, representative of three independent experiments, B) PLC/PRF/5 cell line, representative of one experiment, C) SNU182 cell line, representative of one experiment, D) SNU387 cell line, representative of two independent experiments, E) SNU423 cell line, representative of two independent experiments. After blotting proteins, antibodies against IKKε and β-Actin (loading control) was used to identify their relative protein levels. 20 μg of protein sample per cell line were used in this experiment. p-values are denoted versus respective controls, Student's paired t-test. ns ≥ 0.05, * p<0.05, ** p<0.01, *** p<0.001, **** p<0.0001.

Although 50 ng/ml of PolyI:C treated PLC/PRF/5 cells didn't show statistically significant decline in cell viability (p=0.0592) (Figure 4.6B), it might be significant when the number of biological replicates increased. Additionally, when the copy number of HCC cell lines were analyzed in CCLE database, differences in IKKε and TLR3 copy numbers were observed. Thus, this might be the reason for different responses to Poly I:C upon IKKε depletion (Figure 4.7).

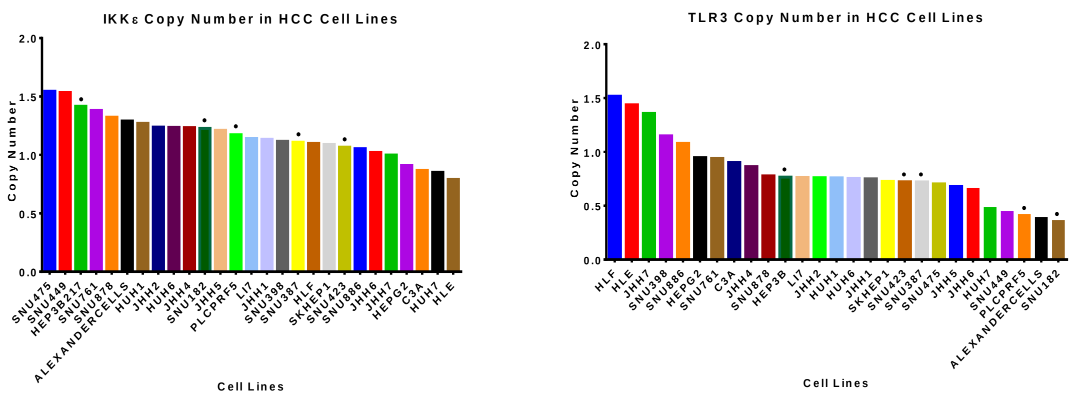

Figure 4.7. Copy number data for IKKε and TLR3 extracted from Cancer Cell Line Encyclopedia by using normalized copy number data. Cell lines that were used

in the cell viability experiments were emphasized with black dot on top of the corresponding bar.

4.4 The role of IKKε in HCC cell proliferation

After understanding the importance of IKKε for cell viability, to validate previous viability results which was conducted by using transiently IKKε transfected HCC cell lines, real time analysis of cell proliferation (RTCA proliferation) was carried out by using both shRNA mediated stably IKKε knocked down and CRISPR/Cas9 mediated IKKε knockout HEP3B cells. RTCA proliferation analysis revealed significant reduction in cell growth of HEP3B cells upon IKKε depletion both with shRNA and CRISPR/Cas9 methods (Figure 4.8). Hence, it is concluded that IKKε is important for cell viability (Figure 4.6) and cell proliferation (Figure 4.8).

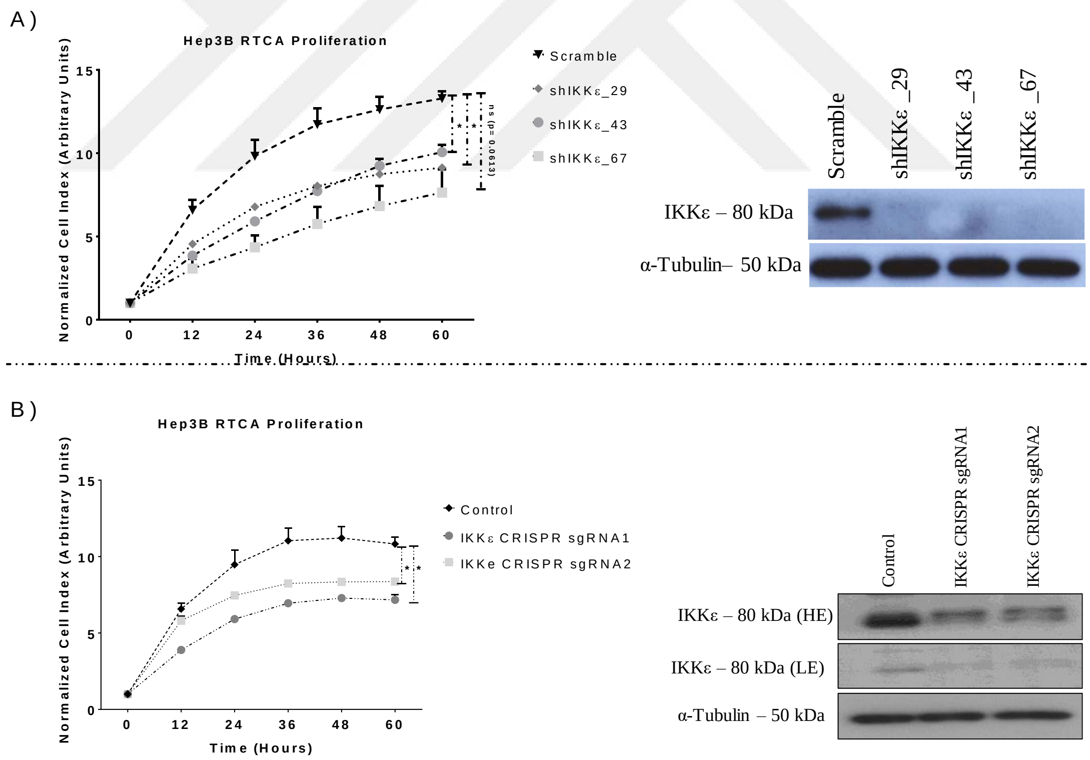

Figure 4.8. ***In vitro*** **real time cell proliferation assay in IKKε depleted HEP3B cells.** RTCA proliferation analysis of shRNA mediated stably IKKε knocked down (A) and CRISPR/Cas9 mediated IKKε knockout (B) HEP3B cells and confirmation of IKKε depletion by western blot. After blotting proteins, antibodies against IKKε and β-Actin

(loading control) was used to identify their relative protein levels. 20 µg of protein sample per cell line were used in this experiment. Data shown as mean ± SEM of duplicate wells and representative of one experiment. p-values are denoted versus respective controls, Student's paired t-test. ns ≥ 0.05, * p<0.05, ** p<0.01, *** p<0.001, **** p<0.0001.

4.5 The role of IKKε in HCC cell migration

After revealing the importance of IKKε for cell viability and proliferation, particularly in HEP3B cell line, wound healing assays were performed to understand role of IKKε in cell migration. For this purpose, HEP3B, HUH7, SNU182 and SNU387 cell lines transiently transfected with IKKε targeting siRNA. Due to the differences in doubling time of the cell lines, gap closure of HEP3B and HUH7 cell lines were followed for 48 hours by taking image at every 24 hours and SNU182 and SNU387 cell lines were tracked for 24 hours by taking image at every 12 hours. Gaps were closed equally in both control and IKKε depleted cells without any significant difference by time. Thus, it is revealed that siRNA mediated IKKε depletion didn't result in a dramatic change in HCC cell migration in all four cell lines (Figure 4.9). To verify this, HEP3B cells stably transfected with IKKε targeting shRNAs were used for wound healing assay. Gap closure of stably transfected HEP3B cells in which serum starvation was applied were tracked for 72 hours by taking their images at every 24 hours. However, gaps were closed equally without any significant change by time. Thus, these findings were correlated with each other (Figure 4.9 & Figure 4.10) and indicating that IKKε does not have a drastic effect on HCC cell migration.

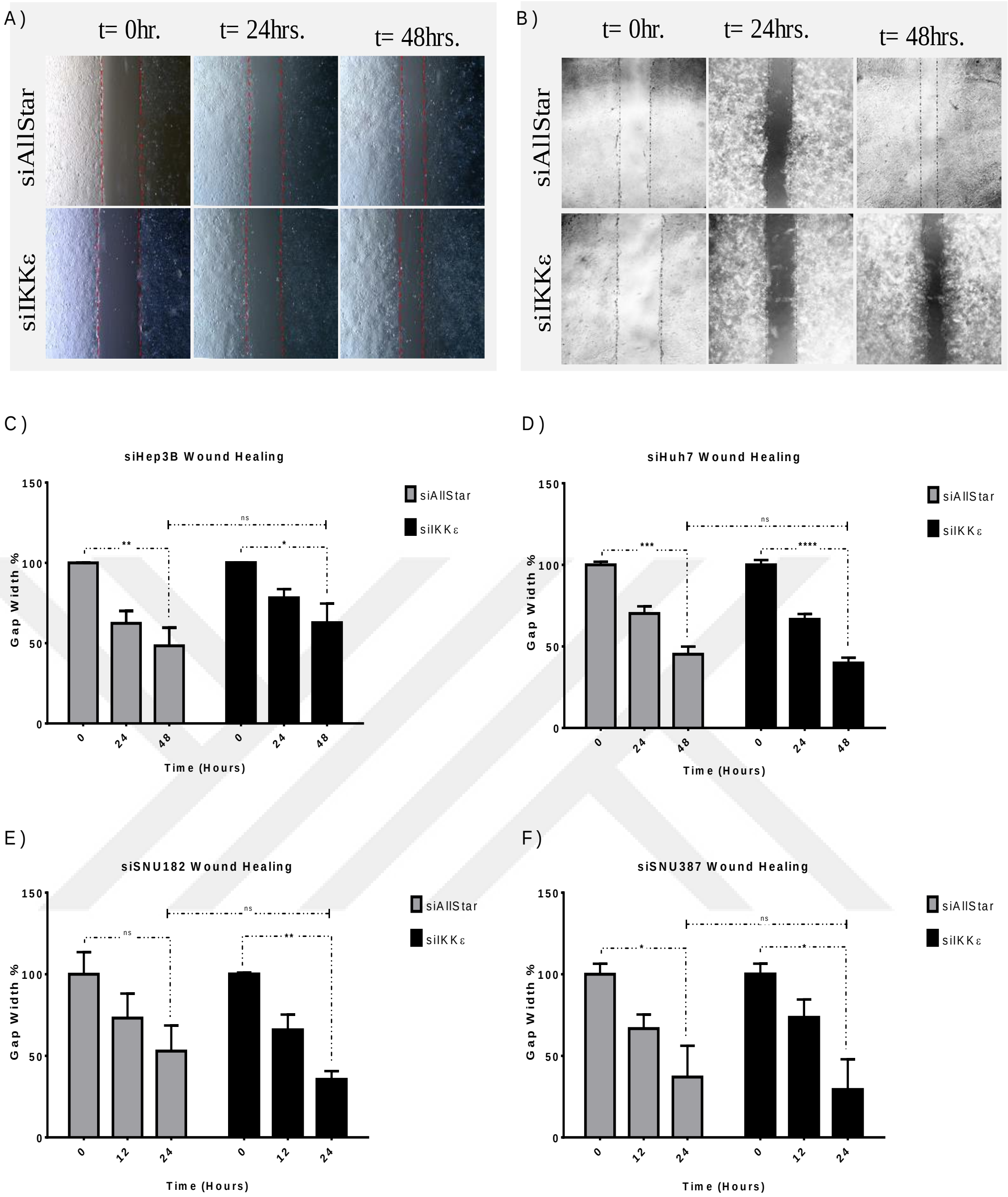

Figure 4.9. The effect of siRNA mediated transient IKKε depletion in HCC cell migration via *in vitro* wound healing assay. A&C) Wound healing assay performed in transiently IKKε depleted A&C) HEP3B cell line and representative images per time point, B&D) HUH7 cell line and representing images per time point. E) SNU182 cell line. F) SNU387 cell line. Data shown as mean ± SEM of triplicate wells and representative of one experiment; ns ≥ 0.05, * p<0.05, ** p<0.01, *** p<0.001, **** p<0.00001. p-values are denoted versus respective controls, Student's paired t-test.

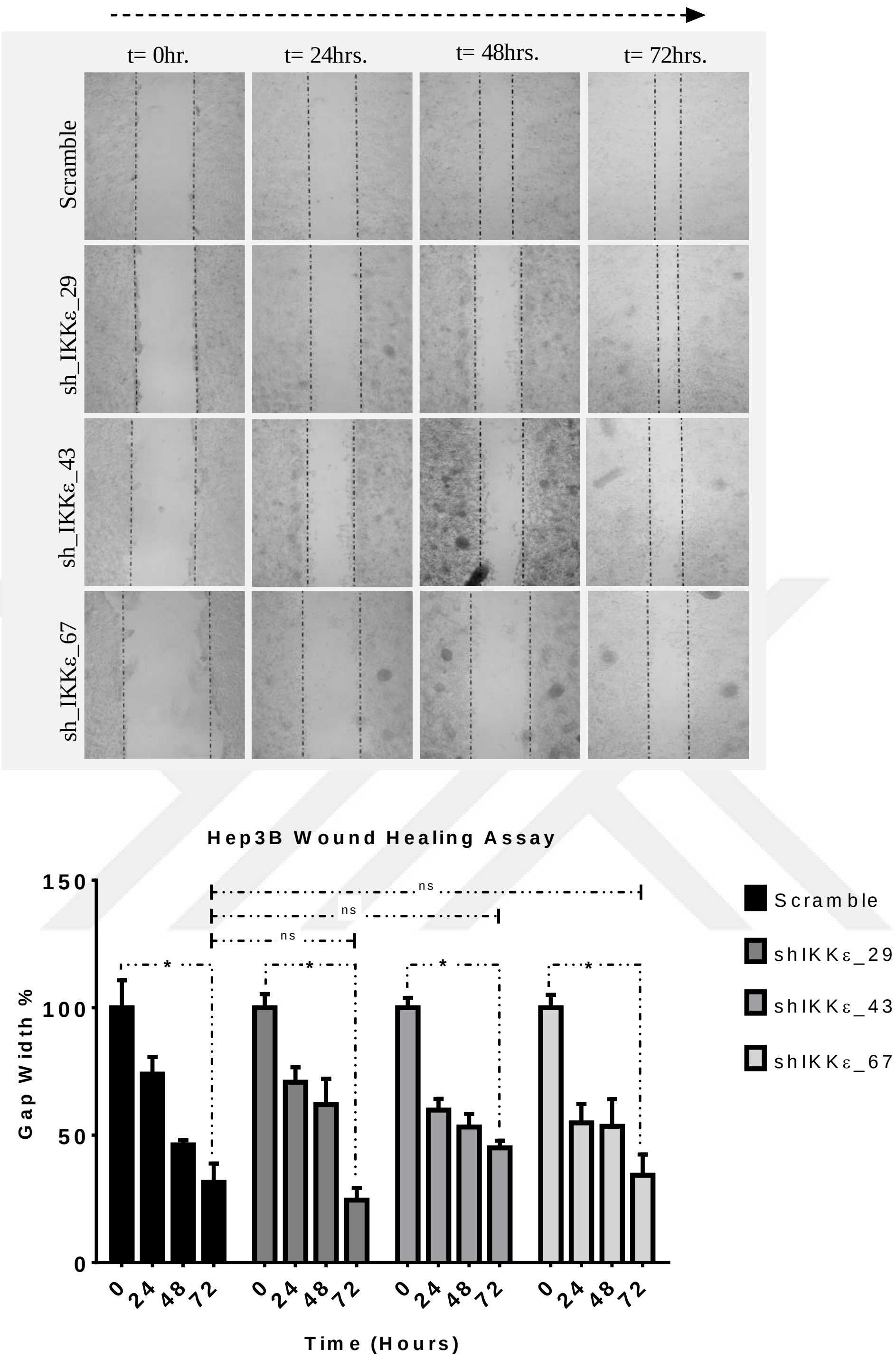

Figure 4.10. The effect of shRNA mediated stable IKKε depletion in HCC cell migration via *in vitro* wound healing assay. Wound healing assay performed in stably IKKε depleted HEP3B cell line and representative images per time point. Data shown as mean ± SEM of triplicate wells and representative of one experiment; ns ≥ 0.05, * p<0.05, ** p<0.01, *** p<0.001, **** p<0.00001. p-values are denoted versus respective controls, Student's paired t-test.

4.6 The role of IKKε in epithelial-to-mesenchymal transition of HEP3B cells

In order to understand whether IKKε plays a role in epithelial-to-mesenchymal transition of HEP3B cells, EMT markers were analyzed by qRT-PCR and western blotting besides the analysis of cell migration by wound healing assay. qRT-PCR and western blot analyses conferred an increase in epithelial markers and decrease in mesenchymal markers upon loss of IKKε, especially in HEP3B cells which were depleted by using CRISPR/Cas9 method (Figure 4.11B, 4.11D, and 4.11F). Although, shRNA depleted cells also demonstrated some non-significant alterations in both epithelial and mesenchymal markers, which didn't exhibit a significant trend in all three IKKε targeting shRNA constructs (Figure 4.11A, 4.11C, and 4.11E), but IKKε knockout HEP3B cells which were stably transfected with CRISPR/Cas9 constructs demonstrated a significant trend both in qRT-PCR and western blot analyses (Figure 4.11). Hence, an increase in epithelial markers and a decrease in mesenchymal markers in IKKε knockout HEP3B cells (Figure 4.11) (especially a dramatic increase of E-cadherin in cells depleted via CRISPR/Cas9 method) didn't lose E-cadherin mediated cell-cell adhesion and their polarity which may explain the reason why absence of IKKε doesn't affect HCC cell migration (Figure 4.9 & Figure 4.10).

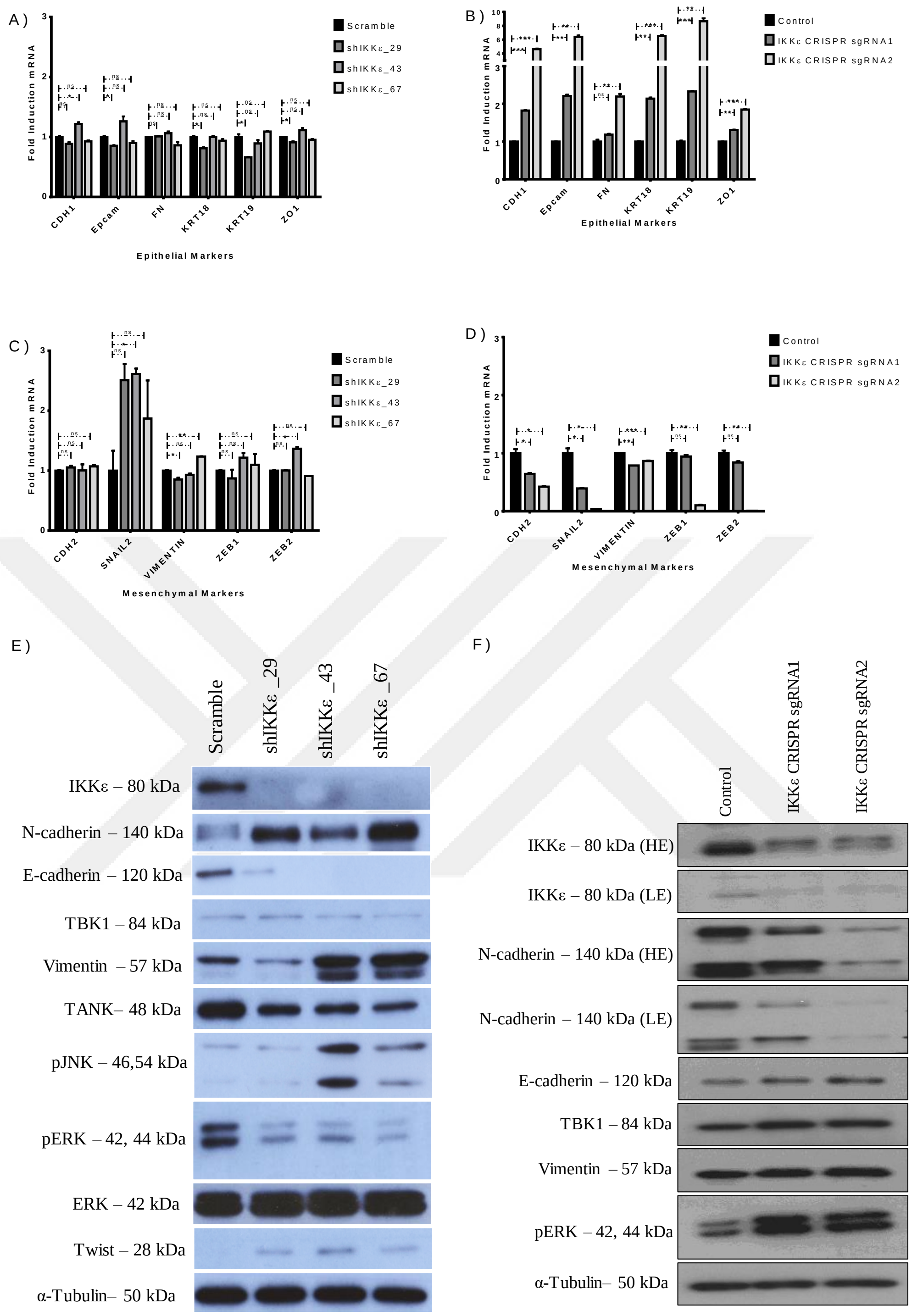

Figure 4.11. The effect of IKKε depletion in epithelial-to-mesenchymal transition in HEP3B cells. Western blot and qRT-PCR analyses revealed an increase in the expression of epithelial markers and decrease in mesenchymal markers upon generation of CRISPR/Cas9 mediated IKKε knockout HEP3B cells. A, C, E) Changes in the expression of A) epithelial markers and C) mesenchymal markers in HEP3B cells depleted by shRNA. B, D, F) Changes in the expression of B) epithelial markers and

D) mesenchymal markers in HEP3B cells depleted by CRISPR/Cas9. After blotting proteins, antibodies against IKKε, TBK1, TANK, E-cadherin, N-cadherin, Vimentin, pJNK, pERK, ERK, Twist and Tubulin-α (loading control) were used to identify their relative protein levels. 20 µg of protein per sample were used in this experiment. Data shown as mean ± SEM of duplicate wells and representative of one experiment; ns ≥ 0.05, * $p<0.05$, ** $p<0.01$, *** $p<0.001$. p-values are denoted versus respective controls, Student's paired t-test.

4.7 The effect of IKKε loss in HEP3B xenograft growth *in vivo*.

HEP3B cells stably transfected by using control and IKKε targeting shRNAs. Subsequently, stably transfected cells were subcutaneously injected to both flanks of nude mice to determine whether IKKε has an effect on HCC tumor growth. Compared to control cells, injection of IKKε depleted cells revealed a substantial decrease in tumor volume (Figure 4.12) correlating with previous findings in which IKKε resulted in a significant reduction of cell proliferation (Figure 4.6 & Figure 4.8). Because of the substantial differences in tumor volumes upon IKKε depletion, it is discovered that IKKε is essential for HCC tumor growth *in vivo* which also highlight the importance of IKKε for cell proliferation.

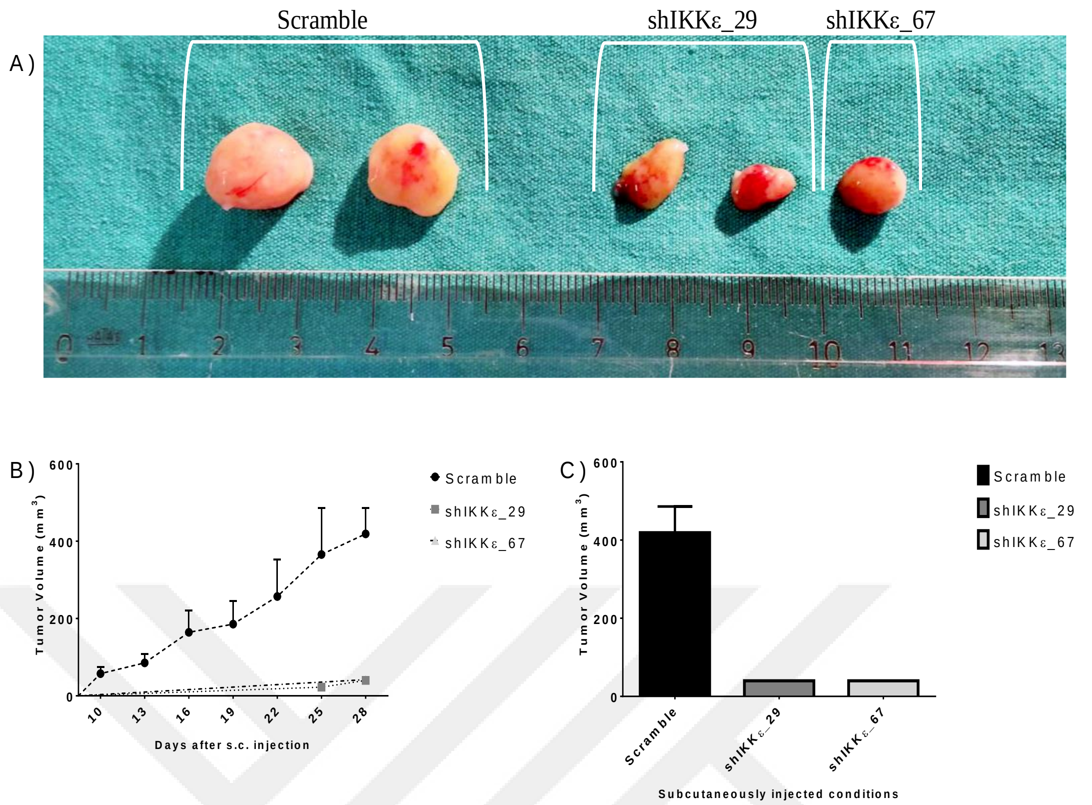

Figure 4.12. The effect of IKKε loss in tumorigenicity of HEP3B cells *in vivo*. 2.5 × 10^6 HEP3B cells stably transfected with control and IKKε targeting shRNAs were injected to nude mice with the help of matrigel ((n=3) except HEP3B shIKKε_29 mice in which one animal died three days after tumor inoculation). Mice were sacrificed 28 days after tumor injection. A) Substantial difference in terms of tumor size. B) Growth curves demonstrating alterations in tumor volume. C) Column bar graph exhibiting the differences in tumor volume.

4.8 The effects of IKKε loss in CRC cell proliferation and anchorage independent growth of CRC cells

In order to test whether IKKε depletion lead to an increase in CRC cell proliferation, DLD1 and SW480 CRC cell lines were selected according to their IKKε expression (Figure 4.5) and stably transfected to deplete IKKε using CRISPR/Cas9 and shRNA constructs. After that, end-point (Cell Titer Glo) analysis for DLD1 cell line and real time cell proliferation analyses for both DLD1 and SW480 cell lines were conducted. End-point analysis of DLD1 cell line conferred meaningful increase in cell growth (20% elevation in shIKKε_29, 30% elevation in shIKKε_43, 10% elevation in shIKKε_67) (Figure 4.13B). Consequently, RTCA proliferation analysis revealed that cell growth significantly increased in IKKε depleted DLD1 cells (Figure 4.13A) . However, although increase in cell growth of IKKε depleted SW480 cells was observed during the experiment (Figure 4.13D), statistical significance was not found at the end. Thus, IKKε may have a role in cell growth and its depletion promotes CRC cell proliferation. Moreover, promotion of CRC cell growth upon IKKε depletion was further recapitulated by clonogenicity assay conducted using SW480 cells (Figure 4.15) and by the anchorage independent growth of IKKε depleted DLD1 cells which show increased cell viability upon depletion (Figure 4.14B). Also, number of colonies smaller than 50 μm diameter were increased in depleted cells compared to control (Figure 4.14A, 4.14C, and 4.14D). All in all, these additional clonogenicity and anchorage independent growth assay data underline the importance of IKKε in cell proliferation.

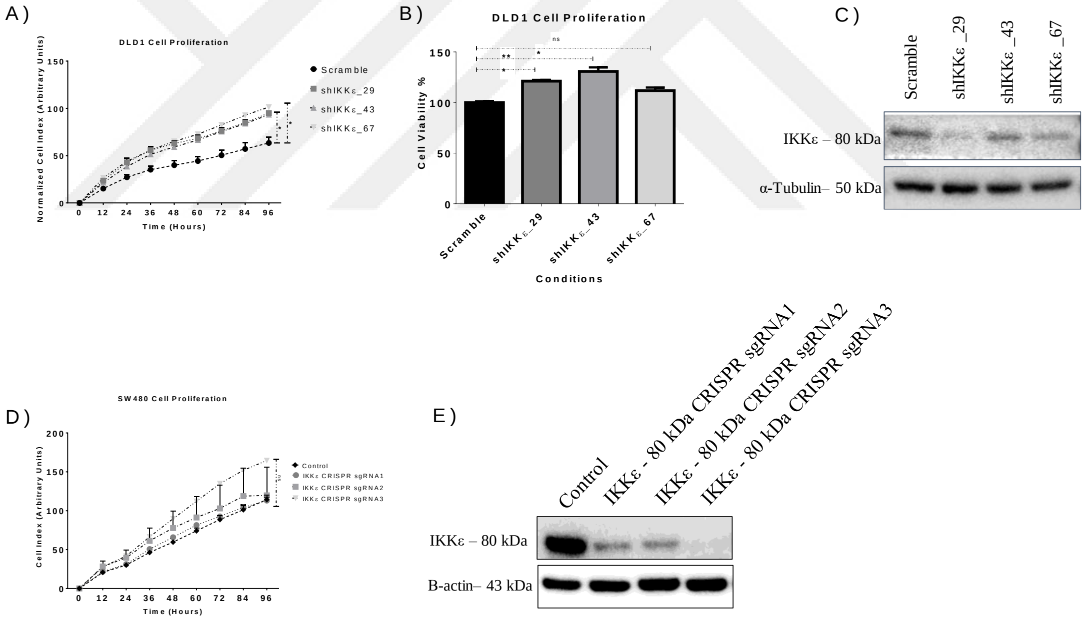

Figure 4.13. ***In vitro* real end-point and real time cell proliferation assay in IKKε depleted DLD1 and SW480 cells.** A) Real-time cell analysis of shRNA mediated IKKε depletion on DLD1 cell line and western blot analysis of IKKε depletion (C). B) End-point analysis of CRISPR/Cas9 mediated IKKε depletion on SW480 cell line and western blot analysis of IKKε depletion (C). D) Real-time cell analysis of CRISPR/Cas9 mediated IKKε depletion on SW480 cell line and western blot analysis of IKKε depletion. Data shown in section Figure 4.13A & 4.13D were as mean ± SEM

of duplicate wells and representative of one experiment and in section C was as mean ± SEM of triplicate wells and representative of one experiment ; ns ≥ 0.05, * p<0.05, ** p<0.01, *** p<0.001, **** p<0.00001. p-values are denoted versus respective controls, Student's paired t-test. After blotting proteins, antibodies against IKKε, β-actin (loading control) and Tubulin-α (loading control) were used to identify their relative protein levels. 20 µg of protein per sample were used in this experiment.

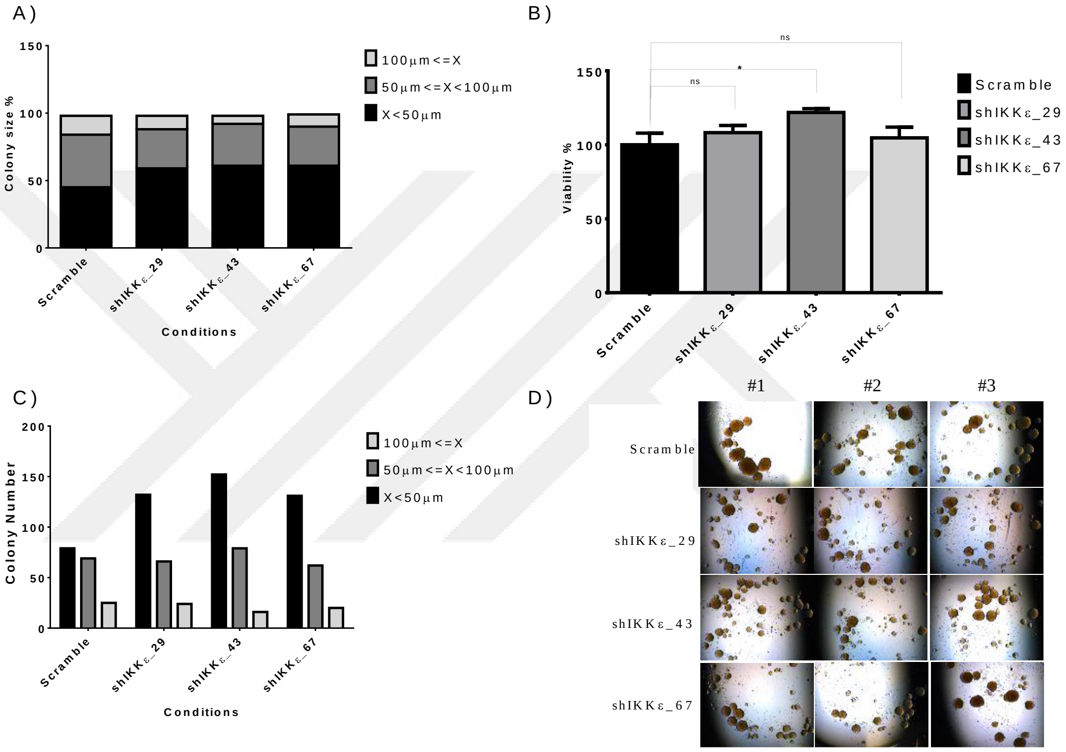

Figure 4.14. The effects of IKKε depletion in viability and anchorage independent growth of DLD1 cells. A) Stacked bar graph representation of colony numbers as percentage representing an increase number of colonies smaller than 50 µm diameter due to depletion. B) Viability of the cells were measured with WST-1 cell proliferation reagent. Although there was a trend in which viability of the IKKε depleted cells increased, only shIKKε _43 condition was statistically significant. Data shown as mean ± SEM of triplicate wells and representative of three experiments; ns ≥ 0.05, * p<0.05, ** p<0.01, *** p<0.001, **** p<0.00001. p-values are denoted versus respective controls, Student's paired t-test. C) Colony numbers according to sizes. D) Representative images of the colonies formed.

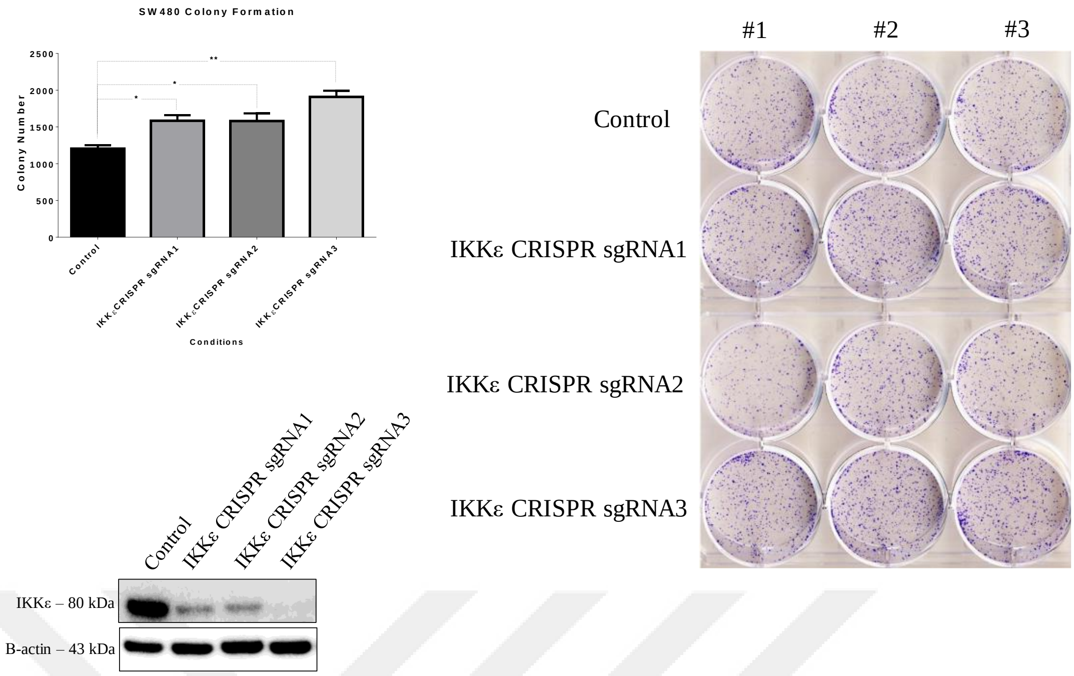

Figure 4.15. The effects of IKKε loss in SW480 colony formation. Thousands of SW480 cells were seeded per well of 6 well plate as triplicates. 10 days later, cells were stained with crystal violet and colonies were counted by Clono-Counter software**.** After blotting proteins, antibodies against IKKε and β-actin (loading control) were used to identify their relative protein levels. 20 μg of protein per sample were used in this experiment. Data shown as mean ± SEM of triplicate wells and representative of one experiment; ns ≥ 0.05, * p<0.05, ** p<0.01, *** p<0.001, **** p<0.00001. p-values are denoted versus respective controls, Student's paired t-test.

4.9 The role of IKKε in CRC cell migration

After understanding the importance of IKKε for cell proliferation in CRC cells, particularly in DLD1 cell line, wound healing assays were performed to understand role of IKKε in cell migration. For this purpose, DLD1 and SW480 cell lines were stably transfected to deplete IKKε using CRISPR/Cas9 and shRNA constructs. Gap closure of DLD1 cell line was followed for 48 hours by taking image at every 24 hours and SW480 cell line in which serum starvation was applied were tracked for 96 hours by taking image at every 24 hours. Gaps were closed equally in both control and IKKε depleted cells without any significant difference by time. Thus, it is revealed that IKKε depletion didn't result in a dramatic change in CRC cell migration in both cell lines

(Figure 4.16 & Figure 4.17). More advanced technique, real time cell migration analysis was conducted by using the same DLD1 cells that are used for wound healing assay to verify previous finding (Figure 4.16). Migration of DLD1 cells were followed for 72 hours by taking measurements for every 15 minutes via RTCA device and RTCA migration analysis revealed insignificant changes in the migration of IKKε depleted DLD1 cells (Figure 4.16B) which correlates with wound healing results and indicates that IKKε does not have a drastic effect on CRC cell migration.

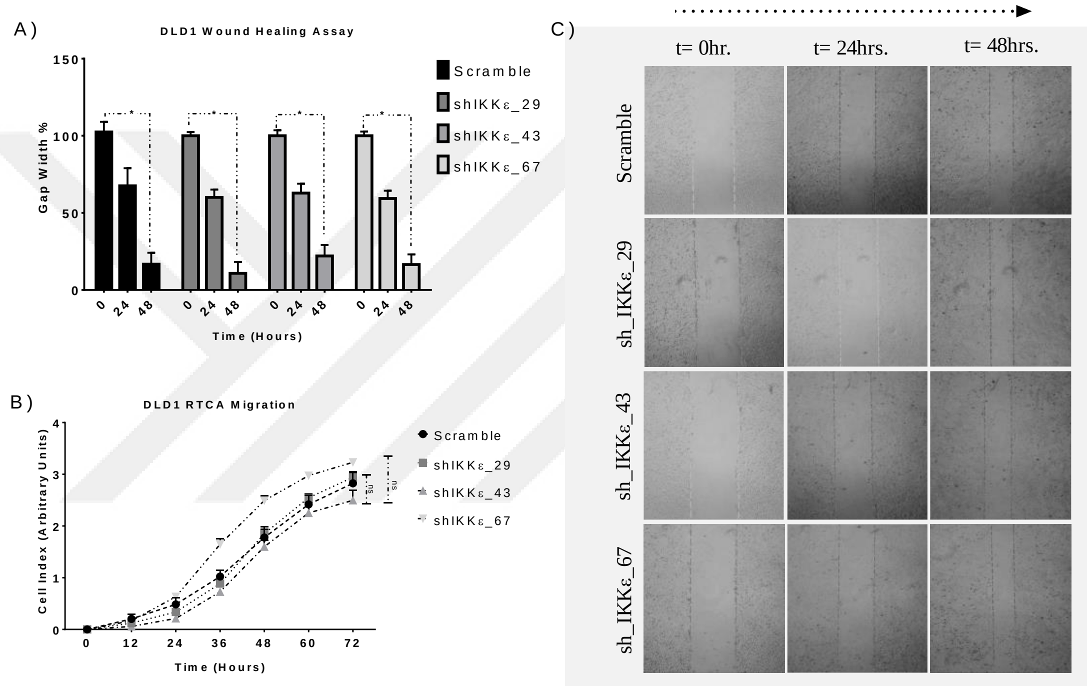

Figure 4.16. The effect of shRNA mediated IKKε depletion in DLD1 cell migration via *in vitro* wound healing and RTCA migration assays. A&C) Wound healing assay performed in DLD1 cells stably transfected with shRNAs and representing images per time point. B) Real-time cell migration analysis of DLD1 cells stably transfected with shRNAs. Data shown as mean ± SEM of triplicate wells and representative of one experiment; ns ≥ 0.05, * p<0.05, ** p<0.01, *** p<0.001, **** p<0.00001. p-values are denoted versus respective controls, Student's paired t-test.

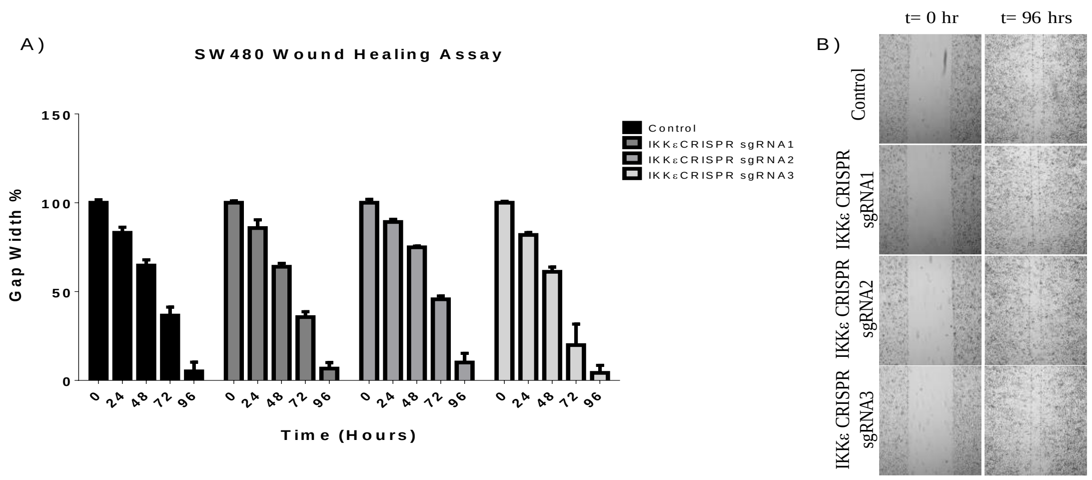

Figure 4.17. The effect of CRISPR/Cas9 mediated IKKε depletion in SW480 cell migration via *in vitro* wound healing assay. A & B) Wound healing assay performed in DLD1 cells stably transfected with CRISPR/Cas9 constructs and representing images per time point. Data shown as mean ± SEM of triplicate wells and representative of one experiment; ns ≥ 0.05, * p<0.05, ** p<0.01, *** p<0.001, **** p<0.00001. p-values are denoted versus respective controls, Student's paired t-test.

4.10 The role of IKKε in epithelial-to-mesenchymal transition of CRC cells

In order to understand whether IKKε plays a role in epithelial-to-mesenchymal transition of CRC cells, EMT markers were analyzed by qRT-PCR and western blotting besides the analysis of cell migration by RTCA and wound healing assay. qRT-PCR and western blot analyses conferred an increase in some epithelial markers such as KRT18, ZO1 and also in Vimentin which is a mesenchymal marker in DLD1 cells (Figure 4.18A, 4.18B). Nevertheless, significant decrease in CDH1 which is another epithelial marker was observed in qRT-PCR of DLD1 cell line (Figure 4.18A). However, the changes detected in the qRT-PCR of DLD1 cell line was not detected by western blot analysis (Figure 4.18C). Moreover, SW480 cells in which IKKε depleted didn't exhibit any significant alteration in EMT marker expression according to qRT-PCR results (Figure 4.19A & B). Interestingly, strange Vimentin expression was detected in the cells which was transfected with IKKε CRISPR sgRNA2 construct (Figure 4.19C).

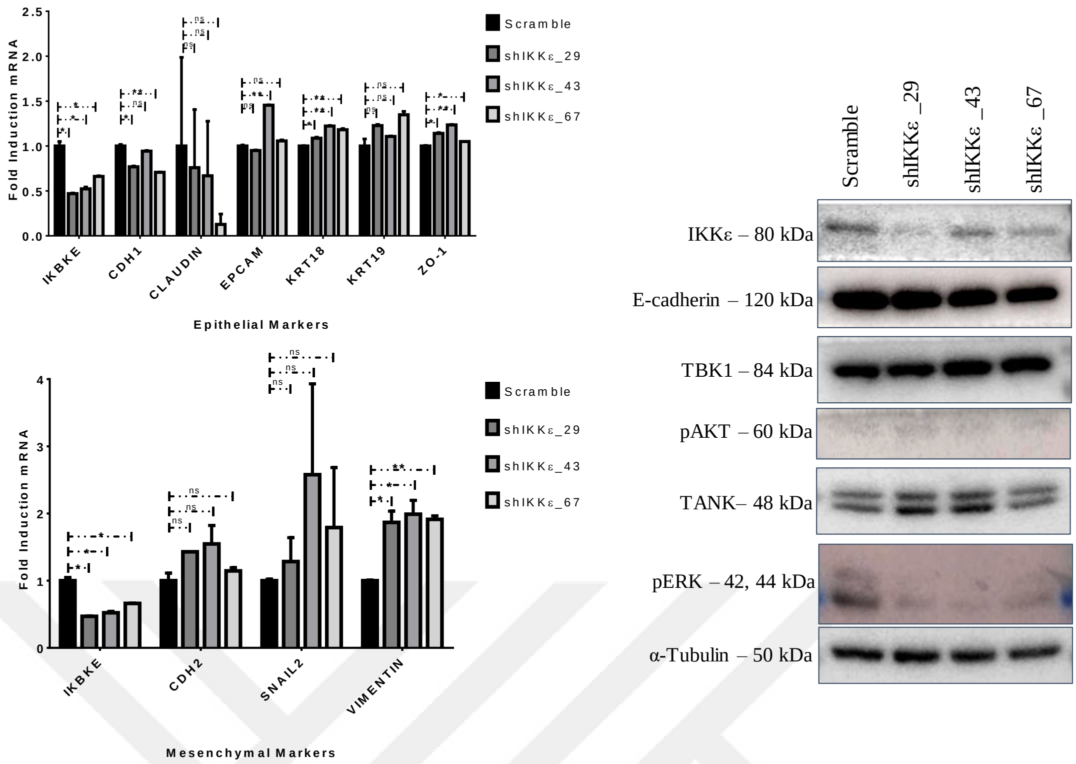

Figure 4.18. Expression of EMT markers upon IKKε depletion in DLD1 cell line. Western blot and qRT-PCR analyses revealed an increase in some epithelial markers such as KRT18, ZO1 and also in Vimentin which is a mesenchymal marker in DLD1 cells. Interestingly, significant decrease in CDH1 which is another epithelial marker was observed in qRT-PCR. However, the changes detected in the qRT-PCR of DLD1 cell line was not detected by western blot analysis. After blotting proteins, antibodies against IKKε, TBK1, TANK, E-cadherin, pERK and Tubulin-α (loading control) were used to identify their relative protein levels. 20 µg of protein sample per sample were used in this experiment. Data shown as mean ± SEM of duplicate wells and representative of one experiment; ns ≥ 0.05, * $p<0.05$, ** $p<0.01$, *** $p<0.001$. p-values are denoted versus respective controls, Student's paired t-test.

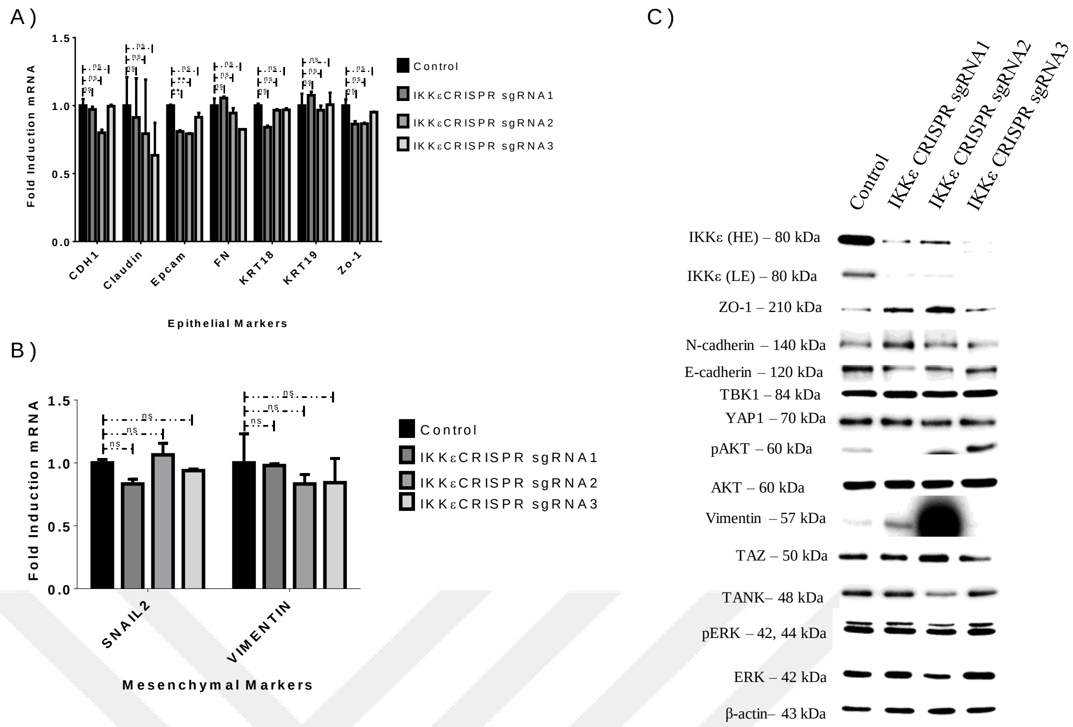

Figure 4.19. Expression of EMT markers upon IKKε depletion in SW480 cell line. A, B, and C) Western blot and qRT-PCR analyses revealed IKKε depleted SW480 cells didn't exhibit any significant alteration in EMT marker. Interestingly, strange Vimentin expression was detected in the cells which was transfected with IKKε CRISPR sgRNA2 construct (C). After blotting proteins, antibodies against IKKε, TBK1, TANK, E-cadherin, N-cadherin, Vimentin, YAP1, TAZ, pAKT, AKT, pERK, ERK and β-catenin (loading control) were used to identify their relative protein levels. 20 µg of protein per sample were used in this experiment. Data shown as mean ± SEM of duplicate wells and representative of one independent experiment; ns ≥ 0.05, * p<0.05, ** p<0.01, *** p<0.001. p-values are denoted versus respective controls, Student's paired t-test.

4.11 The effect of IKKε loss in SW480 xenograft growth *in vivo*.

SW480 cells stably transfected by using control and IKKε targeting CRISPR/Cas9 constructs. Subsequently, stably transfected cells were subcutaneously injected to both flanks of nude mice to determine whether IKKε has an effect on CRC tumor growth. Compared to control cells, injection of IKKε depleted cells promoted a substantial augmentation in tumor volume (Figure 4.20) correlating with previous findings in which IKKε resulted in a significant rise in cell proliferation (Figure 4.13, Figure 4.14 & Figure 4.15). Because of the substantial differences in tumor volumes upon IKKε depletion, it is discovered that IKKε promotes CRC tumor growth *in vivo* which also highlight the importance of IKKε for cell proliferation.

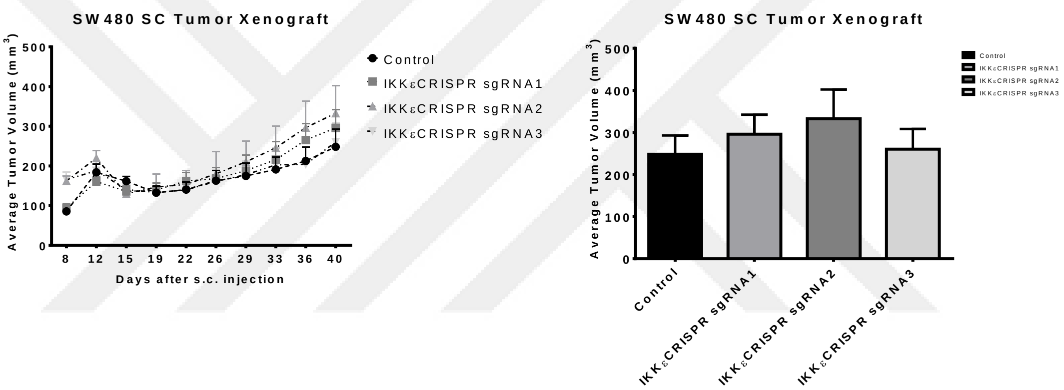

Figure 4.20. The effect of IKKε loss in SW480 xenograft growth *in vivo*. 5×10^6 SW480 cells stably transfected with control and IKKε targeting CRISPR constructs were injected to nude mice with the help of matrigel (n=5). A) Growth curves demonstrating alterations in tumor volume. B) Column bar graph exhibiting the differences in tumor volume.

Chapter 5

Discussion

Although the mechanisms underlying for metastasis and tumor growth are poorly understood, tumor microenvironment is vital for these processes. Cell survival, invasion, proliferation and inflammatory immune responses are various important physiological functions which are regulated by NF-κB and it is proposed that NF-κB is a pivotal link between inflammation and cancer due to its activation in variety of tumors [116, 117]. IKKε and TBK1, non-canonical inhibitor of κB kinases, act as an effector of NF-κB to promote tumorigenesis providing a bridge between NF-κB mediated inflammation and cancer and regulate NF-κB signaling [116, 118, 119]. Furthermore, IKKε either directly phosphorylates NF-κB p65 or phosphorylates Akt, which later phosphorylates and results in p65 activation, to potentiate tumorigenesis and the activity of NF-κB due to its tumor promoting function [58, 59, 100, 101]. Additionally, altered IKKε is able to activate STAT3 by direct phosphorylation which assist oncogenic activation of IKKε in various cancers such as breast and lung cancers [120-122]. IKKε is overexpressed and act like oncogene in glioma [87], esophageal squamous cell carcinoma [88], gastric cancer [89], non-small lung cancer [90], pancreatic ductal adenocarcinoma [91], prostate cancer [92, 93], ovarian cancer [94, 95], breast cancer [96-98] which makes it an important target to combat to treat cancer Despite current studies showing involvement of IKKε in the migration and proliferation of particular cancers, functional role of IKKε in the progression of HCC still unexplored.

In this study, roles played by IKKε has been demonstrated for the first time in hepatocellular carcinogenesis. *In silico* analysis performed by using mRNA RNAseq data of KM Plot database [114] proposed having high levels of IKKε protein expression is closely related to advanced HCC and poor overall survival in male HCC patients (Figure 4.3). Consequently, amplification of IKKε was detected in HCC according to cBioPortal TCGA patient cancer tissues (Figure 4.2). These findings indicate that overexpression of IKKε has strong association with poor prognosis of HCC. First, IKKε protein expression levels of available HCC cell lines were examined and it was indicated that IKKε protein expression was higher in HEP3B cells. Then, HEP3B, PLC/PRF/5, SNU182, SNU387, SNU423 cells with transient IKKε depletion and HEP3B cells with stable knocked-down IKKε were created in order to understand the potential function of IKKε in metastasis and growth of HCC cells. The analysis of cell viability by the end-point (Cell Titer Glo) and proliferation by real time cell proliferation analyses demonstrated that compared with control cells, IKKε silenced cells had lower cell viability and proliferation. Due to reduced HCC cell proliferation upon IKKε depletion, it is proposed that IKKε may not have a role in tumor initiation but in tumor progression. As it was previously shown by Adli et al. [98], IKKε knockdown results in a decrease in HeLa cell proliferation. Moreover, Barbie et al. reported that the use of CYT387 which is JAK/IKKε/TBK1 multi-target inhibitor, reduces triple-negative breast cancer proliferation and survival *in vitro* as well as tumor progression *in vivo* [123]. Moreover, Boehm et al. revealed that IKKε is overexpressed and amplified in breast cancer cell lines as well as in tumors derived from patients. Subsequently, they silenced IKKε and demonstrated a decrease in cell viability [97]. Recently, several groups exhibited that hippo pathway is inactivated by IKKε via negative regulation of LATS1&2 [124-129]. Thus, upon IKKε silencing either by amlexanox, inhibitor of IKKε, or by shRNA and siRNA mediated knockdown, decrease in glioma cell proliferation, survival, metastasis and invasion is demonstrated as well as an increase in apoptosis. Hence, decrease in HCC cell viability and proliferation upon IKKε depletion might be explained through Hippo pathway mechanistically. Nevertheless, wound healing assays didn't exhibit any alteration in the wound recovery upon IKKε depletion compared to control. To observe changes in the wound recovery, epithelial to mesenchymal transition can be induced by using TGF-β [130]. Collectively, IKKε may be concluded as an oncoprotein that mediates HCC cell proliferation. To validate *in vitro* findings, functional role of IKKε in *in vivo* tumor growth was further examined by developing subcutaneous xenograft models injected with IKKε shRNA or scrambled HEP3B cells in nude mice. As can be seen in Figure 4.12, IKKε silenced HEP3B cells formed significantly small xenograft tumors compared to scrambled HEP3B cells. When these results considered, IKKε might be a promising therapeutic target and prognostic marker in human HCCs.

Data produced for the roles played by IKKε in HCC are too preliminary to claim a mechanism but 90% of HCC incidences are linked to the NAFLD, NASH, and viral hepatitis, reminding us the characteristic of HCC as inflammation related cancer [45]. Due to interaction of macrophages, lymphocytes, endothelial cells and stellate cells in chronically inflamed liver with hepatocytes, tumor growth is favored [33]. In hepatocytes, NF-κB signaling pathway is activated by the release of TNF from macrophages in hepatic infiltrates causing promotion of hepatocarcinogenesis via decrease in sensitivity of apoptosis. Moreover, JAK-STAT and NF-κB signaling pathways are induced by inflammatory cytokines in chronically inflamed liver and cause further promotion of HCC [45, 47-49]. Due to its variable roles in tissue regeneration and inflammation, NF-κB signaling pathway has placed to the center among the pathways connecting inflammatory regulation of tumor microenvironment and cellular plasticity. Thus, observed effect of IKKε in hepatocellular carcinogenesis might be due to interaction between different cells in tumor microenvironment instead of oncogenic mechanism.

Although oncogenic roles of IKKε in early phases of CRC development is known, this study has been conducted to understand whether IKKε has totally different roles in later stages. After analyses of cell proliferation *in vivo* and *in vitro* with different methods, it was observed that IKKε silenced cells had higher proliferation compared to control cells and form relatively xenograft tumors compared to scrambled cells. Thus, it is concluded that IKKε depletion promotes CRC cell proliferation. Although this data looks as if it is contradicting with the current studies [65, 131], Göktuna et al. demonstrated the importance of IKKε for inflammation and tumor progression via the animal models related to signaling pathways in the early stages of tumors. Proposed relation is not because of oncogenic mechanisms but due to the formation of inflammatory cytokine signaling cascades as a result of interaction between different cells in tumor microenvironment [65]. Additionally, a study of Chen et al. shows IKKε as a negative regulator of β-catenin-dependent transcription and also links IKKε inhibition and excessive β-catenin signaling, resulting in CRC cell proliferation in a subset of human CRC cells with high levels of β-catenin expression [131]. Thus, it can be deduced that IKKε may regulate cancer development differently depending on the tumor stage through different signal pathways. Furthermore, compensation of IKKε inhibition by TBK1, another non-canonical IκB kinases with 66% sequence homology to IKKε, in mice was shown by Reilly et al. [132]. Thus, increase in CRC cell proliferation upon IKKε depletion might be explained via compensation of IKKε by

TBK1 which later activates AKT protein by direct phosphorylation [133]. Activated AKT induces pro-survival signaling and cause inhibition of FOXO3a by phosphorylation leading to advanced cell proliferation, cell survival and eluding apoptosis [100].

Epithelial to mesenchymal transition is a double-faced biological phenomenon took place in cancer progression, tissue regeneration and embryogenesis [134-136]. Augmentation in epithelial markers such as; E-cadherin, cytokeratin 18, cytokeratin 19, occludin and reduction of mesenchymal markers such as; N-cadherin Vimentin, slug and snail can encourage tumor metastasis and invasion in primary tumors [134-136]. NF-κB, WNT, PI3K/Akt pathways are known as regulators of EMT [134-136]. Recently, a study conducted by Lu et al. demonstrated direct interaction between IKKε and two indispensable downstream transcription factor of Hippo pathway, YAP1 and TEAD2 [126]. Moreover, silencing of IKKε in glioblastoma cells results in notable reduction in YAP1 and TEAD2 and reverses EMT process [126]. As a result, their study demonstrates IKKε could affect EMT via Hippo pathway as well as mentioned pathways above [126].

In this study, whether downregulation of IKKε in CRC and HCC cells affecting their migration ability was tested. Results showed that IKKε does not affecting migration abilities of HCC and CRC cells. According to qRT-PCR and WB analyses conducted, epithelial markers such as; E-cadherin, EpCAM, Fibronectin, cytokeratin 18, cytokeratin 19, and ZO-1 levels increased while N-cadherin, snail, vimentin, zeb1, zeb2 levels decreased in HEP3B cells in which IKKε depleted by CRISPR constructs. These findings suggesting that EMT process might be reversed upon IKKε depletion in HCC cells. Although HEP3B IKKε-shRNA findings exhibited unchanged N-cadherin mRNA expression in qRT-PCR analysis, increased N-cadherin and Vimentin levels, and decreased E-cadherin levels in western blot analysis was observed. Differences of N-cadherin might be explained by post-translational modification influenced by IKKε. Although CRISPR and shRNA findings of IKKε depleted HEP3B cells looks like conflicting, the difference may stem from the different methods used for IKKε depletion. In CRISPR mediated knockout method, a guide RNA direct Cas9 nuclease to the target site and then generates double-strand breaks resulting in small deletions and functional gene knockout whereas hairpin-forming RNAs complexes with target mRNAs and results in translational inhibition or mRNA degradation in shRNA mediated knockdown method [137, 138]. Despite the alterations causing complete loss of gene function induced by CRISPR/Cas9 method are stable and permanent, partial loss of gene function because of leftover functional mRNA can be observed in shRNA method [137, 138]. Thus, CRISPR gene editing is more advantageous and good-to-use for elimination of any functional target gene remnants [137, 138]. As a result, the discrepancy in shRNA EMT marker results may be due to residual functional mRNAs from shRNA-mediated silencing. For this reason, CRISPR results are thought to give more reliable results in understanding the function of IKKε. In CRC, although DLD1 IKKε-shRNA findings exhibited decreased E-cadherin mRNA expression cadherin level was not detected by western blotting. Thus, it might be concluded that IKKε knockdown could influence these EMT markers on mRNA level and cause not full but partial-EMT [139] due to increase of other epithelial markers in mRNA level. Furthermore, stimulating CRC cells with TGF-β to understand the role of IKKε in cell migration and to observe changes in the wound recovery, might be necessary to make a distinct conclusion [130]. Overall, IKKε acts like an oncogene in HCC and its depletion suppresses HCC cell proliferation probably via Hippo pathway. Nevertheless, depletion of IKKε in CRC cells confer growth advantage and increases CRC cell proliferation.

Chapter 6

Conclusion and Future perspectives

Firstly, in this study, the functional roles of IKKε involvement in hepatocellular carcinogenesis have been explored. Our findings suggest that IKKε may be considered as an oncoprotein regulating cellular growth of HCC cells. According to *in silico* data, higher IKKε protein expression has been associated with poor overall survival only in male HCC patients. Additionally, we observed that HCC cell proliferation reduced upon IKKε depletion both *in vitro* and *in vivo* settings. When these results combined, IKKε might be a promising therapeutic target and prognostic marker in human HCCs. However, at the moment, it is not possible to fully explain our observations mechanistically with the available data. Yet, we can suggest that tumor promoting effects of IKKε may be due to increased proliferation and survival of HCC cells. Still further studies with sporadic tumor models are required to fully appreciate IKKε involvement in HCC tumor microenvironment

Secondly, potential oncogenic roles played by IKKε in the progression and metastasis of CRC were studied. Upon IKK□ depletion in CRC cell lines, increased proliferation both *in vitro* and *in vivo* has been observed, which suggest that IKKε loss in CRC cells confer growth advantage leading to increased proliferation. From the previous studies, we know that IKKε phosphorylates Akt and maintain its constitutive activation, which then induce pro-survival signaling through inhibition of FOXO3a leading to advanced cell proliferation, cell survival and eluding apoptosis [100]. Previously, Xie et al. have shown *in vitro* robust activation of Akt due to phosphorylation of hydrophobic motif and activation loop of Akt by TBK1 and IKKε [59]. Moreover, another study represents Akt as a TBK1 substrate playing a role in cancer cell survival [133]. Thus, TBK1 may compensate IKKε and activate Akt resulting an increased CRC cell proliferation. To test this claim, phosphorylation of TBK1 and Akt as well as Cyclin D1 and Cdk4 levels, downstream of Akt, upon IKKε depletion might be checked by western blot and qRT-PCR.

Thirdly, experiments conducted to understand the role of IKKε in HCC and CRC cell migration didn't demonstrate significant difference between IKKε-silenced and control cells. Technically, wound healing assay didn't show any alteration with or without serum starvation of cells. Furthermore, RTCA migration assay which is a state-of-art technology didn't demonstrate significant difference in IKKε depleted DLD1 cell migration. To be sure, *in vitro* another assays such as Boyden chamber assay or cell exclusion zone assay may be applied as well as developing *in vivo* metastasis model by the injection of IKKε depleted cells to the tail-vein of immune compromised mice. However, it can be speculated that IKKε depletion does not affect neither HCC nor CRC cell migration *in vitro*. As well as migration assays, invasion assays such as real time cell invasion analysis (RTCA invasion) and Transwell invasion assays should be carried out to learn more about the metastatic role of IKKε in HCC and CRC.

Last but not least, epithelial markers have been increased together with IKKε silencing in HCC cells, suggesting that EMT process might be reversed upon IKKε depletion and this process might be mediated via Hippo pathway. Thus, IKKε could enhance epithelial to mesenchymal transition of HCC cells via Hippo signaling pathway, especially its two downstream molecules, YAP1 and TEAD2 [126]. To enlighten the interaction between Hippo pathway and IKKε in EMT of HCC cells, downstream molecules of Hippo pathway can be checked in IKKε depleted cells as well as IKKε and EMT markers can be checked in YAP1 and TEAD2 depleted cell by qRT-PCR and western blotting. Moreover, partial EMT has been observed in IKKε depleted CRC cells. To understand the role of IKKε in EMT, IKKε silenced HCC and CRC cells might be treated with EMT inducer, TGF-β [130].

Finally, these *in vitro* and *in vivo* findings should be further supported by transgenic mice models such as IKKε knockout mice and also overexpression of IKKε in other HCC and CRC cell lines, especially the ones with low endogenous IKKε level. To sum up, in the light of the current results, it can be attributed that IKKε plays an oncogenic role in HCC but not in CRC.

Bibliography

1. Torre, L.A., et al., *Global cancer statistics, 2012.* CA Cancer J Clin, 2015. **65**(2): p. 87-108.
2. Lee, J.G., et al., *The actual five-year survival rate of hepatocellular carcinoma patients after curative resection.* Yonsei Med J, 2006. **47**(1): p. 105-12.
3. Torre, L.A., et al., *Global Cancer Incidence and Mortality Rates and Trends--An Update.* Cancer Epidemiol Biomarkers Prev, 2016. **25**(1): p. 16-27.
4. Ahmed, I.L., D.N., *Malignant tumours of the liver.* Surgery, 2009. **27**(1): p. 30-37.
5. Yu, L.X., Y. Ling, and H.Y. Wang, *Role of nonresolving inflammation in hepatocellular carcinoma development and progression.* NPJ Precis Oncol, 2018. **2**(1): p. 6.
6. Lee, J.S., et al., *Classification and prediction of survival in hepatocellular carcinoma by gene expression profiling.* Hepatology, 2004. **40**(3): p. 667-76.
7. Chiang, D.Y., et al., *Focal gains of VEGFA and molecular classification of hepatocellular carcinoma.* Cancer Res, 2008. **68**(16): p. 6779-88.
8. Hoshida, Y., et al., *Molecular classification and novel targets in hepatocellular carcinoma: recent advancements.* Semin Liver Dis, 2010. **30**(1): p. 35-51.
9. Zucman-Rossi, J., et al., *Genetic Landscape and Biomarkers of Hepatocellular Carcinoma.* Gastroenterology, 2015. **149**(5): p. 1226-1239 e4.
10. Villanueva, A., et al., *Pivotal role of mTOR signaling in hepatocellular carcinoma.* Gastroenterology, 2008. **135**(6): p. 1972-83, 1983 e1-11.
11. Newell, P., et al., *Ras pathway activation in hepatocellular carcinoma and anti-tumoral effect of combined sorafenib and rapamycin in vivo.* J Hepatol, 2009. **51**(4): p. 725-33.
12. Boyault, S., et al., *Transcriptome classification of HCC is related to gene alterations and to new therapeutic targets.* Hepatology, 2007. **45**(1): p. 42-52.
13. Coulouarn, C., V.M. Factor, and S.S. Thorgeirsson, *Transforming growth factor-beta gene expression signature in mouse hepatocytes predicts clinical outcome in human cancer.* Hepatology, 2008. **47**(6): p. 2059-67.
14. Lachenmayer, A., et al., *Wnt-pathway activation in two molecular classes of hepatocellular carcinoma and experimental modulation by sorafenib.* Clin Cancer Res, 2012. **18**(18): p. 4997-5007.
15. Keng, V.W., et al., *Sex bias occurrence of hepatocellular carcinoma in Poly7 molecular subclass is associated with EGFR.* Hepatology, 2013. **57**(1): p. 120-30.
16. European Association for Study of, L., R. European Organisation for, and C. Treatment of, *EASL-EORTC clinical practice guidelines: management of hepatocellular carcinoma.* Eur J Cancer, 2012. **48**(5): p. 599-641.
17. El-Serag, H.B. and K.L. Rudolph, *Hepatocellular carcinoma: epidemiology and molecular carcinogenesis.* Gastroenterology, 2007. **132**(7): p. 2557-76.
18. Yang, J.D., et al., *Cirrhosis is present in most patients with hepatitis B and hepatocellular carcinoma.* Clin Gastroenterol Hepatol, 2011. **9**(1): p. 64-70.
19. Lok, A.S., et al., *Incidence of hepatocellular carcinoma and associated risk factors in hepatitis C-related advanced liver disease.* Gastroenterology, 2009. **136**(1): p. 138-48.
20. Hsu, I.C., et al., *Mutational hotspot in the p53 gene in human hepatocellular carcinomas.* Nature, 1991. **350**(6317): p. 427-8.
21. Kuipers, E.J., et al., *Colorectal cancer.* Nat Rev Dis Primers, 2015. **1**: p. 15065.

22. Farazi, P.A., et al., *Differential impact of telomere dysfunction on initiation and progression of hepatocellular carcinoma.* Cancer Res, 2003. **63**(16): p. 5021-7.

23. Zhao, R. and F. Michor, *Patterns of proliferative activity in the colonic crypt determine crypt stability and rates of somatic evolution.* PLoS Comput Biol, 2013. **9**(6): p. e1003082.

24. Beasley, R.P., *Hepatitis B virus. The major etiology of hepatocellular carcinoma.* Cancer, 1988. **61**(10): p. 1942-56.

25. Lavanchy, D., *Hepatitis B virus epidemiology, disease burden, treatment, and current and emerging prevention and control measures.* J Viral Hepat, 2004. **11**(2): p. 97-107.

26. Nault, J.C., et al., *Recurrent AAV2-related insertional mutagenesis in human hepatocellular carcinomas.* Nat Genet, 2015. **47**(10): p. 1187-93.

27. Mittal, S., et al., *Temporal trends of nonalcoholic fatty liver disease-related hepatocellular carcinoma in the veteran affairs population.* Clin Gastroenterol Hepatol, 2015. **13**(3): p. 594-601 e1.

28. Bruix, J., M. Sherman, and D. American Association for the Study of Liver, *Management of hepatocellular carcinoma: an update.* Hepatology, 2011. **53**(3): p. 1020-2.

29. Hartmann, D., et al., *Telomerase gene mutations are associated with cirrhosis formation.* Hepatology, 2011. **53**(5): p. 1608-17.

30. Calado, R.T., et al., *Constitutional telomerase mutations are genetic risk factors for cirrhosis.* Hepatology, 2011. **53**(5): p. 1600-7.

31. Gunes, C. and K.L. Rudolph, *The role of telomeres in stem cells and cancer.* Cell, 2013. **152**(3): p. 390-3.

32. Satyanarayana, A., et al., *Mitogen stimulation cooperates with telomere shortening to activate DNA damage responses and senescence signaling.* Mol Cell Biol, 2004. **24**(12): p. 5459-74.

33. Llovet, J.M., et al., *Hepatocellular carcinoma.* Nat Rev Dis Primers, 2016. **2**: p. 16018.

34. Neuveut, C., Y. Wei, and M.A. Buendia, *Mechanisms of HBV-related hepatocarcinogenesis.* J Hepatol, 2010. **52**(4): p. 594-604.

35. Wang, J., et al., *Hepatitis B virus integration in a cyclin A gene in a hepatocellular carcinoma.* Nature, 1990. **343**(6258): p. 555-7.

36. Audard, V., et al., *Cholestasis is a marker for hepatocellular carcinomas displaying beta-catenin mutations.* J Pathol, 2007. **212**(3): p. 345-52.

37. Totoki, Y., et al., *Trans-ancestry mutational landscape of hepatocellular carcinoma genomes.* Nat Genet, 2014. **46**(12): p. 1267-73.

38. Guichard, C., et al., *Integrated analysis of somatic mutations and focal copy-number changes identifies key genes and pathways in hepatocellular carcinoma.* Nat Genet, 2012. **44**(6): p. 694-8.

39. Schulze, K., et al., *Exome sequencing of hepatocellular carcinomas identifies new mutational signatures and potential therapeutic targets.* Nat Genet, 2015. **47**(5): p. 505-511.

40. Sung, W.K., et al., *Genome-wide survey of recurrent HBV integration in hepatocellular carcinoma.* Nat Genet, 2012. **44**(7): p. 765-9.

41. Fei, Q., et al., *Histone methyltransferase SETDB1 regulates liver cancer cell growth through methylation of p53.* Nat Commun, 2015. **6**: p. 8651.

42. Wong, C.M., et al., *Up-regulation of histone methyltransferase SETDB1 by multiple mechanisms in hepatocellular carcinoma promotes cancer metastasis.* Hepatology, 2016. **63**(2): p. 474-87.

43. Hanahan, D. and R.A. Weinberg, *Hallmarks of cancer: the next generation.* Cell, 2011. **144**(5): p. 646-74.

44. Grivennikov, S.I., F.R. Greten, and M. Karin, *Immunity, inflammation, and cancer.* Cell, 2010. **140**(6): p. 883-99.

45. Hernandez-Gea, V., et al., *Role of the microenvironment in the pathogenesis and treatment of hepatocellular carcinoma.* Gastroenterology, 2013. **144**(3): p. 512-27.

46. Finkin, S., et al., *Ectopic lymphoid structures function as microniches for tumor progenitor cells in hepatocellular carcinoma.* Nat Immunol, 2015. **16**(12): p. 1235-44.

47. Pikarsky, E., et al., *NF-kappaB functions as a tumour promoter in inflammation-associated cancer.* Nature, 2004. **431**(7007): p. 461-6.

48. Karin, M. and F.R. Greten, *NF-kappaB: linking inflammation and immunity to cancer development and progression.* Nat Rev Immunol, 2005. **5**(10): p. 749-59.

49. Bauer, J., et al., *Lymphotoxin, NF-kB, and cancer: the dark side of cytokines.* Dig Dis, 2012. **30**(5): p. 453-68.

50. Zhang, D.Y., et al., *A hepatic stellate cell gene expression signature associated with outcomes in hepatitis C cirrhosis and hepatocellular carcinoma after curative resection.* Gut, 2016. **65**(10): p. 1754-64.

51. Haggar, F.A. and R.P. Boushey, *Colorectal cancer epidemiology: incidence, mortality, survival, and risk factors.* Clin Colon Rectal Surg, 2009. **22**(4): p. 191-7.

52. Fedirko, V., et al., *Alcohol drinking and colorectal cancer risk: an overall and dose-response meta-analysis of published studies.* Ann Oncol, 2011. **22**(9): p. 1958-72.

53. Liang, P.S., T.Y. Chen, and E. Giovannucci, *Cigarette smoking and colorectal cancer incidence and mortality: systematic review and meta-analysis.* Int J Cancer, 2009. **124**(10): p. 2406-15.

54. Botteri, E., et al., *Smoking and colorectal cancer: a meta-analysis.* JAMA, 2008. **300**(23): p. 2765-78.

55. Dahm, C.C., et al., *Dietary fiber and colorectal cancer risk: a nested case-control study using food diaries.* J Natl Cancer Inst, 2010. **102**(9): p. 614-26.

56. Song, M., W.S. Garrett, and A.T. Chan, *Nutrients, foods, and colorectal cancer prevention.* Gastroenterology, 2015. **148**(6): p. 1244-60 e16.

57. Raskov, H., et al., *Colorectal carcinogenesis--update and perspectives.* World J Gastroenterol, 2014. **20**(48): p. 18151-64.

58. Datta, S.R., A. Brunet, and M.E. Greenberg, *Cellular survival: a play in three Akts.* Genes Dev, 1999. **13**(22): p. 2905-27.

59. Xie, X., et al., *IkappaB kinase epsilon and TANK-binding kinase 1 activate AKT by direct phosphorylation.* Proc Natl Acad Sci U S A, 2011. **108**(16): p. 6474-9.

60. Taniguchi, K. and M. Karin, *NF-kappaB, inflammation, immunity and cancer: coming of age.* Nat Rev Immunol, 2018. **18**(5): p. 309-324.

61. Hisamuddin, I.M. and V.W. Yang, *Molecular Genetics of Colorectal Cancer: An Overview.* Curr Colorectal Cancer Rep, 2006. **2**(2): p. 53-59.

62. Vasen, H.F., I. Tomlinson, and A. Castells, *Clinical management of hereditary colorectal cancer syndromes.* Nat Rev Gastroenterol Hepatol, 2015. **12**(2): p. 88-97.

63. Tiwari, A.K., H.K. Roy, and H.T. Lynch, *Lynch syndrome in the 21st century: clinical perspectives.* QJM, 2016. **109**(3): p. 151-8.

64. Pancione, M., A. Remo, and V. Colantuoni, *Genetic and epigenetic events generate multiple pathways in colorectal cancer progression.* Patholog Res Int, 2012. **2012**: p. 509348.

65. Goktuna, S.I., et al., *The Prosurvival IKK-Related Kinase IKKepsilon Integrates LPS and IL17A Signaling Cascades to Promote Wnt-Dependent Tumor Development in the Intestine.* Cancer Res, 2016. **76**(9): p. 2587-99.

66. Barnes, D.E. and T. Lindahl, *Repair and genetic consequences of endogenous DNA base damage in mammalian cells.* Annu Rev Genet, 2004. **38**: p. 445-76.

67. Shin, Y.J., et al., *Post-translational regulation enables robust p53 regulation.* BMC Syst Biol, 2013. **7**: p. 83.

68. Richardson, R.B., *p53 mutations associated with aging-related rise in cancer incidence rates.* Cell Cycle, 2013. **12**(15): p. 2468-78.

69. Wang, S. and W.S. El-Deiry, *Requirement of p53 targets in chemosensitization of colonic carcinoma to death ligand therapy.* Proc Natl Acad Sci U S A, 2003. **100**(25): p. 15095-100.

70. Dobre, M., et al., *K-ras gene mutation status in colorectal cancer: comparative analysis of pyrosequencing and PCR-RFLP.* Rom J Morphol Embryol, 2013. **54**(3): p. 567-74.

71. Bettington, M., et al., *The serrated pathway to colorectal carcinoma: current concepts and challenges.* Histopathology, 2013. **62**(3): p. 367-86.

72. Leggett, B. and V. Whitehall, *Role of the serrated pathway in colorectal cancer pathogenesis.* Gastroenterology, 2010. **138**(6): p. 2088-100.

73. Markman, B., et al., *EGFR and KRAS in colorectal cancer.* Adv Clin Chem, 2010. **51**: p. 71-119.

74. Bond, C.E., et al., *Microsatellite stable colorectal cancers stratified by the BRAF V600E mutation show distinct patterns of chromosomal instability.* PLoS One, 2014. **9**(3): p. e91739.

75. Sideris, M. and S. Papagrigoriadis, *Molecular biomarkers and classification models in the evaluation of the prognosis of colorectal cancer.* Anticancer Res, 2014. **34**(5): p. 2061-8.

76. Goktuna, S.I., M.A. Diamanti, and T.L. Chau, *IKKs and tumor cell plasticity.* FEBS J, 2018.

77. Jess, T., C. Rungoe, and L. Peyrin-Biroulet, *Risk of colorectal cancer in patients with ulcerative colitis: a meta-analysis of population-based cohort studies.* Clin Gastroenterol Hepatol, 2012. **10**(6): p. 639-45.

78. Sun, B. and M. Karin, *Obesity, inflammation, and liver cancer.* J Hepatol, 2012. **56**(3): p. 704-13.

79. Berasain, C., et al., *Inflammation and liver cancer: new molecular links.* Ann N Y Acad Sci, 2009. **1155**: p. 206-21.

80. Wang, K. and M. Karin, *Tumor-Elicited Inflammation and Colorectal Cancer.* Adv Cancer Res, 2015. **128**: p. 173-96.

81. Terzic, J., et al., *Inflammation and colon cancer.* Gastroenterology, 2010. **138**(6): p. 2101-2114 e5.

82. DiDonato, J.A., F. Mercurio, and M. Karin, *NF-kappaB and the link between inflammation and cancer.* Immunol Rev, 2012. **246**(1): p. 379-400.

83. Grivennikov, S.I., *Inflammation and colorectal cancer: colitis-associated neoplasia.* Semin Immunopathol, 2013. **35**(2): p. 229-44.

84. Coussens, L.M. and Z. Werb, *Inflammation and cancer.* Nature, 2002. **420**(6917): p. 860-7.

85. Bergmann, A., *IKK epsilon signaling: not just NF-kappaB.* Curr Biol, 2006. **16**(15): p. R588-90.

86. Peters, R.T., S.M. Liao, and T. Maniatis, *IKKepsilon is part of a novel PMA-inducible IkappaB kinase complex.* Mol Cell, 2000. **5**(3): p. 513-22.

87. Guan, H., et al., *IKBKE is over-expressed in glioma and contributes to resistance of glioma cells to apoptosis via activating NF-kappaB.* J Pathol, 2011. **223**(3): p. 436-45.

88. Kang, M.R., et al., *NF-kappaB signalling proteins p50/p105, p52/p100, RelA, and IKKepsilon are over-expressed in oesophageal squamous cell carcinomas.* Pathology, 2009. **41**(7): p. 622-5.

89. Lee, S.E., et al., *IKKepsilon and TBK1 expression in gastric cancer.* Oncotarget, 2017. **8**(10): p. 16233-16242.

90. Guo, J., et al., *IKBKE is induced by STAT3 and tobacco carcinogen and determines chemosensitivity in non-small cell lung cancer.* Oncogene, 2013. **32**(2): p. 151-9.

91. Zubair, H., et al., *Glucose Metabolism Reprogrammed by Overexpression of IKKepsilon Promotes Pancreatic Tumor Growth.* Cancer Res, 2016. **76**(24): p. 7254-7264.

92. Peant, B., et al., *IkappaB-Kinase-epsilon (IKKepsilon) over-expression promotes the growth of prostate cancer through the C/EBP-beta dependent activation of IL-6 gene expression.* Oncotarget, 2017. **8**(9): p. 14487-14501.

93. Peant, B., et al., *Over-expression of IkappaB-kinase-epsilon (IKKepsilon/IKKi) induces secretion of inflammatory cytokines in prostate cancer cell lines.* Prostate, 2009. **69**(7): p. 706-18.

94. Guo, J.P., et al., *Deregulation of IKBKE is associated with tumor progression, poor prognosis, and cisplatin resistance in ovarian cancer.* Am J Pathol, 2009. **175**(1): p. 324-33.

95. Hsu, S., et al., *IKK-epsilon coordinates invasion and metastasis of ovarian cancer.* Cancer Res, 2012. **72**(21): p. 5494-504.

96. Hutti, J.E., et al., *Phosphorylation of the tumor suppressor CYLD by the breast cancer oncogene IKKepsilon promotes cell transformation.* Mol Cell, 2009. **34**(4): p. 461-72.

97. Boehm, J.S., et al., *Integrative genomic approaches identify IKBKE as a breast cancer oncogene.* Cell, 2007. **129**(6): p. 1065-79.

98. Adli, M. and A.S. Baldwin, *IKK-i/IKKepsilon controls constitutive, cancer cell-associated NF-kappaB activity via regulation of Ser-536 p65/RelA phosphorylation.* J Biol Chem, 2006. **281**(37): p. 26976-84.

99. Shen, R.R., et al., *IkappaB kinase epsilon phosphorylates TRAF2 to promote mammary epithelial cell transformation.* Mol Cell Biol, 2012. **32**(23): p. 4756-68.

100. Guo, J.P., D. Coppola, and J.Q. Cheng, *IKBKE protein activates Akt independent of phosphatidylinositol 3-kinase/PDK1/mTORC2 and the pleckstrin homology domain to sustain malignant transformation.* J Biol Chem, 2011. **286**(43): p. 37389-98.

101. Buss, H., et al., *Constitutive and interleukin-1-inducible phosphorylation of p65 NF-{kappa}B at serine 536 is mediated by multiple protein kinases including I{kappa}B kinase (IKK)-{alpha}, IKK{beta}, IKK{epsilon}, TRAF family member-associated (TANK)-binding kinase 1 (TBK1), and an unknown kinase and couples p65 to TATA-binding protein-associated factor II31-mediated interleukin-8 transcription.* J Biol Chem, 2004. **279**(53): p. 55633-43.

102. Zhou, A.Y., et al., *IKKepsilon-mediated tumorigenesis requires K63-linked polyubiquitination by a cIAP1/cIAP2/TRAF2 E3 ubiquitin ligase complex.* Cell Rep, 2013. **3**(3): p. 724-33.

103. He, G. and M. Karin, *NF-kappaB and STAT3 - key players in liver inflammation and cancer.* Cell Res, 2011. **21**(1): p. 159-68.

104. Guo, J.P., et al., *IKBKE phosphorylation and inhibition of FOXO3a: a mechanism of IKBKE oncogenic function.* PLoS One, 2013. **8**(5): p. e63636.

105. Eddy, S.F., et al., *Inducible IkappaB kinase/IkappaB kinase epsilon expression is induced by CK2 and promotes aberrant nuclear factor-kappaB activation in breast cancer cells.* Cancer Res, 2005. **65**(24): p. 11375-83.

106. Shimada, T., et al., *IKK-i, a novel lipopolysaccharide-inducible kinase that is related to IkappaB kinases.* Int Immunol, 1999. **11**(8): p. 1357-62.

107. Bulek, K., et al., *The inducible kinase IKKi is required for IL-17-dependent signaling associated with neutrophilia and pulmonary inflammation.* Nat Immunol, 2011. **12**(9): p. 844-52.

108. Gulen, M.F., et al., *Inactivation of the enzyme GSK3alpha by the kinase IKKi promotes AKT-mTOR signaling pathway that mediates interleukin-1-induced Th17 cell maintenance.* Immunity, 2012. **37**(5): p. 800-12.

109. Chau, T.L., et al., *Are the IKKs and IKK-related kinases TBK1 and IKK-epsilon similarly activated?* Trends Biochem Sci, 2008. **33**(4): p. 171-80.

110. Bibeau-Poirier, A., et al., *Involvement of the IkappaB kinase (IKK)-related kinases tank-binding kinase 1/IKKi and cullin-based ubiquitin ligases in IFN regulatory factor-3 degradation.* J Immunol, 2006. **177**(8): p. 5059-67.

111. *Retraction notice to "Triptolide, histone acetyltransferase inhibitor, suppresses growth and chemosensitizes leukemic cells through inhibition of gene expression regulated by TNF-TNFR1-TRADD-TRAF2-NIK-TAK1-IKK pathway" [Biochem. Pharmacol. 82 (2011) 1134-1144].* Biochem Pharmacol, 2016. **102**: p. 141.

112. Chiang, S.H., et al., *The protein kinase IKKepsilon regulates energy balance in obese mice.* Cell, 2009. **138**(5): p. 961-75.

113. Sanjana, N.E., O. Shalem, and F. Zhang, *Improved vectors and genome-wide libraries for CRISPR screening.* Nat Methods, 2014. **11**(8): p. 783-784.

114. Szasz, A.M., et al., *Cross-validation of survival associated biomarkers in gastric cancer using transcriptomic data of 1,065 patients.* Oncotarget, 2016. **7**(31): p. 49322-49333.

115. Bianchi, F., et al., *Exploiting poly(I:C) to induce cancer cell apoptosis.* Cancer Biol Ther, 2017. **18**(10): p. 747-756.

116. Shen, R.R. and W.C. Hahn, *Emerging roles for the non-canonical IKKs in cancer.* Oncogene, 2011. **30**(6): p. 631-41.

117. Kondylis, V., et al., *The interplay of IKK, NF-kappaB and RIPK1 signaling in the regulation of cell death, tissue homeostasis and inflammation.* Immunol Rev, 2017. **277**(1): p. 113-127.

118. D'Ignazio, L., D. Bandarra, and S. Rocha, *NF-kappaB and HIF crosstalk in immune responses.* FEBS J, 2016. **283**(3): p. 413-24.

119. Gudkov, A.V. and E.A. Komarova, *p53 and the Carcinogenicity of Chronic Inflammation.* Cold Spring Harb Perspect Med, 2016. **6**(11).

120. Rajurkar, M., et al., *IKBKE Is Required during KRAS-Induced Pancreatic Tumorigenesis.* Cancer Res, 2017. **77**(2): p. 320-329.

121. Verstrepen, L. and R. Beyaert, *Receptor proximal kinases in NF-kappaB signaling as potential therapeutic targets in cancer and inflammation.* Biochem Pharmacol, 2014. **92**(4): p. 519-29.

122. Wei, C., et al., *Elevated expression of TANK-binding kinase 1 enhances tamoxifen resistance in breast cancer.* Proc Natl Acad Sci U S A, 2014. **111**(5): p. E601-10.

123. Barbie, T.U., et al., *Targeting an IKBKE cytokine network impairs triple-negative breast cancer growth.* J Clin Invest, 2014. **124**(12): p. 5411-23.

124. Zhang, Z., et al., *IKBKE promotes glioblastoma progression by establishing the regulatory feedback loop of IKBKE/YAP1/miR-Let-7b/i.* Tumour Biol, 2017. **39**(7): p. 1010428317705575.

125. Wang, L., S. Guo, and H. Zhang, *MiR-98 Promotes Apoptosis of Glioma Cells via Suppressing IKBKE/NF-kappaB Pathway.* Technol Cancer Res Treat, 2017. **16**(6): p. 1226-1234.

126. Lu, J., et al., *IKBKE regulates cell proliferation and epithelial-mesenchymal transition of human malignant glioma via the Hippo pathway.* Oncotarget, 2017. **8**(30): p. 49502-49514.

127. Liu, Y., et al., *Amlexanox, a selective inhibitor of IKBKE, generates anti-tumoral effects by disrupting the Hippo pathway in human glioblastoma cell lines.* Cell Death Dis, 2017. **8**(8): p. e3022.

128. Tian, Y., et al., *MicroRNAs let-7b/i suppress human glioma cell invasion and migration by targeting IKBKE directly.* Biochem Biophys Res Commun, 2015. **458**(2): p. 307-12.

129. Li, H., et al., *Silencing of IKKepsilon using siRNA inhibits proliferation and invasion of glioma cells in vitro and in vivo.* Int J Oncol, 2012. **41**(1): p. 169-78.

130. Xu, J., S. Lamouille, and R. Derynck, *TGF-beta-induced epithelial to mesenchymal transition.* Cell Res, 2009. **19**(2): p. 156-72.

131. Chen, J., et al., *Hyper activation of beta-catenin signalling induced by IKKepsilon inhibition thwarts colorectal cancer cell proliferation.* Cell Prolif, 2017. **50**(4).

132. Reilly, S.M., et al., *An inhibitor of the protein kinases TBK1 and IKK-varepsilon improves obesity-related metabolic dysfunctions in mice.* Nat Med, 2013. **19**(3): p. 313-21.

133. Ou, Y.H., et al., *TBK1 directly engages Akt/PKB survival signaling to support oncogenic transformation.* Mol Cell, 2011. **41**(4): p. 458-70.

134. Nieto, M.A., et al., *Emt: 2016.* Cell, 2016. **166**(1): p. 21-45.

135. Brabletz, T., *EMT and MET in metastasis: where are the cancer stem cells?* Cancer Cell, 2012. **22**(6): p. 699-701.

136. Brabletz, T., et al., *EMT in cancer.* Nat Rev Cancer, 2018. **18**(2): p. 128-134.

137. Boettcher, M. and M.T. McManus, *Choosing the Right Tool for the Job: RNAi, TALEN, or CRISPR.* Mol Cell, 2015. **58**(4): p. 575-85.

138. Evers, B., et al., *CRISPR knockout screening outperforms shRNA and CRISPRi in identifying essential genes.* Nat Biotechnol, 2016. **34**(6): p. 631-3.

139. Zhang, J., et al., *TGF-beta-induced epithelial-to-mesenchymal transition proceeds through stepwise activation of multiple feedback loops.* Sci Signal, 2014. **7**(345): p. ra91.

Appendix

Copyright Permissions

ELSEVIER LICENSE
TERMS AND CONDITIONS

Jul 04, 2018

This Agreement between Mr. Ugur Kahya ("You") and Elsevier ("Elsevier") consists of your license details and the terms and conditions provided by Elsevier and Copyright Clearance Center.

License Number	4365060471264
License date	Jun 09, 2018
Licensed Content Publisher	Elsevier
Licensed Content Publication	Surgery (Oxford)
Licensed Content Title	Malignant tumours of the liver
Licensed Content Author	Irfan Ahmed,Dileep N. Lobo
Licensed Content Date	Jan 1, 2009
Licensed Content Volume	27
Licensed Content Issue	1
Licensed Content Pages	8
Start Page	30
End Page	37
Type of Use	reuse in a thesis/dissertation
Portion	figures/tables/illustrations
Number of figures/tables /illustrations	3
Format	both print and electronic
Are you the author of this Elsevier article?	No
Will you be translating?	No
Original figure numbers	Table 1 table 2 Table 5
Title of your thesis/dissertation	Identification of the Roles Played by IKKε in Hepatocellular and Colorectal Carcinogenesis
Expected completion date	Jul 2018
Estimated size (number of pages)	100
Requestor Location	Mr. Ugur Kahya Bilkent Universitesi Merkez Kampusu Molekuler Biyoloji ve Genetik Bolumu Bilkent, Cankaya, Ankara, Turkiye Ankara, 06800 Turkey Attn: Mr. Ugur Kahya
Publisher Tax ID	GB 494 6272 12
Total	0.00 USD

SPRINGER NATURE LICENSE
TERMS AND CONDITIONS

Jul 04, 2018

This Agreement between Mr. Ugur Kahya ("You") and Springer Nature ("Springer Nature") consists of your license details and the terms and conditions provided by Springer Nature and Copyright Clearance Center.

License Number	4382191462585
License date	Jul 04, 2018
Licensed Content Publisher	Springer Nature
Licensed Content Publication	Nature Reviews Disease Primers
Licensed Content Title	Hepatocellular carcinoma
Licensed Content Author	Josep M. Llovet, Jessica Zucman-Rossi, Eli Pikarsky, Bruno Sangro, Myron Schwartz et al.
Licensed Content Date	Apr 14, 2016
Licensed Content Volume	2
Type of Use	Thesis/Dissertation
Requestor type	academic/university or research institute
Format	print and electronic
Portion	figures/tables/illustrations
Number of figures/tables /illustrations	1
High-res required	no
Will you be translating?	no
Circulation/distribution	>50,000
Author of this Springer Nature content	no
Title	Identification of the Roles Played by IKKε in Hepatocellular and Colorectal Carcinogenesis
Instructor name	n/a
Institution name	n/a
Expected presentation date	Jul 2018
Portions	Figure 3
Requestor Location	Mr. Ugur Kahya Bilkent Universitesi Merkez Kampusu Molekuler Biyoloji ve Genetik Bolumu Bilkent, Cankaya, Ankara, Turkiye Ankara, 06800 Turkey Attn: Mr. Ugur Kahya
Billing Type	Invoice
Billing Address	Mr. Ugur Kahya Bilkent Universitesi Merkez Kampusu Molekuler Biyoloji ve Genetik Bolumu Bilkent, Cankaya, Ankara, Turkiye Ankara, Turkey 06800 Attn: Mr. Ugur Kahya
Total	0.00 USD

SPRINGER NATURE LICENSE
TERMS AND CONDITIONS

Jul 04, 2018

This Agreement between Mr. Ugur Kahya ("You") and Springer Nature ("Springer Nature") consists of your license details and the terms and conditions provided by Springer Nature and Copyright Clearance Center.

License Number	4382200023083
License date	Jul 04, 2018
Licensed Content Publisher	Springer Nature
Licensed Content Publication	Nature Reviews Disease Primers
Licensed Content Title	Colorectal cancer
Licensed Content Author	Ernst J. Kuipers, William M. Grady, David Lieberman, Thomas Seufferlein, Joseph J. Sung et al.
Licensed Content Date	Nov 5, 2015
Licensed Content Volume	1
Type of Use	Thesis/Dissertation
Requestor type	academic/university or research institute
Format	print and electronic
Portion	figures/tables/illustrations
Number of figures/tables /illustrations	1
High-res required	no
Will you be translating?	no
Circulation/distribution	>50,000
Author of this Springer Nature content	no
Title	Identification of the Roles Played by IKKε in Hepatocellular and Colorectal Carcinogenesis
Instructor name	n/a
Institution name	n/a
Expected presentation date	Jul 2018
Portions	Figure 3
Requestor Location	Mr. Ugur Kahya Bilkent Universitesi Merkez Kampusu Molekuler Biyoloji ve Genetik Bolumu Bilkent, Cankaya, Ankara, Turkiye Ankara, 06800 Turkey Attn: Mr. Ugur Kahya
Billing Type	Invoice
Billing Address	Mr. Ugur Kahya Bilkent Universitesi Merkez Kampusu Molekuler Biyoloji ve Genetik Bolumu Bilkent, Cankaya, Ankara, Turkiye Ankara, Turkey 06800 Attn: Mr. Ugur Kahya
Total	0.00 USD

ELSEVIER LICENSE
TERMS AND CONDITIONS

Jul 04, 2018

This Agreement between Mr. Ugur Kahya ("You") and Elsevier ("Elsevier") consists of your license details and the terms and conditions provided by Elsevier and Copyright Clearance Center.

License Number	4382200124705
License date	Jul 04, 2018
Licensed Content Publisher	Elsevier
Licensed Content Publication	European Journal of Cancer
Licensed Content Title	EASL–EORTC Clinical Practice Guidelines: Management of hepatocellular carcinoma
Licensed Content Date	Mar 1, 2012
Licensed Content Volume	48
Licensed Content Issue	5
Licensed Content Pages	43
Start Page	599
End Page	641
Type of Use	reuse in a thesis/dissertation
Intended publisher of new work	other
Portion	figures/tables/illustrations
Number of figures/tables /illustrations	1
Format	both print and electronic
Are you the author of this Elsevier article?	No
Will you be translating?	No
Original figure numbers	Figure 3
Title of your thesis/dissertation	Identification of the Roles Played by IKKε in Hepatocellular and Colorectal Carcinogenesis
Expected completion date	Jul 2018
Estimated size (number of pages)	100
Requestor Location	Mr. Ugur Kahya Bilkent Universitesi Merkez Kampusu Molekuler Biyoloji ve Genetik Bolumu Bilkent, Cankaya, Ankara, Turkiye Ankara, 06800 Turkey Attn: Mr. Ugur Kahya
Publisher Tax ID	GB 494 6272 12
Total	0.00 USD